AD-A170 203 STUDIES OF PHASE-CONJUGATE OPTICAL DEVICE CONCEPTS(U) 1/2
ROCKWELL INTERNATIONAL THOUSAND OAKS CA SCIENCE CENTER
P YEH ET AL. JUN 86 SC5424.AR N00014-85-C-0219
UNCLASSIFIED F/G 20/6 NL

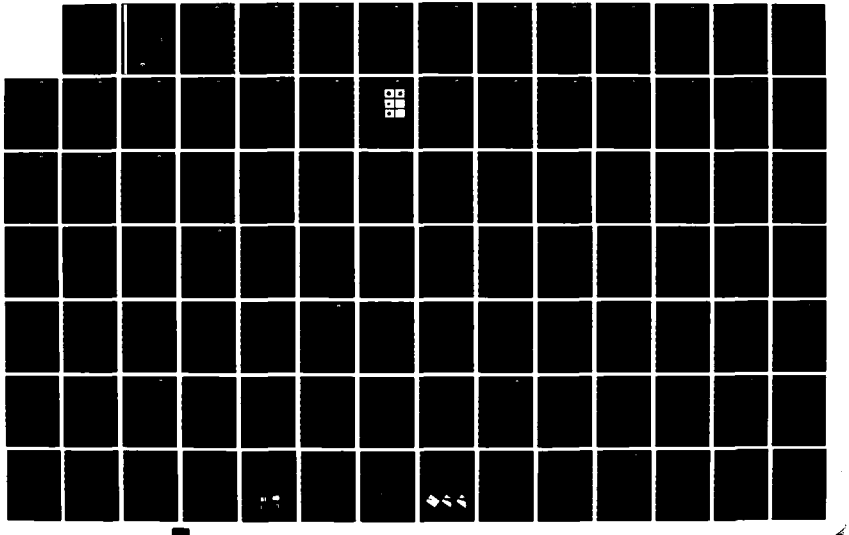

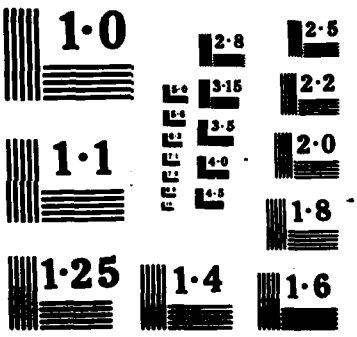
1·0
1·1
1·25
1·4
1·6
1·8
2·0
2·2
2·5
2·8
3·15
3·5
4·0
4·5

(12)

SC5424.AR

Copy No. 3

SC5424.AR

AD-A170 203

STUDIES OF PHASE-CONJUGATE OPTICAL DEVICE CONCEPTS

ANNUAL TECHNICAL REPORT FOR THE PERIOD
April 01, 1985 through March 31, 1986

CONTRACT NO. N00014-85-C-0219

Prepared for:

Dr. Herschel Pilloff
Office of Naval Research
Physics Division, Code 412
800 N. Quincy Street
Arlington, VA 22217-5000

Pochi Yeh
Ian McMichael

JUNE 1986

Approved for public release; distribution unlimited

Rockwell International
Science Center

86

TABLE OF CONTENTS

LIST OF FIGURES

LIST OF TABLES

1.0 SUMMARY

1.1 Contract Description

This contract studies the phase-reversal property of optical phase conjugation for navigational and other device applications. The study focuses on the development of the phase-conjugate fiber-optic gyro and the generation of new device concepts.

1.2 Scientific Problem

Although much attention is paid to the aberration correction property of phase conjugation, little attention is paid to the phase reversal property. The phase-reversal property has important applications in inertial navigation devices. The general problem for this program is to generate new device concepts using the phase-reversal property of phase conjugation.

Polarization scrambling is a well-known source of noise and signal fading in fiber-optic gyros. Some gyros avoid this problem by using polarization-preserving fibers and couplers to decouple the polarization modes. This program studies a new approach in which polarization-preserving phase conjugation is used to correct for polarization scrambling without the need for polarization-preserving fibers and couplers.

1.3 Progress

There are several areas of significant progress in the first year of this program that are directly related to the development of the phase-conjugate fiber-optic gyro. These include:

- First experimental observation of the phase-conjugate Sagnac phase shift.
- First demonstrations of rotation sensing with a phase-conjugate gyro and with a self-pumped phase-conjugate fiber-optic gyro.

- First measurement of a nonreciprocal phase shift (Faraday effect) in a double phase-conjugate interferometer.

- Development of a polarization-preserving phase-conjugate mirror that operates at milliwatt power levels.

- First demonstration of the correction of polarization scrambling in multimode fibers by polarization-preserving phase conjugation.

- First measurements of the phase of phase-conjugate reflections.

In addition to the progress mentioned above, we have also carried out other interesting scientific research and have achieved many significant results. These include:

- Frequency shifts of photorefractive resonators

- Resonator model and frequency shifts of self-pumped phase conjugate resonators

- Photorefractive conical diffraction, and

- Parallel image subtraction via phase-conjugate Michelson interferometry.

The results are published (or to be published) in the papers and conference presentations listed in Section 1.5.

1.4 Special Significance of Results

It should be noted that two of the above mentioned areas of progress are of special significance in that they are not restricted in their use to the phase-conjugate fiber-optic gyro. The polarization-preserving phase-conjugate

mirror opens a whole new area of interferometry with multimode fibers. Measurements of the phase of the phase-conjugate reflection can be used to determine the phase shift (with respect to the intensity pattern) and the type of grating (index, absorption, gain, or mixture) involved in degenerate four-wave mixing in nonlinear media. Proper selection of nonlinear media will allow the construction of phase-conjugate interferometers that "self-quadrature" for high sensitivity and linear response. The phase shift of phase conjugators also plays an important role in the frequency shift of double phase-conjugate resonators.

1.5 Publications and Presentations

Publications

"Self-Pumped Phase-Conjugate Fiber-Optic Gyro," Ian McMichael and Pochi Yeh, submitted to Optics Letters, (1986).

"Polarization-Preserving Phase Conjugator," Ian McMichael, Monte Khoshnevisan and Pochi Yeh, to appear in Opt. Lett., August (1986).

"Absolute Phase Shift of Phase Conjugators," Ian McMichael, Pochi Yeh and Monte Khoshnevisan, to appear in Proc. SPIE 613, 32 (1986).

"Phase-Conjugate Fiber-Optic Gyro," Pochi Yeh, Ian McMichael and Monte Khoshnevisan, Appl. Opt. 25, 1029 (1986).

* "Theory of Unidirectional Photorefractive Ring Oscillators," Pochi Yeh, J. Opt. Soc. Am. B2, 1924 (1985).

* "Frequency Shift and Cavity Length in Photorefractive Resonators," M.D. Ewbank and Pochi Yeh, Opt. Lett., 10, 496-498 (1985).

* "Frequency Shift of Self-Pumped Phase Conjugator," M.D. Ewbank and Pochi Yeh, SPIE Proc. 613, 59 (1986).

* "Parallel Image Subtraction Using a Phase Conjugate Michelson Interferometer," A.E.T. Chiou and Pochi Yeh, Opt. Lett. 11, 306 (1986).

*Works only partially supported by this contract.

* "Photorefractive Conical Diffraction in $BaTiO_3$," M.D. Ewbank, Pochi Yeh and J. Feinberg, to appear in Opt. Comm. (1986).

Presentations

"Self-Pumped Phase-Conjugate Fiber-Optic Gyro," Ian McMichael and Pochi Yeh, submitted to the 1986 OSA Annual Meeting in Seattle, WA.

"Measurements of the Phase of Phase-Conjugate Reflections," Ian McMichael, Pochi Yeh and Monte Khoshnevisan, presented at IQEC'86 in San Francisco, CA.

"Absolute Phase Shift of Phase Conjugators," Ian McMichael, Pochi Yeh and Monte Khoshnevisan, presented at O-E LASE'86 in Los Angeles, CA.

"Phase-Conjugate Fiber-Optic Gyro," Pochi Yeh, Ian McMichael and Monte Khoshnevisan, presented at the 1985 OSA Annual Meeting in Washington, D.C.

"Scalar Phase Conjugation Using a Barium Titanate Crystal," Ian McMichael and Monte Khoshnevisan, presented at CLEO'85 in Baltimore, MD.

* "Photorefractive Resonators," M.D. Ewbank and Pochi Yeh, paper presented at the 1985 OSA Annual Meeting in Washington, D.C. (October 14-18, 1985).

* "Frequency Shift of Self-Pumped Phase Conjugator," M.D. Ewbank and Pochi Yeh, paper presented at Conference on Nonlinear Optics and Applications, January 21-22, 1986, Los Angeles, CA.

* "Coherent Image Subtraction Using Phase Conjugate Interferometry," A.E.T. Chiou, Pochi Yeh and Monte Khoshnevisan, paper presented at Conference on Nonlinear Optics and Applications, January 21-22, 1986, Los Angeles, CA.

*Works only partially supported by this contract.

2.0 TECHNICAL DISCUSSION

Optical phase conjugation has been a subject of considerable interest during the past several years. Much attention has been focused on the wavefront correction property of this process by means of degenerate four-wave mixing.[1-3] Very little attention was paid to the phase reversal property, the Doppler-free reflection, and the phase-sensitive coupling of degenerate four-wave mixing. These properties have many interesting and important applications in inertial navigation devices. In this section, we will first briefly describe some of the nonlinear optical phenomena and then discuss the phase-conjugate fiber-optic gyro.

2.1 Phase Reversal and Doppler-Free Reflection

Phase reversal is a unique property of degenerate four-wave mixing which is not available in the conventional adaptive optics. A very interesting situation arises as a result of the phase reversal. Consider the situation when a laser beam is incident on a phase-conjugate reflector (abbreviated here as ϕ^* reflector). Let $E \exp[i(\omega t - kz + \phi)]$ be the incident electric field. The ϕ^* reflector will generate a reflected wave of the form $\rho E \exp[i(\omega t + kz - \phi)]$. The interference pattern formed by the incident and reflected waves is of the form

$$I = E^2 [1 + |\rho|^2 + 2|\rho| \cos (2kz - 2\phi + \sigma)] \qquad (1)$$

where σ is the constant phase of the complex reflection coefficient ρ. Note that the phase ϕ contains the information of the source. If the source frequency fluctuates, ϕ will be a function of time and the interference pattern also fluctuates. This means that the phase of the interference pattern is determined by the source, not the reflector. In other words, the interference pattern is independent of the position (or motion) of the ϕ^* reflector. This property can also be explained in terms of the Doppler-free reflection. Since there is no Doppler shift in frequency due to the motion of the ϕ^* reflector,[4]

the incident beam and the reflected beam have the same frequency which leads to a stationary interference pattern.

If the ϕ^* reflector were replaced by an ordinary mirror, the interference pattern would have a phase which depends on the position of the mirror. Such an interference pattern would move with the mirror and does not contain any phase information about the source. Since ϕ does not appear in the interference pattern, any frequency fluctuation (or phase fluctuation) of the source will not affect the pattern. In other words, the interference pattern is determined by the mirror. This property also can be explained in terms of the Doppler shift upon reflection from a moving mirror. Since the reflected wave is shifted in frequency by $(2v\omega/c)$, the interference pattern is traveling at a speed equal to the speed of the mirror.

The Doppler-free reflection via four-wave mixing has been demonstrated experimentally by the author and his co-workers.[4]

2.2 Polarization-Preserving Phase Conjugator

In many of the early experiments on wavefront correction,[1,2] the change of polarization state upon phase-conjugate reflection had no effect on the fidelity of aberration correction because the distorting media were optically isotropic. There are many situations where the distorting media may become optically anisotropic due to external perturbations such as electric field, magnetic field, strain, etc. Under these circumstances, the polarization state of the phase-conjugated wave becomes an important issue.

Consider an optical wave of frequency ω moving in the +z direction

$$\vec{E}_1 = \vec{A}_1(\vec{r})e^{i(\omega t - kz)} \tag{2}$$

where $\vec{A}_1(\vec{r})$ is the complex amplitude and k is the wave number. This wave satisfies the wave equation

$$\vec{\nabla}\times(\vec{\nabla}\times\vec{E}) - \omega^2\,\mu\varepsilon(\vec{r})\vec{E} = 0 \tag{3}$$

where ε is the dielectric constant and μ is the permeability constant.

We now consider a case where in some region of space near z_0, we generate a field $\vec{E}_2$ (e.g., via degenerate four-wave mixing) which is related to the phase-conjugate of $\vec{E}_1$, and described locally by

$$\vec{E}_2 = \rho \vec{A}_1^{\,*}(\vec{r}) e^{i(\omega t + kz)} \quad , \tag{4}$$

where ρ is, in general, a 3 × 3 tensor. It can then be shown that the amplitude of the reflected wave $\vec{E}_2$ will remain $\rho \vec{A}_1^{\,*}(\vec{r})$ in the region $z < z_0$, provided $\vec{E}_2$ and $\vec{E}_1$ satisfy the same wave equation in this region. This is the basic principle of wavefront correction via optical phase-conjugation. If the dielectric function $\varepsilon(\vec{r})$, which describes the property in the region $z < z_0$, is a tensor (i.e., has nonzero off-diagonal terms), then the wave $\vec{E}_2$ may not satisfy the wave equation (3) because the matrix multiplication is, in general, not commutative. If the phase-conjugate reflectance tensor ρ reduces to a scalar, then $\vec{E}_2$ also satisfies the wave equation (3), because for scalar ρ, $\rho\varepsilon = \varepsilon\rho$, even if ε is a tensor. Thus, a scalar phase conjugator can serve to restore polarization scrambling, as well as wavefront aberration. Such a reflector is called a polarization preserving phase conjugator.

To further illustrate the polarization restoration, we consider the propagation of polarized light through a series of birefringent plates (see Fig. 2-1). At the end of the birefringent system, a phase-conjugate reflector

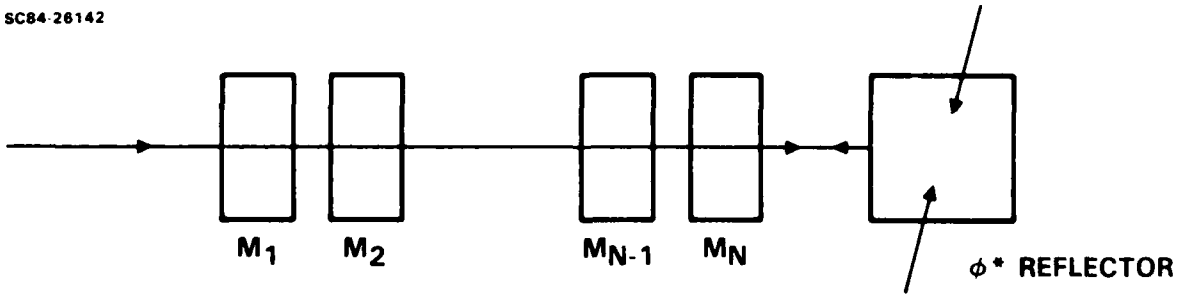

Fig. 2-1 Phase conjugator for polarization restoration in a birefringent system.

retroreflects the polarized light. Let us now examine the polarization state of the light as it propagates through the system. Let $\vec{A}_1(0)$ be the input polarization state and $\vec{A}_1(L)$ be the output polarization state. $\vec{A}_1(0)$ and $\vec{A}_1(L)$ are related by

$$\vec{A}_1(L) = M_N M_{N-1} \cdots M_3 M_2 M_1 \vec{A}_1(0) \tag{5}$$

where M_i $(i = 1,2,..N)$ is the Jones matrix for the i-th plate. Upon reflection from the phase-conjugator, the polarization state becomes $\rho\vec{A}_1^*(L)$. When the reflected light propagates backward through the birefringent system, the final polarization state $\vec{A}_2(0)$ is given by

$$\vec{A}_2(0) = M_1 M_2 M_3 \cdots M_{N-1} M_N \rho \vec{A}_1^*(L) \quad . \tag{6}$$

Using Eqs. (5) and (6), this polarization state can be written

$$\vec{A}_2(0) = M_1 M_2 M_3 \cdots M_{N-1} M_N \rho M_N^* M_{N-1}^* \cdots M_3^* M_2^* M_1^* \vec{A}_1^*(0) \quad . \tag{7}$$

If ρ is a scalar, then Eq. (7) reduces to

$$\vec{A}_2(0) = \rho \vec{A}_1^*(0) \tag{8}$$

because all the Jones matrices are unitary (i.e., $MM^* = 1$).[5] Equation (8) indicates that $\vec{A}_1(0)$ and $\vec{A}_2(0)$ have exactly the same polarization state (i.e., same ellipticity, handedness, helicity). If ρ cannot be reduced to a scalar, then Eq. (7) indicates that the polarization state $\vec{A}_2(0)$ is different from $\vec{A}_1(0)$. Thus, a polarization-preserving phase-conjugator can be used to restore the polarization state.

Consider now the tensor property of a phase-conjugator which consists of a nonlinear isotropic medium pumped by a pair of counter-propagating beams. Let the electric fields of the incident probe beam and the pump beams be $\vec{A}(\vec{r})e^{i(\omega t - kz)}$, $\vec{B}e^{i(\omega,t-\vec{k}\cdot\vec{r})}$ and $\vec{C}e^{i(\omega t - \vec{k}\cdot\vec{r})}$, respectively. The nonlinear polarization which is responsible for the generation of the phase-conjugated wave is[6]

$$\vec{P}^{NL} = 2\chi_{1111}[\vec{A}^*(\vec{B}\cdot\vec{C}) + \vec{B}(\vec{A}^*\cdot\vec{C}) + \vec{C}(\vec{A}^*\cdot\vec{B})]e^{i(\omega t+kz)} \quad , \qquad (9)$$

where we assume that the material has an instantaneous polarization response (i.e., lossless) and use the relationships $\chi_{1111} = 3\chi_{1122}$ and $\chi_{1122} = \chi_{1221} = \chi_{1212}$.[7] The last two terms in the square brackets are responsible for the analogy between the degenerate four-wave mixing and holography. The first term has no holographic analog and may be the dominant term in the event of a two-photon resonance.[3] In general, all three terms contribute to the generation of the phase-conjugated wave whose amplitude is proportional to $\vec{P}^{NL}$.

According to Eq. (9), a polarization-preserving phase-conjugator can be obtained by arranging the pump beams in such a way that the holographic terms vanish. This can be achieved by making the polarization state of the pump beams orthogonal to that of the probe beam. For the case of probing incidence along the +z direction, the polarization state of the probe wave lies in the xy plane. Thus, the pump beams must be polarized along the z-direction in order to have zero holographic terms. Such a geometry is depicted in Fig. 2-2(a). In this scheme, the nonlinear polarization

$$\vec{P}^{NL} = 2\chi_{1111}\vec{A}^*(\vec{B}\cdot\vec{C}) \qquad (10)$$

will generate a phase-conjugated wave which preserves the polarization state. This example shows that polarization-preserving phase-conjugation exists.

Figures 2-2(b) and 2-2(c) show two other schemes which can also achieve polarization-preserving phase conjugation. In these two schemes, the phase conjugators are operated in the holographic regime (e.g., photorefractive effect) such that they respond to one linear polarization state only and have no effect on the other polarization state. By using a polarizing beam splitter (see Fig. 2-2(c)) or using two stages in cascade (Fig. 2-2(b)), it is possible to conjugate each polarization component individually and then recombine the conjugated components. By proper alignment of the crystals, it is possible to achieve polarization-preserving phase conjugation.

A scheme, similar to that shown in Fig. 2-2(c), which utilizes self-pumped phase conjugation in a Michelson interferometer can also be employed to achieve polarization-preserving phase conjugation. This approach is described in the progress section.

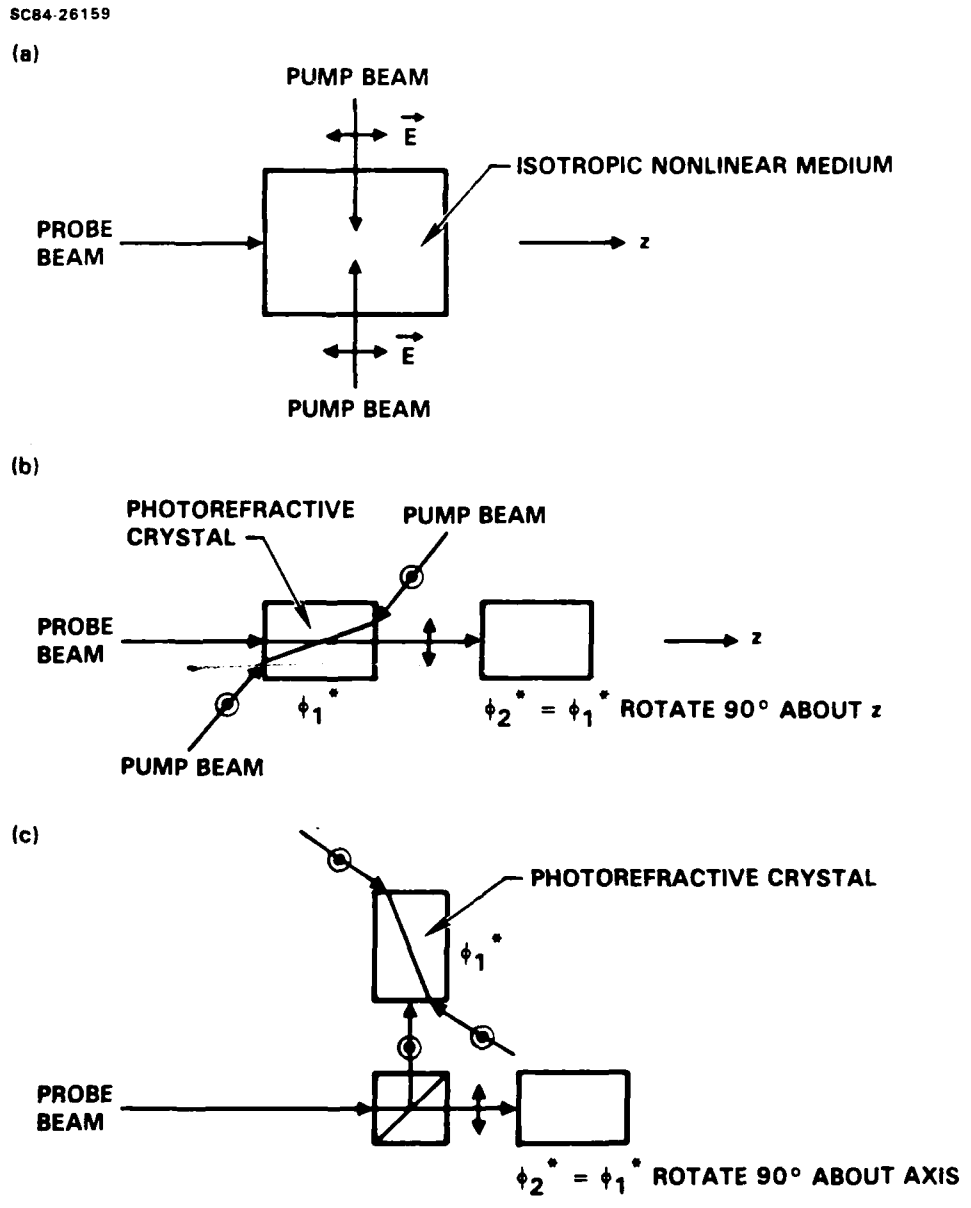

Fig. 2-2 Schematic drawings of polarization-preserving phase conjugators.

2.3 Phase-Conjugate Fiber-Optic Gyros

Polarization scrambling is a well-known noise source in fiber-optic gyros. Birefringent polarization-holding fibers can be used to decouple the two states of polarization and hence improve the sensitivity.[8,9] In the phase-conjugate fiber-optic gyro, which we are studying, a polarization-preserving phase conjugator can be used to restore severely scrambled waves to their original state of polarization. This eliminates the noise due to polarization scrambling.

Referring to Fig. 2-3, we consider a fiber-optic gyro which contains a phase-conjugate reflector (abbreviated as ϕ^* reflector) at the end of the fiber loop. We now examine the phase shift of light. In the clockwise trip from the input coupling to the ϕ^* detector, the phase shift is $\phi_1 = kL - 2\pi LR\Omega/(\lambda c)$, where L is the length of the fiber, R is the radius of the loop, Ω is the rotation rate, λ is the wavelength, $k = 2\pi n/\lambda$, and c is the velocity of light. In the counterclockwise trip, the phase shift is $\phi_2 = kL + 2\pi LR\Omega/(\lambda c)$. Due to the phase reversal nature of the ϕ^* reflector, the net phase shift in a round trip is $\Delta\phi = \phi_2 - \phi_1 = 4\pi LR\Omega/(\lambda c)$. Such a net phase change is proportional to the rotation rate and can be used for rotation sensing.

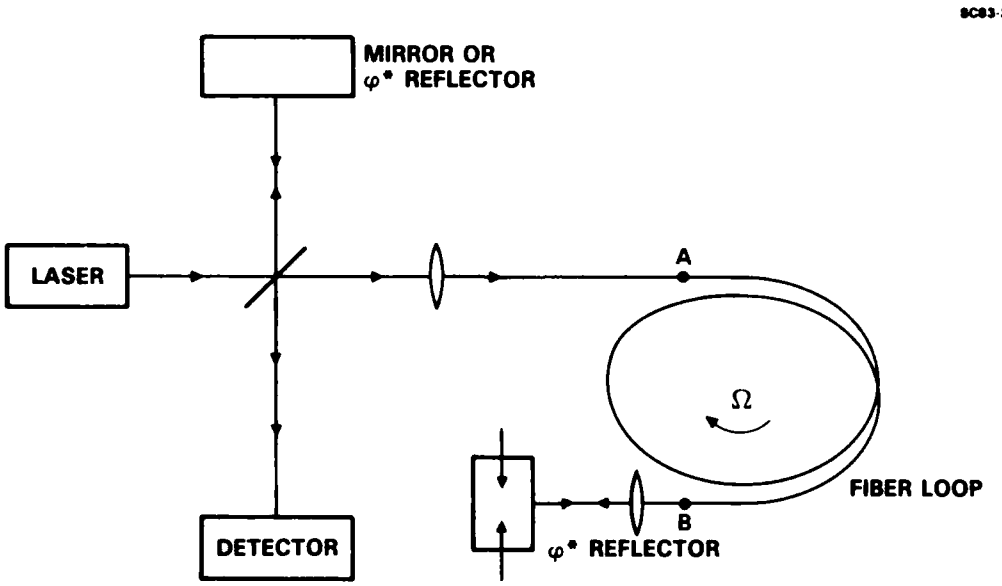

Fig. 2-3 Schematic of the phase-conjugate fiber-optic gyro.

In addition, if the ϕ^* reflector can preserve the polarization state, then the polarization state will not change upon reflection. Such a polarization-preserving ϕ^* reflector will produce a true time-reversed version of the incident wave and will undo all the reciprocal changes (e.g., polarization scrambling, modal aberration) when the light propagates backward from ϕ^* reflector to the input coupling. Thus, the problem of polarization scrambling as well as modal aberration in multimode fibers can be solved by using polarization-preserving phase conjugation.

3.0 PROGRESS

During the first year of this research program, there were many areas of significant progress. These include the experimental demonstration of the phase-conjugate Sagnac effect and the polarization-preserving phase conjugator. In addition, we have proposed and demonstrated a scheme to measure the absolute phase shift of phase-conjugate reflections. This phase shift plays an important role in the detection of the Sagnac phase shift due to rotation. This progress is summarized below.

3.1 Phase-Conjugate Fiber-Optic Gyro

Our first objective was to demonstrate that the phase-conjugate fiber-optic gyro (PCFOG) described in Section 2.3 is sensitive to rotation. A proof of concept experiment was set up for this objective using an externally pumped crystal of barium titanate as the phase-conjugate mirror. Since the phase-conjugate mirror in this preliminary experiment did not preserve polarization, the fiber-optic coil was made of polarization-preserving fiber. Our report of the first demonstration of rotation-sensing is included as Appendix Section 5.4. The results of this proof of concept experiment demonstrate that as predicted, the PCFOG is sensitive to the nonreciprocal phase shift produced by the Sagnac effect and therefore it can be used to sense rotation.

In the proof of concept demonstration of the PCFOG described above, we were limited to a fiber-optic coil having an optical path length of 10 m by the coherence length of the laser. As a result, we were not able to measure low rotation rates. However, there are other configurations of the PCFOG that allow for longer lengths of fiber and hence greater sensitivity. For example, a Michelson interferometer in which both arms are terminated by the same self-pumped phase-conjugate mirror is also sensitive to nonreciprocal phase shifts. We first demonstrated this fact by measuring the nonreciprocal phase shift introduced by the Faraday effect in such an interferometer. The results of this demonstration implied that a PCFOG can be made by placing fiber-optic coils in

the arms of this interferometer. In this configuration the two fiber-optic coils can be of any length as long as the difference between their lengths does not exceed the coherence length of the source. We recently demonstrated rotation sensing with this configuration of a PCFOG, and our report of that demonstration is included as Appendix Section 5.1. Since this configuration uses self-pumped phase conjugation, it has the obvious advantage of not having to provide external pumping waves that are coherent and form a phase-conjugate pair.

3.2 Polarization-Preserving Phase Conjugator

Our ultimate goal is the demonstration of a phase-conjugate fiber-optic gyro using multimode fiber. Such a demonstration requires the polarization-preserving phase conjugator (PPPC) described in Section 2.2 to correct for the environmentally dependent birefringence and modal aberration of multimode fibers. With this motivation we developed the first polarization-preserving phase conjugator that operates at milliwatt power levels. The polarization-preserving phase conjugator works by decomposing a light beam into its two polarization components, rotating one of these components with a half-wave plate, and reflecting both components from the same phase-conjugate mirror. When the two reflected components recombine they form a phase-conjugate wave that has the same polarization as the incident wave. Our report of this development is included in Appendix Section 5.2. The report presents results demonstrating that the phase-conjugate wave produced by the polarization-preserving phase conjugator has the same ellipticity and helicity of polarization as the incident wave.

To demonstrate the ability of the polarization-preserving phase conjugator to correct for the modal and polarization scrambling of multimode fibers, we performed the experiment shown in Fig. 3-1. The highly reflective beamsplitter BS1 isolates the laser from retroreflections of its output. The polarizer P1 ensures that light entering the multimode fiber MMF is linearly polarized in the plane of the figure. Light exiting from the fiber is retro-

reflected by either a normal mirror M, a nonpolarization-preserving phase conjugator, or by the polarization-preserving phase-conjugator PPPC. After propagating back through the fiber the light is sampled by the beamsplitter BS2, analyzed by the polarizer P2, and photographed by the camera D. The resulting photographs are shown in Fig. 3-2. The upper photographs, taken with a normal mirror at the end of the fiber, demonstrate complete polarization scrambling by the fiber. The middle photographs, taken with a phase-conjugate mirror (nonpolarization preserving) at the end of the fiber, demonstrate partial correction of the polarization scrambling. Finally, the lower photographs demonstrate complete correction of the polarization scrambling by the polarization-preserving phase conjugator.

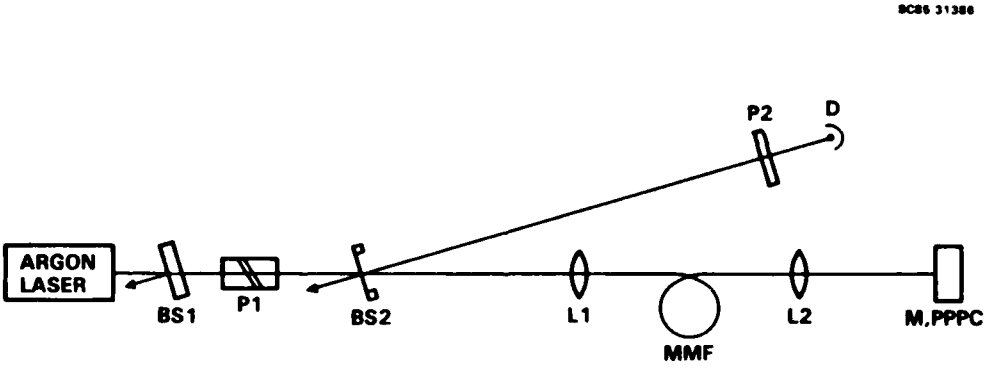

Fig. 3-1 Experiment used to demonstrate correction of polarization scrambling in multimode fibers by polarization-preserving phase conjugation.

The results presented above and in Appendix Section 5.2 are for a polarization-preserving phase conjugator that utilizes self-pumped phase conjugation. A more recent experiment, with similar results, demonstrates a polarization-preserving phase conjugator that utilizes externally pumped phase conjugation. This experiment is shown in Fig. 3-3. The polarization-preserving phase conjugator consists of components BS2, M1, M2, $BaTiO_3$, PBS, M3, and $\lambda/2$ (not shown as a dashed line). This arrangement is a polarization-preserving

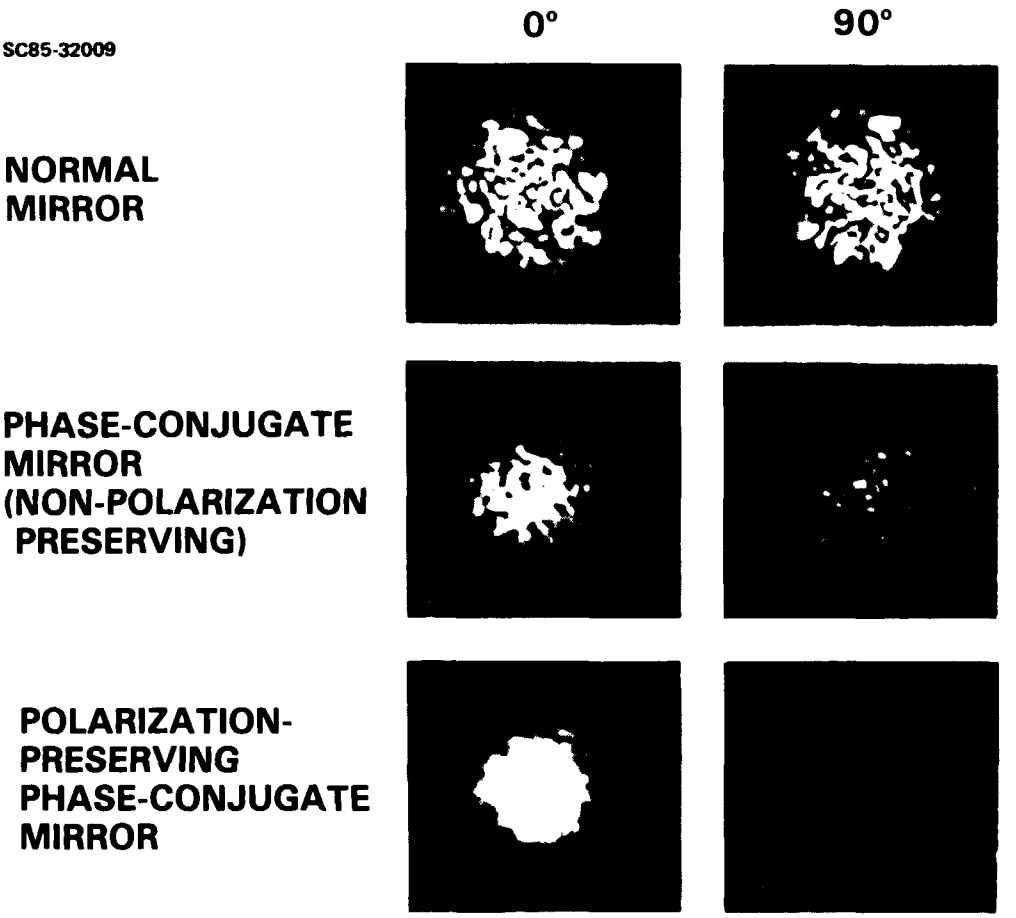

Fig. 3-2 Correction of polarization scrambling and modal aberration in a multimode fiber by polarization-preserving phase conjugation.

phase conjugator for light incident from the left on the polarizing beamsplitter PBS. The remaining components are used to test the polarization-preserving phase conjugator. The external pumping waves for degenerate four-wave mixing in the crystal of barium titanate are provided by the reflections from mirrors M1 and M2. The components transmitted and reflected by PBS are probe waves. To test the polarization-preserving phase conjugator, either a half-wave retarder $\lambda/2$ (shown as dashed line) or quarter-wave retarder $\lambda/4$ is used to alter the

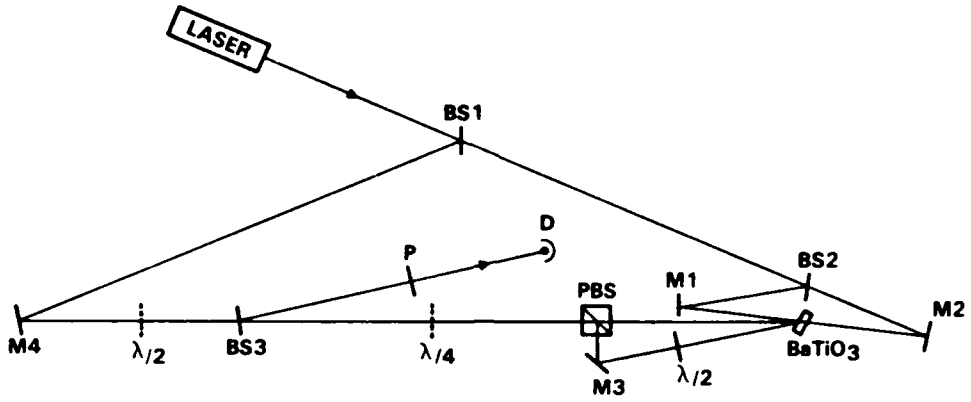

Fig. 3-3 Externally pumped polarization-preserving phase-conjugate mirror.

polarization state of the light incident on the PPPC. The reflected light is sampled by the beamsplitter BS2, and analyzed by the combination of polarizer P and detector D. Since BS2 is an uncoated pellicle beamsplitter used near normal incidence (the angle of incidence is exaggerated in the figure; the actual angle of incidence is 2°), the reflection coefficients for the s and p polarizations are nearly equal and the polarization measured by P and D is nearly the same as that of the reflection.

Figure 3-4 shows the measured angle of polarization for the reflection from the polarization-preserving phase conjugator, PPPC, as a function of the angle of polarization of the light incident on the PPPC, for various orientations of the half-wave retarder. Zero degrees corresponds to polarization in the plane of the previous figures. The open circles are the data (with diameters corresponding to the uncertainty), and the solid line indicates what is expected in the case of an ideal polarization-preserving phase conjugator. The measured ellipticity of the polarization for the light reflected by the PPPC (defined as the ratio of the minor polarization axis to the major polarization axis) never exceeded 5%.

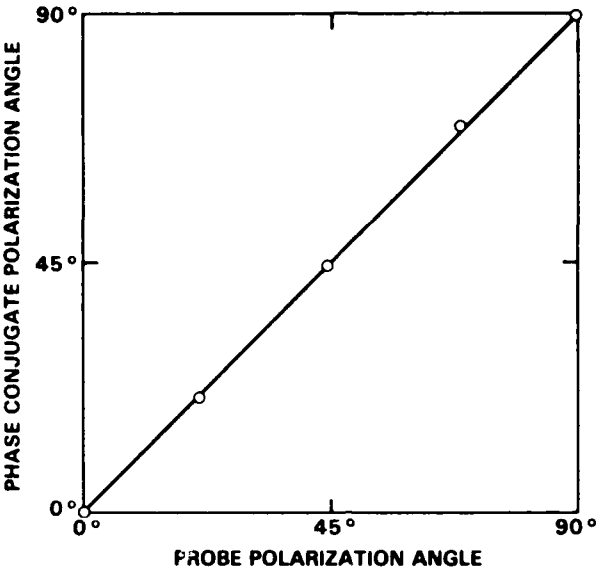

Fig. 3-4 Measured angle of polarization for the reflection from the polarization-preserving phase conjugator vs the angle of polarization of the incident wave.

The results shown in Fig. 3-4 demonstrate that the reflection from the PPPC reproduces the angle of polarization of the incident wave. To show that it reproduces the helicity of the polarization of the incident wave, the quarter-wave retarder $\lambda/4$ is placed between the sampling beam splitter and the polarizing beam splitter and is oriented such that the light incident on the mirror is converted from linearly polarized light to circularly polarized light. Figure 3-5 shows the measured polarization ellipses for the reflections from a normal mirror and from the polarization-preserving phase conjugator. Light reflected from the normal mirror changes helicity. After passing back through the quarter-wave retarder, the polarization of the reflected light is orthogonal to the incident light. This is the principle by which quarter-wave isolation works. On the other hand, light reflected by the polarization-preserving phase conjugator has the same helicity as the incident light and returns to its original polarization state after passing back through the quarter-wave retarder.

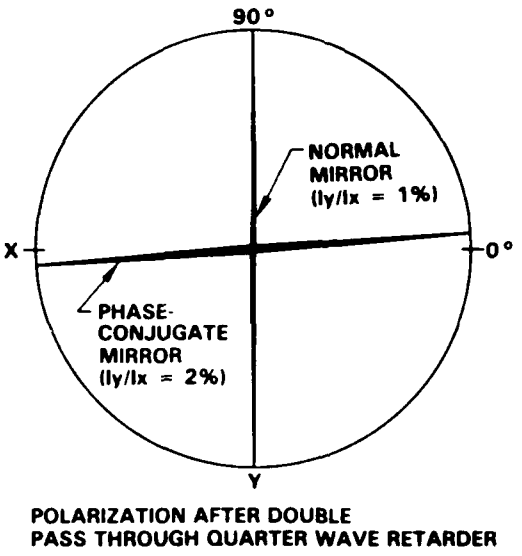

Fig. 3-5 Reproduction of the helicity of polarized light by the externally pumped polarization-preserving phase conjugator.

3.3 Phase of Phase-Conjugate Reflections

The phase of the phase-conjugate reflection determines the operating point in some configurations of the phase-conjugate fiber-optic gyro. If this phase can be controlled, the PCFOG can be biased at the operating point of highest sensitivity and linear response (quadrature). With this motivation we measured the phase of phase-conjugate reflections by determining the operating point of a phase-conjugate interferometer and developed a theory to explain our results. The detailed report of this work is included as Appendix Section 5.3 and a summary of the results is given here.

If the complex amplitude A_4 of the phase-conjugate reflection of an incident wave having complex amplitude A_3 is written as

$$A_4 = r\, e^{i\phi_0} A_1 A_2 A_3^* / |A_1 A_2| \tag{11}$$

where A_1 and A_2 are the complex amplitudes of the pumping waves, then ϕ_0 is referred to as the phase of the phase-conjugate. This phase is given by,

$$\phi_0 = \phi_{\Delta k} + \phi_g + \pi/2 \tag{12}$$

$$\phi_o = \phi_{\Delta k} + \phi_g + \pi/2 \qquad (12)$$

where $\phi_{\Delta k}$ is a term that depends on the type of grating involved in the phase conjugation (index, absorption, or gain) and ϕ_g is the phase shift of the grating with respect to the light intensity pattern that produces the grating. For photorefractive media in which the index grating ($\phi\Delta_k = 0$) is shifted by $\pi/2$ radians we expect $\phi_o = 0$ or π radians. For thermo-optic media in which the index grating is in phase with the light intensity pattern we expect $\phi_o = \pi/2$ radians.

Our experimental measurements of ϕ_o for various nonlinear media are given in Table 1, where θ is the angle between the grating k vector and the crystal axis. For the photorefractive materials, barium titanate and strontium barium niobate, the measured values of ϕ_o compare well with the expected values. The small discrepancies for barium titanate at $\theta = 0°$ and 180° indicate that the index grating is not shifted by exactly $\pi/2$ radians, as is often assumed. We have verified this fact by an independent measurement of the two-wave mixing gain as a function of the frequency detuning between the two waves. The fact that the grating is not shifted by exactly $\pi/2$ radians may be due to the existence of a photovoltaic field. Since for ruby $\phi_o \approx \pi/2$ radians, the grating is probably dominated by an index change rather than an absorption change.

Table 1
Phase of Phase-Conjugate Reflections

Material	θ	ϕ_o
$BaTiO_3$	0°	(19±3)°
	45°	(6±4)°
	135°	(176±3)°
	180°	(164±3)°
SBN	0°	(3±3)°
	180°	(175±5)°
Ruby	-	(80±5)°

These results demonstrate that the proper choice of nonlinear material for the phase-conjugate mirror can automatically bias the phase-conjugate fiber-optic gyro at the point of maximum sensitivity and linear response.

3.4 Photorefractive Phenomena

3.4.1 Frequency Shift of Photorefractive Resonators

Photorefractive resonators exhibit an extremely small frequency difference ($\Delta f/f \sim 10^{-15}$) between the oscillating and pump beams. In addition, the photorefractive ring resonator seems to oscillate over a large range of cavity detuning despite the narrow gain bandwidth. A theory is developed which describes how the oscillating mode attains the round-trip phase condition. The theory predicts that the frequency difference between the oscillating and pump beams is proportional to the cavity detuning. This dependence is explained by a photorefractive phase shift due to slightly nondegenerate two-wave mixing that compensates the cavity detuning and allows the electric field to reproduce itself after each round trip. Such a theory is validated experimentally. The measured frequency and oscillating intensity agree with theory.

The details are given in the reprints of our papers which are attached as Appendix Sections 5.5 and 5.6.

3.4.2 Frequency Shift of Self-Pumped Phase Conjugators

The reflection from most photorefractive, self-pumped phase conjugators differs in frequency from the incident beam by a small amount ($\Delta\omega/\omega \sim 10^{-15}$). This frequency shift has been attributed to moving photorefractive gratings which Doppler shift the diff -ted light. However, the physical mechanism responsible for the moving grati . is not well understood.

The frequency shift first manifested itself as a frequency scanning when a self-pumped $BaTiO_3$ was coupled to a dye laser. Since those initial observations, numerous experiments and theories involving self-pumped phase conjugators and/or photorefractive resonators have addressed, either directly or

indirectly, the frequency shift issue. However, a general theory and the conclusive experiments are not available.

We have developed a theory and carried out the supporting experiments which explain such frequency shifts of most self-pumped phase conjugators. In our theory, self-pumped phase conjugation results from an internal self-oscillation. The optical resonance cavity which supports such oscillation is formed by either external mirrors or crystal surfaces. The oscillating beams provide the counterpropagating pump beams which are required in the four-wave mixing process. The frequency shift is proportional to the cavity length detuning.

When the self-pumping beams are spontaneously generated via photorefractive coupling in a linear resonance cavity with two external mirrors on opposite sides of a photorefractive crystal such as $BaTiO_3$, we observe that the frequency shift of the phase-conjugate reflection is directly proportional to cavity-length detuning. In the case where the self-pumping beams arise from internal reflections off the photorefractive crystal's surfaces, we experimentally prove that previous descriptions of the self-pumping process are inadequate and we show that a closed-looped resonance cavity forming inside the crystal is a better description.

The details are given in the reprint of a paper which is attached as Appendix Section 5.7.

3.4.3 Photorefractive Conical Diffraction

A single beam of coherent light incident on a $BaTiO_3$ crystal can cause a cone of light to emerge from the far face of the crystal. This cone has a polarization orthogonal to that of the incident ray and appears when the incident beam is an extraordinary ray in the crystal. There have been previous accounts of rings, fans, and other forms of photoinduced light scattering in photorefractive crystals, which have been attributed to a variety of physical mechanisms.[11-19] Recently, similar light cones in $BaTiO_3$ have been reported and shown to be due to stimulated two-wave mixing via the photorefractive effect.[20]

Here, we account for the phase-matching condition in $BaTiO_3$ for anisotropic Bragg scattering[21] by using a simple geometrical construction to predict the angular position of the light in the exit plane. We also show that precise measurements of the cone angle can be used to determine the dispersion of the birefringence, $\Delta n = n_e - n_o$, of a $BaTiO_3$ sample.

The details are given in the preprint of a paper which is attached as Appendix Section 5.8.

4.0 REFERENCES

1. B. Ya. Zel'dovich, V.I. Popovichev, V.V. Ragul'skii and F.S. Faizullov, Sov. Phys. JETP 15, 109 (1972).

2. A. Yariv, IEE J. Quantum Electronics QE14, 650 (1978).

3. C.R. Giuliano, Physics Today 27 (April 1981).

4. P. Yeh, M. Ewbank, M. Khoshnevisan and J. Tracy, "Doppler-Free-Phase-Conjugate Reflection," Opt. Lett. 9, 41-43 (1984).

5. See, for example, A. Yariv and P. Yeh, "Optical Waves in Crystals," (Wiley, NY, 1984), p. 124.

6. Reference 5, p. 553.

7. R.W. Hellwarth, "Third-Order Optical Susceptibilities of Liquids and Solids," Prog. Quant. Electr. 5, 1-68 (Pergammon Press, 1977).

8. T.G. Giallorenzi, J.A. Burcaro, A. Dandridge, G.H. Sigel, Jr., J.H. Cole, S.C. Rashleigh and R.G. Priest, "Optical Fiber Sensor Technology," IEEE, J. QE, QE-18, 626-664 (1982).

9. W.K. Burns, R.P. Moeller, C.A. Villarruel and M. Abebe, "Fiber Optic Gyroscopes with Polarization Holding Fiber," Opt. Lett. 8, 540-542 (1983).

10. P. Yeh, "Scalar Phase Conjugator for Polarization Correction," Opt. Comm. 51, 195-197 (1984).

11. W. Phillips, J.J. Amodei and D.L. Staebler, RCA Rev. 33, 94 (1972).

12. J.M. Morgan and I.P. Kaminow, Appl. Opt. 12, 1964 (1973).

13. M.R.B. Forhsaw, Appl. Opt. 13, 2 (1974).

14. R. Magnusson and T.K. Gaylord, Appl. Opt. 13, 1545 (1974).

15. S.I. Ragnarsson, Appl. Opt. 17, 116 (1978).

16. I.R. Dorosh, Yu.S. Kuzminov, N.M. Polozkov, A.M. Prokhorov, V.V. Osiko, N.V. Tkachenko, V.V. Voronov and D.Kh. Nurligareev, Phys. Stat. Sol. (1) 65, 513 (1981).

17. E.M. Avakyan, K.G. Belabaev and S.G. Odoulov, Sov. Phys. Sol. St. 25, 1887 (1983).

18. R. Grousson, S. Mallick and S. Odoulov, Opt. Comm. 51, 342 (1984).

19. S. Odoulov, K. Belabaev and I. Kiseleva, Opt. Lett. 10, 31 (1985).

20. D.A. Temple and C. Warde, J. Opt. Soc. Am. 1B3, 337 (1986).

21. N.V. Kukhtarev, E. Kratzig, H.C. Kulich and R.A. Rupp, Appl. Phys. B35, 17 (1984).

APPENDIX 5.1

Self-Pumped Phase-Conjugate Fiber-Optic Gyro

(Paper submitted to Optics Letters)

SELF-PUMPED PHASE-CONJUGATE FIBER-OPTIC GYRO

Ian McMichael and Pochi Yeh
Rockwell International Science Center
1049 Camino Dos Rios
Thousand Oaks, CA 91360

ABSTRACT

We describe a new type of phase-conjugate fiber-optic gyro that uses self-pumped phase conjugation. The self-pumped configuration is simpler than externally pumped configurations and permits the use of sensing fibers longer than the coherence length of the laser. A proof-of-principle demonstration of rotation sensing with the device is presented.

Several types of phase-conjugate gyros are described in the literature,[1-4] and we recently reported on the first demonstration of rotation sensing with a phase conjugate gyro.[5] The passive phase-conjugate fiber-optic gyros described in references 3 and 5 are Michelson interferometers in which the arms contain fiber-optic coils that are terminated by externally pumped phase-conjugate mirrors. Since the phase-conjugate mirrors produce time-reversed waves, all reciprocal phase changes in the optical paths are compensated and do not effect the output of the interferometer. However, since the phase shift produced by the Sagnac effect is nonreciprocal, the output of the interferometer is sensitive to rotation and can be used as a gyro.

Standard fiber-optic gyros[6] are Sagnac interferometers that are inherently insensitive to reciprocal phase changes and sensitive to nonreciprocal phase changes. This is true only when their operation is restricted to a single polarization mode,[7] and the best fiber-optic gyros use polarization-preserving fibers and couplers.[8] However, if the phase-conjugate mirrors in the phase-conjugate fiber-optic gyro preserve polarization,[9] then nonpolarization preserving single-mode fibers, and even multimode fibers, can be used in the gyro.

In the externally pumped configurations described in references 3 and 5, the fiber-optic coils can be no longer than the coherence length of the laser. This limits the sensitivity of the device. It is true that longer coils can be used if a polarization-preserving fiber of equal length is used to carry the pumping waves to the phase-conjugate mirrors. However,

this defeats the above mentioned advantage in that the phase-conjugate gyro can use inexpensive multimode fibers and couplers. In this letter, we describe and demonstrate a self-pumped configuration of the phase-conjugate fiber-optic gyro that is not only simpler than the externally pumped configurations, but also allows for the use of fiber-optic coils that are longer than the coherence length of the laser.

Figure 1 shows a schematic of a self-pumped phase-conjugate fiber-optic gyro. Light from a laser is split by beamsplitter BS into two fibers F1 and F2. Fibers F1 and F2 are coiled such that light travels clockwise in F1 and counterclockwise in F2. Light waves traversing fibers F1 and F2 experience reciprocal phase shifts,

$$\varnothing_{r_1} = \int k_1 \, dl_1 \text{ and } \varnothing_{r_2} = \int k_2 \, dl_2, \tag{1}$$

respectively, where dl_1 and dl_2 are elements of length along F1 and F2, and $k_{1,2} = 2\pi n_{1,2}/\lambda$. In addition, the nonreciprocal phase shifts,

$$\varnothing_{nr_1} = +2\pi R_1 L_1 \Omega/\lambda c \text{ and } \varnothing_{nr_2} = -2\pi R_2 L_2 \Omega/\lambda c \tag{2}$$

are due to the Sagnac effect, where $R_{1,2}$ and $L_{1,2}$ are the lengths and radii of the fiber loops, and Ω is the rotation rate. The net phase shifts are then, $\varnothing_{r_1} + \varnothing_{nr_1}$ and $\varnothing_{r_2} + \varnothing_{nr_2}$. On reflection from the phase-conjugate mirror, the phase shifts become, $-\varnothing_{r_1} - \varnothing_{nr_1}$ and $-\varnothing_{r_2} - \varnothing_{nr_2}$, where we

have dropped the phase shift of the phase conjugator[10,11] since it is common to both waves, and we are only interested in the phase difference. It should be noted that the phase shift of the phase conjugator is common to both waves, only when both waves are reflected from the same phase-conjugate mirror, or when the phase-conjugate mirrors are coupled[12]. In the case of self-pumped phase conjugation in barium titanate, the two incident waves interact by coherently pumping the oscillation of a resonator formed by internal reflectons in the crystal[13]. The counterpropagating waves in the resonator provide the pumping waves for degenerate four wave mixing (DFWM) with the incident waves. Due to the resonance condition, the DFWM pumping waves may be frequency shifted[14,15] with respect to the incident waves and result in a frequency shift or time varying phase shift for the phase conjugate reflections. But again, since the two incident waves see the same pumping waves, this phase shift is common to both and does not effect the operation of this device since it is only sensitive to the phase difference. The phase shifts for the return trip in the fiber are given by, $\phi_{r_1} - \phi_{nr_1}$ and $\phi_{r_2} - \phi_{nr_2}$, noting that the sign of the reciprocal contribution is the same as before whereas the nonreciprocal contribution has opposite sign. In the round trip, the reciprocal contributions cancel and net phase shifts are given by, $-2\phi_{nr_1}$ and $-2\phi_{nr_2}$. The phase difference measured by the interference at detector D,

$$\phi = -2(\phi_{nr_2} - \phi_{nr_1}) = 4\pi(R_1L_1 + R_2L_2)\Omega/\lambda c, \qquad (3)$$

is proportional to the rotation rate Ω, and can be used to sense rotation.

This configuration has several advantages over our previously reported configuration.[5] Here, we can use self-pumped phase conjugation, with the obvious advantage of not having to provide external pump waves that are coherent and form a phase-conjugate pair. In the externally pumped configuration, the pump beam(s) involved in the writing of the index grating must be coherent with the probe wave to within the response time of the phase conjugator, and the two counterpropagating pump beams must be phase conjugates of each other to obtain a high fidelity phase-conjugate reflection. In initial experiments where an entire externally pumped phase-conjugate gyro was mounted on a rotating table, due to the slow time response of phase conjugation in the barium titanate crystal used, vibrations of the mounts providing the external pumping washed out the gratings involved in the phase conjugation, and precluded the measurement of rotation. As an additional advantage of the self-pumped configuration, the sensing fibers F1 and F2 can be made longer (thereby increasing the sensitivity) than the coherence length of the laser provided that they are equal in length to within the coherence length.

Figure 2 shows the experimental setup of the self-pumped phase-conjugate fiber-optic gyro. Instead of using two separate fibers as shown in Fig.1, we use the two polarization modes of a single polarization-preserving fiber coil. All experiments are done with the

argon laser running multilongitudinal mode at 515 nm. The highly reflective beamsplitter BS1 isolates the laser from retroreflections. The polarization-preserving fiber F1 couples light from the laser to the remaining part of the apparatus that is mounted on a rotating table. The output end of F1 is oriented such that the polarization of light exiting from the fiber is at 45° to the plane of the figure. The component polarized in the plane of the page is transmitted by the polarizing beamsplitter PBS1 and travels counterclockwise in the fiber coil, whereas the component polarized perpendicular to the page travels clockwise in the fiber coil. The fiber coil is made of approximately 9 m of polarization-preserving fiber coiled in a square of 0.57 m sides, and is oriented such that the polarization of the clockwise and counterclockwise waves are preserved. When the two waves exit from the coil they are separated by a Rochon polarizer PBS2. The polarization of the light that travels straight through PBS2 is rotated by the polarization rotator PR such that its polarization becomes identical to that of the light deflected by PBS2. Both beams are incident as extraordinary waves on a barium titanate crystal such that self-pumped phase conjugation occurs[16]. The reflected waves retraverse the fiber in an opposite sense, recombine at PBS1, and travel back toward the laser with a phase difference $\phi = 8\pi RL\Omega/\lambda c$. These waves are sampled by the uncoated pellicle beamsplitter BS2, and an additional phase delay of $\pi/2$ radians is impressed on them when they propagate through the quarter-wave retarder $\lambda/4$. The half-wave retarder is oriented such that

the intensities of the interferences measured by detectors D1 and D2 are proportional to sin ø and -sin ø, respectively. The signals from these detectors go to a differential amplifier and a chart recorder.

Figure 3 shows the signal from the chart recorder. For t<0, the gyro was stationary. At t=0, the gyro was rotated first clockwise, then counterclockwise in a square-wave fashion for four cycles with an amplitude of approximately 6°/s. The experimentally measured phase shift is in good agreement with the predicted phase shift of 0.04 radians. The fast rotation rate is necessary for the signal to overcome the noise that is evident in the phase shift recorded during the time t<0. Although we are not certain of the major noise source, we believe it is rapid reciprocal phase shifts that are not corrected due to the finite response time of the phase conjugator.

Although this experiment does not demonstrate the the correction of polarization scrambling in multimode fibers, it does demonstrate the measurement of the Sagnac phase shift Eq. (3). To demonstrate a self-pumped phase-conjugate fiber-optic gyro using multimode fibers, one must use two multimode fibers terminated by the same self-pumped polarization-preserving phase-conjugate mirror. Simply replacing the polarization-preserving fiber in Fig. 2 with a multimode fiber does not work, since the polarization of light after traveling down the fiber is scambled and when the light reaches PBS1 part of it will go to the detectors without being reflected from the phase-conjugate mirror. In addition to the added complication of using two fibers and associated

complexity of terminating them on the same self-pumped polarization-preserving phase-conjugate mirror (four beams going into one crystal), it is necessary to insure that the light waves from the two fibers are coherent to within the response time of the phase conjugator (the change in phase shifts for the two waves due to environmental effects on the fibers must be slower than the response time of the phase conjugator). The second of the above mentioned effects can be reduced by wrapping the two fibers together so that they see nearly the same environment.

In conclusion, we have described a new type of phase-conjugate fiber-optic gyro in which self-pumped phase conjugation can be employed to allow the use of sensing fibers that are longer than the coherence length of the laser source. In previous externally pumped configurations, it is possible to use fibers longer than the coherence length of the laser, by using a fiber to carry the pumping waves. This however complicates the setup and defeats some of the advantages of using phase conjugation. We have constructed a self-pumped phase-conjugate fiber-optic gyro and demonstrated rotation sensing.

This work is supported by the Office of Naval Research contract #N0014-85-C-0219.

REFERENCES

1. J.-C. Diels and I. C. McMichael, Opt. Lett. **6**, 219 (1981).
2. P. Yeh, J. Tracy, and M. Khoshnevisan, Proc. SPIE **412**, 240 (1983).
3. C. J. Bord'e, in *Experimental Gravitation and Measurement Theory*, P. Meystre and M. O. Scully, Eds. (Plenum, New York, 1983) 269.
4. B. Fischer and S. Sternklar, Appl. Phys. Lett. **47**, 1 (1985).
5. P. Yeh, I. McMichael, and M. Khoshnevisan, Appl. Opt. **25**, 1029 (1986).
6. R. Bergh, H. Lefevre and H. Shaw, IEEE J. Lightwave Tech. **2**, 91 (1984).
7. R. Ulrich, Opt. Lett. **5**, 173 (1980).
8. W. Burns, R. Moeller, C. Villarruel, and M. Abebe, Opt. Lett. **8**, 540 (1983).
9. I. McMichael, M. Khoshnevisan, and P. Yeh, Opt. Lett. **14**, XXX (1986).
10. I. McMichael, P. Yeh, and M. Khoshnevisan, Proc. SPIE **613**, XXX (1986).
11. S. Kwong, A. Yariv, M. Cronin-Golomb, and B. Fischer, J. Opt. Soc. Am. A **3**, 157 (1986).
12. M. Ewbank, P. Yeh, M. Khoshnevisan, and J. Feinberg, Opt. Lett. **10**, 282 (1985).
13. M. Ewbank and P. Yeh, Proc. SPIE **613**, XXX (1986).
14. P. Yeh, J. Opt. Soc. Am. B **2**, 1924 (1985).
15. M. Ewbank and P. Yeh, Opt. Lett. **10**, 496 (1985).
16. J. Feinberg, Opt. Lett. **7**, 486 (1982).

FIGURE CAPTIONS

Fig. 1 Schematic of a self-pumped phase-conjugate fiber-optic gyro. Light from a laser is split by beamsplitter BS into two fibers F1 and F2 that are coiled such that light travels clockwise in F1 and counterclockwise in F2. Light traversing the fibers experiences phase shifts due to thermal, mechanical, and rotational effects. The self-pumped phase-conjugate mirror PCM produces time reversed waves that compensate for the reciprocal phase changes produced by thermal and mechanical effects, but do not compensate for the nonreciprocal phase shift produced by rotation (Sagnac effect). Therefore, rotation can be sensed by measuring the interference between the recombining waves at detector D.

Fig. 2. Experimental setup of the self-pumped phase-conjugate fiber-optic gyro. Instead of the two fibers shown in Fig. 1, the experimental setup shown here uses the two polarization modes of the polarization-preserving fiber-optic coil. Light from the laser is incident on polarizing beamsplitter PBS1 with its polarization at 45° to the plane of the page. The components reflected and transmitted by PBS1 travel clockwise and counterclockwise respectivly, in the fiber coil. The two beams recombine at PBS1 and are then split at PBS2. One of the beams has its polarization rotated by PR, and both beams are incident on a barium titanate crystal such that self-pumped phase conjugation occurs. The

reflected waves retraverse the fiber in an opposite sense, recombine at PBS1, and travel back toward the laser with a phase difference $\varnothing$, that is proportional to the rotation rate. These waves are sampled by the beamsplitter BS2 and an additional phase delay of $\pi/2$ radians is impressed on them when they propagate through the quarter-wave retarder $\lambda/4$. The half-wave retarder is oriented such that the intensities of the interferences measured by detectors D1 and D2 are proportional to sin $\varnothing$ and -sin $\varnothing$, respectively.

Fig. 3. Measurement of the Sagnac phase shift in the self-pumped phase-conjugate fiber-optic gyro. This figure shows a chart recording of the output of a differential amplifier connected to detectors D1 and D2 in the experimental set up of a self-pumped phase-conjugate fiber-optic gyro shown in Fig. 2. For $t<0$, the gyro was stationary. At $t=0$, the gyro was rotated first clockwise, then counterclockwise in a square-wave fashion for four cycles with an amplitude of approximately 6°/s. The experimentally measured phase shift is in good agreement with the predicted phase shift of 0.04 radians.

SC36018

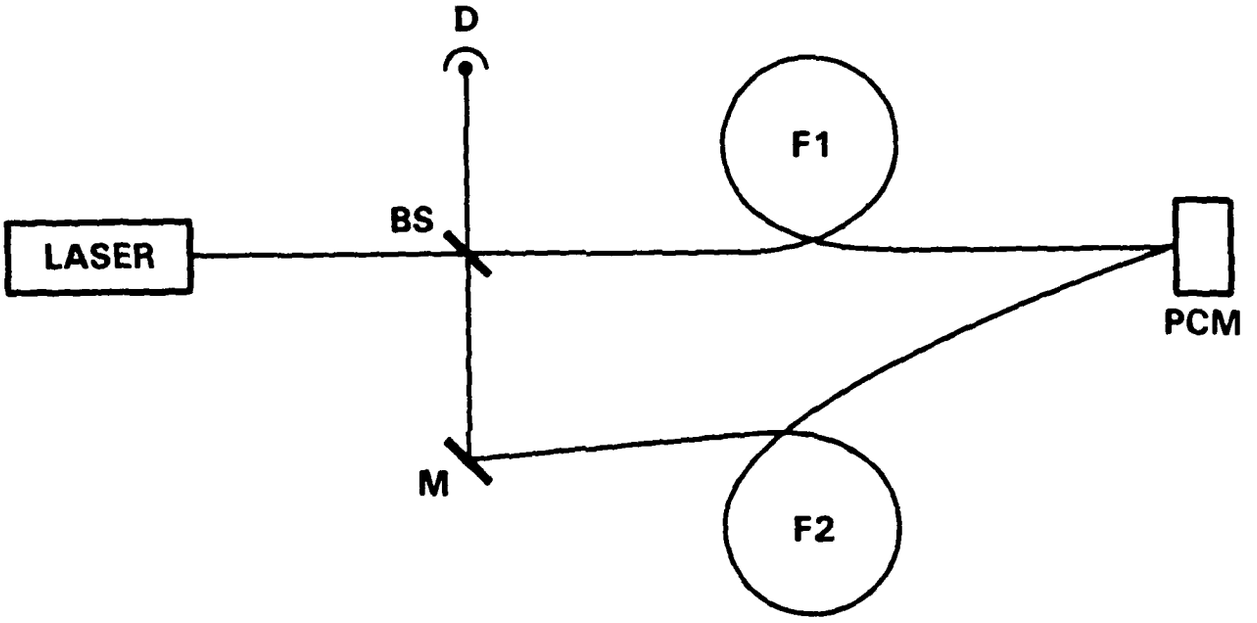

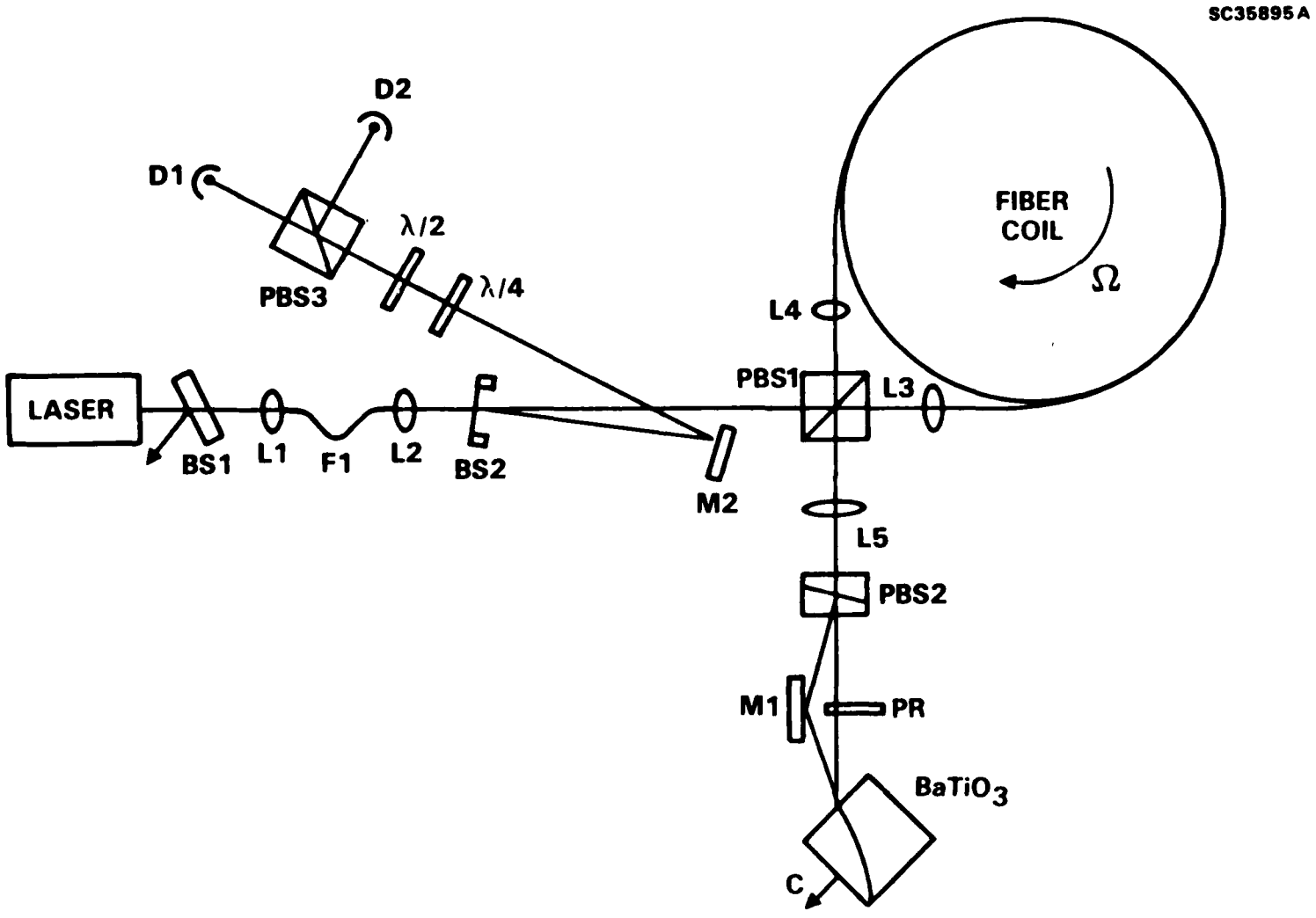
SC35895A
D2
D1
λ/2
PBS3
λ/4
FIBER
COIL
Ω
L4
LASER
PBS1
L3
BS1
L1
F1
L2
BS2
M2
L5
PBS2
M1
PR
BaTiO3
C

SC36017

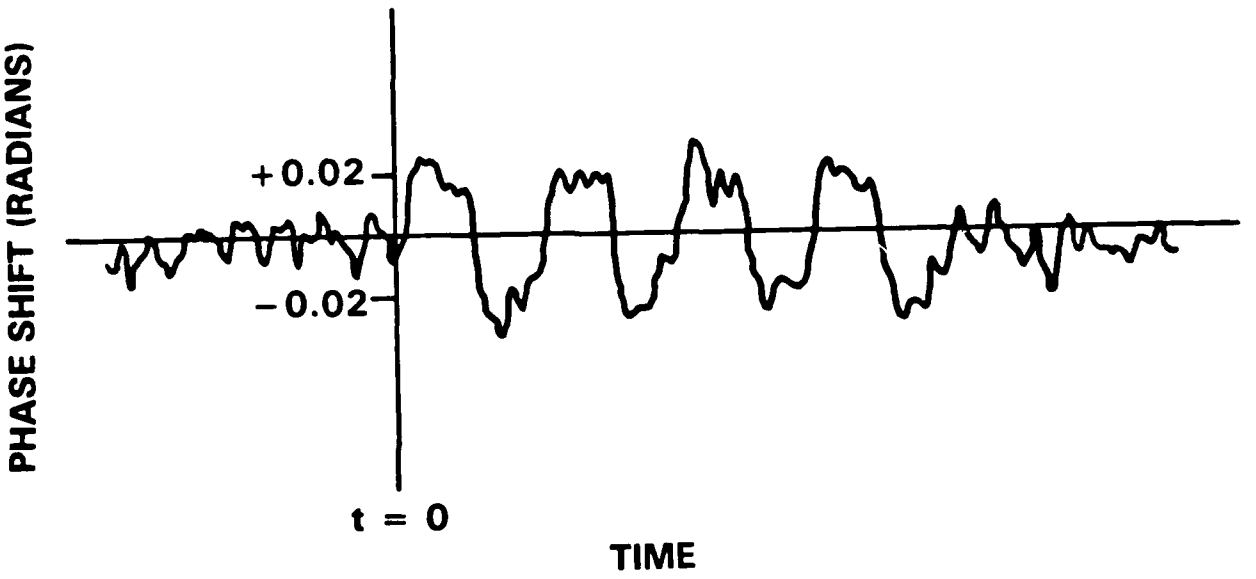

APPENDIX 5.2

Polarization-Preserving Phase Conjugator

(Paper to appear in Opt. Lett., August (1986))

SC5424.AR

POLARIZATION-PRESERVING PHASE CONJUGATOR

Ian McMichael, Monte Khoshnevisan and Pochi Yeh

Rockwell International Science Center
Thousand Oaks, CA 91360

ABSTRACT

Using a single self-pumped crystal of barium titanate, we demonstrate a method for producing the phase-conjugate of an incident wave having arbitrary polarization. Our experimental results show that the phase-conjugate wave produced by this method reproduces both the ellipticity and the helicity of the polarization of the incident wave.

Most demonstrations of the correction of wavefront distortions by phase conjugation use linearly polarized light and optically isotropic wavefront-distorting media. In some cases, however, one may also wish to correct for the changes in polarization induced by optically anisotropic media. For example, one may wish to correct for the polarization scrambling due to environmentally dependent birefringence that is a source of noise and signal fading in fiber-optic gyros.[1] Self-pumped phase conjugation is very efficient in barium titanate,[2] but only for extraordinary light since it utilizes the large electro-optic coefficients r_{42} and r_{51}. In this letter, we demonstrate a scheme for using a single self-pumped crystal of barium titanate to produce the phase-conjugate of a wave having aribitrary polarization.

In general, the reflectivity of a phase-conjugate mirror is described a 2 × 2 tensor that determines the amplitude, phase, and polarization state of the reflected light. Only when this tensor reduces to a scalar can a phase-conjugate mirror correct for both the wavefront distortions and the changes in polarization induced by optically anisotropic wavefront-distorting media.[3] We call a phase-conjugate mirror for which the reflectivity tensor reduces to a scalar, a polarization-preserving phase conjugator (PPPC). To show that a PPPC can correct for the change in polarization state introduced by optically anisotropic media, consider the situation of a plane wave with polarization state described by a vector amplitude A,

$$A = \begin{bmatrix} A_x \\ A_y \end{bmatrix} \tag{1}$$

that is incident on an optically anisotropic medium, followed by a phase-conjugate mirror. After passing through the anisotropic medium, the amplitude becomes

$$A' = TA, \qquad T = \begin{bmatrix} t_{xx} & t_{xy} \\ t_{yx} & t_{yy} \end{bmatrix} \tag{2}$$

where T is a Jones matrix[4] that describes transmission through the anisotropic medium, and where t_{xx}, t_{xy}, t_{yx} and t_{yy} are the tensor elements. After reflection from the phase-conjugate mirror, the amplitude becomes

$$A'' = R(TA)^*, \qquad R = \begin{bmatrix} r_{xx} & r_{xy} \\ r_{yx} & r_{yy} \end{bmatrix} \tag{3}$$

where R is a tensor that describes reflection from the phase-conjugate mirror, and where r_{xx}, r_{xy}, r_{yx} and r_{yy} are the tensor elements. After passing back through the anisotropic medium, the amplitude of the returning wave is given by

$$TRT^*A^*. \tag{4}$$

Since in general this is not proportional to the phase-conjugate of the amplitude of the incident wave, the returning wave does not have the same polarization as the incident wave. However, if the reflectivity tensor reduces to a scalar r, then the amplitude of the reflected wave becomes

$$rTT^*A^*, \quad \text{for } R = \begin{bmatrix} r & 0 \\ 0 & r \end{bmatrix} = r\,. \tag{5}$$

For optically anisotropic media, such as birefringent or optically active media, the Jones matrix has the property, $TT^* = 1$. In this case, the amplitude of the reflected wave becomes,

$$rA^*, \quad \text{for } R = r,\ TT^* = 1. \tag{6}$$

Since this is proportional to the phase-conjugate of the incident wave, the polarization of the reflected wave is identical to that of the incident wave. Thus, we have shown that a PPPC can correct for the change in polarization state introduced by optically anisotropic media. The PPPC cannot correct for the changes in polarization introduced by nonreciprocal phenomena such as the Faraday effect, where $TT^* \neq 1$.

Several methods have been proposed for polarization-preserving phase conjugation.[3,5,6] Polarization-preserving phase conjugators can be made using media that have a tensor reflectivity, by decomposing the incident wave into two components having orthogonal polarizations, phase-conjugating these components, and recombining the conjugates.[5] The result is a polarization-preserving phase conjugator only if the components recombine with the correct amplitude and phase. This is insured if the losses and the amplitudes and phases of the complex phase-conjugate reflectivities are the same for both components. A schematic of our polarization-preserving phase conjugator that uses this method is shown in Fig. 1. To understand how it works, consider an incident wave having a polarization described by a complex vector amplitude A = (a_1, a_2). This wave is decomposed into two orthogonally polarized components, $(a_1, 0)$ and $(0, a_2)$, by the polarizing beam splitter PBS. The component with polarization orthogonal to the plane of the figure $(0, a_2)$ has its polarization rotated by the half-wave retarder $\lambda/2$ such that its polarization state becomes $(a_2, 0)$. Both components are incident on a barium titanate crystal at an angle such that self-pumped phase conjugation occurs.[7] Since both components have the same polarization and are reflected from the same phase-conjugate mirror, they experience the same complex phase-conjugate reflectivity r, becoming $r(a_1^*, 0)$ and $r(a_2^*, 0)$. The half-wave retarder restores the second of these components to its original polarization, $r(0, a_2^*)$. When the two components recombine at the polarizing beam splitter, they form the phase-conjugate with the same polarization as the incident wave, $r(a_1^*, a_2^*) = rA^*$. Thus, the configuration shown in Fig. 1 acts like a polarization-preserving phase conjugator, and henceforth we refer to it as "the PPPC".

Using the self-pumped configuration in the PPPC results in a frequency shift between the components incident on the crystal and their conjugates.[8,9] However, since both components are incident on the same region of the crystal, they see the same pumping waves, and therefore they experience the same frequency shift and phase-conjugate reflectivity. In fact, the two beams can be thought of as two components of a single probe beam. In the experiment, the two beams are made to overlap by aligning mirror M4 while observing the scattered

light from the beams in the crystal. This procedure is sufficient to obtain the results presented here, and exact alignment is not required. The two beams interact by coherently pumping the oscillation of a resonator formed by internal reflections in the crystal.[10] The counterpropagating waves in the resonator then provide the pump waves for DFWM. Since the two beams entering the crystal see the same pump waves, they experience the same DFWM reflectivity. It should be noted that the two beams entering the crystal must be coherent to within the response time of the crystal. In the experiment, the path lengths from the polarizing beam splitter to the crystal were made equal to within the coherence length of the laser. The excellent frequency locking[11] of the conjugates when both beams are present is indicated by the fact that no beating is detected in the return from the PPPC.

Attention paid to experimental details results in improved operation of the PPPC. For example, the analysis above assumes that the polarizing beam splitter completely separates the two polarization components. Although many types of polarizing beam splitters do not do this, we now use a Rochon type that does. In our first experiments, we used a Glan-laser polarizing beam splitter that does not completely separate the two polarization components (some p polarization is reflected along with the s polarization). The p polarization that is reflected by the polarizing beam splitter is not reflected by the phase-conjugate mirror, and is lost. When the conjugated waves recombine at the polarizing beamsplitter, although the two polarization components have the correct phase relationship, they do not have the correct intensity ratio required to reproduce the polarization of the incident wave. This resulted in imperfect operation of the PPPC. For example, with a linear polarized input wave, the polarization of the reflected wave was rotated by as much as 8°. The analysis also assumes no losses in the system, or at least losses that are equal for both components. Among other things, this suggests that the half-wave retarder should be antireflection coated. Our half-wave plate has a total loss of less than 0.5%. Keeping the angle between the two components incident on the crystal small helps to insure that they experience the same complex phase-conjugate reflection coefficient. In our experiment this angle is $\sim 1°$. It should also be

noted that this experimental configuration is an interferometer. Phase changes occurring on a time scale faster than the response time of the crystal that are not common to both components alter the polarization of the reflected wave. Therefore, the setup should be compact and rigid.

To show that the PPPC reproduces the ellipticity of polarized light, we use the experimental setup shown in Fig. 2(a). A highly reflective beam splitter BS1 isolates the laser from any retroreflections of its output. The polarizer P1 insures that the light is linearly polarized in the plane of the figure. In all the experiments presented here, the power after P1 is ~ 1 mW at 514.5 nm. Either a half-wave retarder $\lambda/2$ or quarter-wave retarder $\lambda/4$ is used to alter the polarization state of the light. This light is then reflected from either a normal mirror M (multilayer dielectric high reflector), or the PPPC. The reflected light is sampled by the beam splitter BS2, and it is analyzed by the combination of polarizer P2 and detector D. Since BS2 is an uncoated pellicle beam splitter used near normal *incidence* (the angle of incidence is exaggerated in the figure; the actual angle of incidence is 2°), the reflection coefficients for the s and p polarizations are nearly equal and the polarization measured by P2 and D is nearly the same as that reflected by M.

Figure 2(b) shows the measured angle of polarization for the reflection from the polarization-preserving phase conjugator, PPPC, as a function of the measured angle of polarization for the reflection from the normal mirror M, for various orientations of the <u>half-wave</u> retarder. Zero degrees corresponds to polarization in the plane of the previous figures. The open circles are the data (with diameters corresponding to the uncertainty), and the solid line indicates what is expected in the case of an ideal polarization-preserving phase conjugator. The measured ellipticity of the polarization for the light reflected by the PPPC (defined as the ratio of the minor polarization axis to the major polarization axis) never exceeded 1%.

Figure 2(c) shows the measured polarization ellipse for the reflection from the polarization-preserving phase conjugator (dotted line), and the measured polarization ellipse for the reflection from the normal mirror (solid

line), for various orientations of the quarter-wave retarder. Zero degrees corresponds to orientation of the axis of the quarter-wave retarder in the plane of the previous figures. The ellipticity of the reflected light is measured by rotating polarizer P2, and noting the minimum and maximum intensities at detector D.

The results shown in Fig. 2 demonstrate that the reflection from the PPPC reproduces the ellipticity of the polarization of the incident wave. To show that it reproduces the helicity of the polarization of the incident wave, we use the setup shown in Fig. 3(a). A quarter-wave retarder $\lambda/4$ is placed between the sampling beam splitter and the mirror and is oriented such that the light incident on the mirror is converted from linearly polarized light to circularly polarized light. Figure 3(b) shows the measured polarization ellipses for the normal mirror and the polarization-preserving phase conjugator. Light reflected from the normal mirror changes helicity. After passing back through the quarter-wave retarder, the polarization of the reflected light is orthogonal to the incident light. This is the principle by which quarter-wave isolation works. On the other hand, light reflected by the polarization-preserving phase conjugator has the same helicity as the incident light and returns to its original polarization state after passing back through the quarter-wave retarder.

In order to quantify how well the technique works when there is an aberration in the beam, a multimode fiber is placed at the position of the quarter-wave retarder in Fig 2(a). The multimode fiber scrambles the polarization of the input wave. With a normal mirror at the end of the fiber, approximately 50% of the power returns in each of the two linear polarization states (parallel and orthogonal to the linear input polarization). With the polarization preserving phase conjugator at the end of the fiber, less than 1% of the light returns with the orthogonal polarization.

In conclusion, we have demonstrated a polarization-preserving phase conjugator that is capable of correcting for both the phase distortions and the changes in polarization induced by optically anisotropic phase distorting media. Potential applications of this device include the phase-conjugate fiber-optic gyro[12,13] and interferometry with multimode fibers.[14]

This work is partially supported by the Office of Naval Research.

REFERENCES

1. R. Ulrich and M. Johnson, Opt. Lett. 4, 152 (1979).

2. J. Feinberg and R.W. Hellwarth, Opt. Lett. 5, 519 (1980).

3. P. Yeh, Opt. Comm. 51, 195 (1984).

4. See, for example, A. Yariv and P. Yeh, "Optical Waves in Crystals," (Wiley, New York, 1984).

5. N.G. Basov, V.F. Efimkov, I.G. Zuberev, A.V. Kotov, S.I. Mikhailov, and M.G. Smirnov, JETP Lett. 4, 197 (1978).

6. G. Martin, L.K. Lam, and R.W. Hellwarth, Opt. Lett. 5, 185 (1980).

7. J. Feinberg, Opt. Lett. 7, 486 (1982).

8. W.B. Whitten and J.M. Ramsey, Opt. Lett. 9, 44 (1984).

9. J. Feinberg and G.D. Bacher, Opt. Lett 9, 420 (1984).

10. M. Ewbank and P. Yeh, SPIE Proceedings 613, XXX (1986).

11. M.D. Ewbank, P. Yeh, M. Khoshnevisan, and J. Feinberg, Opt. Lett. 10, 282 (1985).

12. C.J. Borde, NATO Advanced Study Institute in Quantum Optics, "Experimental Gravitation and Measurement Theory," P. Meystre and M.O. Scully, eds. (Plenum Press, 1983).

13. P. Yeh, I. McMichael, and M. Khoshnevisan, Appl. Opt. 25, XXX, April 1, 1986.

14. B. Fischer and S. Sternkler, Appl. Phys. Lett. 46, 113 (1985).

FIGURE CAPTIONS

Fig. 1 Polarization-preserving phase conjugator "PPPC". Light incident on the polarizing beam splitter PBS is decomposed into two orthogonally polarized components. One component is rotated 90° by the half-wave retarder $\lambda/2$. Both components are incident on a barium titanate crystal such that self-pumped phase conjugation occurs. When the two conjugates recombine at PBS, they form a conjugate wave that reproduces the polarization of the incident light.

Fig. 2 Reproduction of the ellipticity of polarized light by the PPPC. (a) Experimental setup. A half- or quarter-wave retarder alters the polarization state of light incident on a normal mirror M or the PPPC. (b) Measured angle of polarization for the reflection from the PPPC vs that from M. (c) Measured polarization ellipse for the reflection from the PPPC (dotted line) compared with that from M (solid line).

Fig. 3 Reproduction of the helicity of polarized light by the PPPC. (a) Experimental setup. The quarter-wave retarder $\lambda/4$ is oriented such that the light incident on M, or the PPPC is converted from linearly polarized light to circularly polarized light. (b) Measured polarization ellipses for the reflections from M and the PPPC after retraversing $\lambda/4$.

SC85-31387

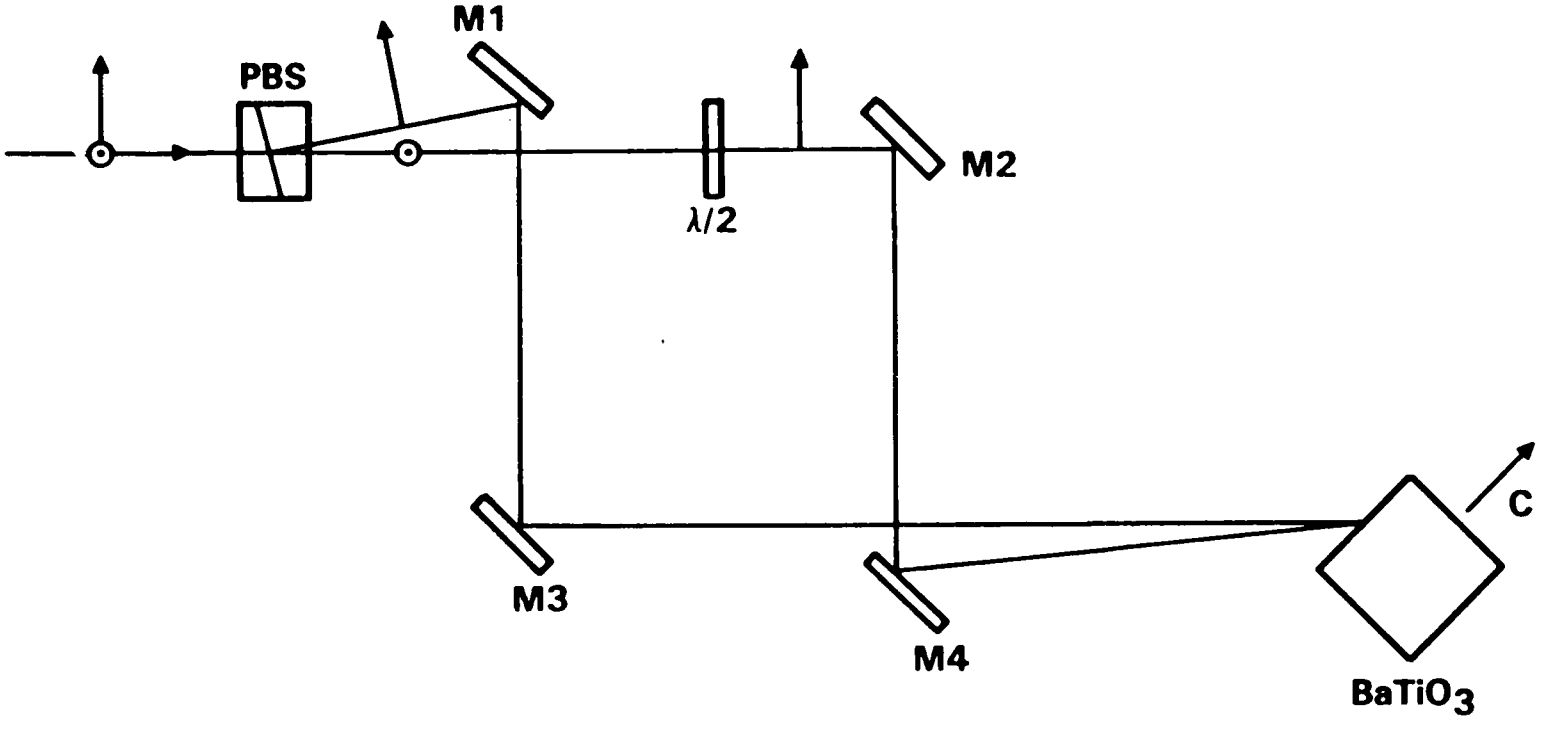

SC85-31390

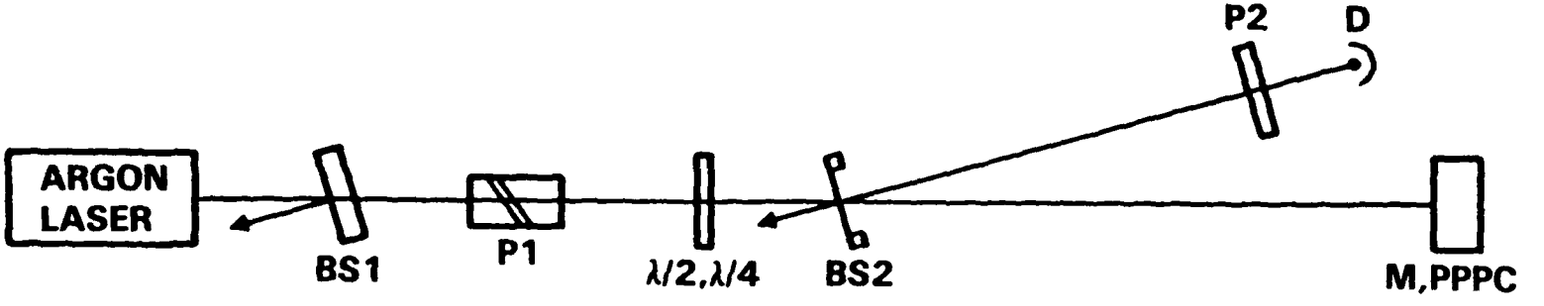

SC85-31389

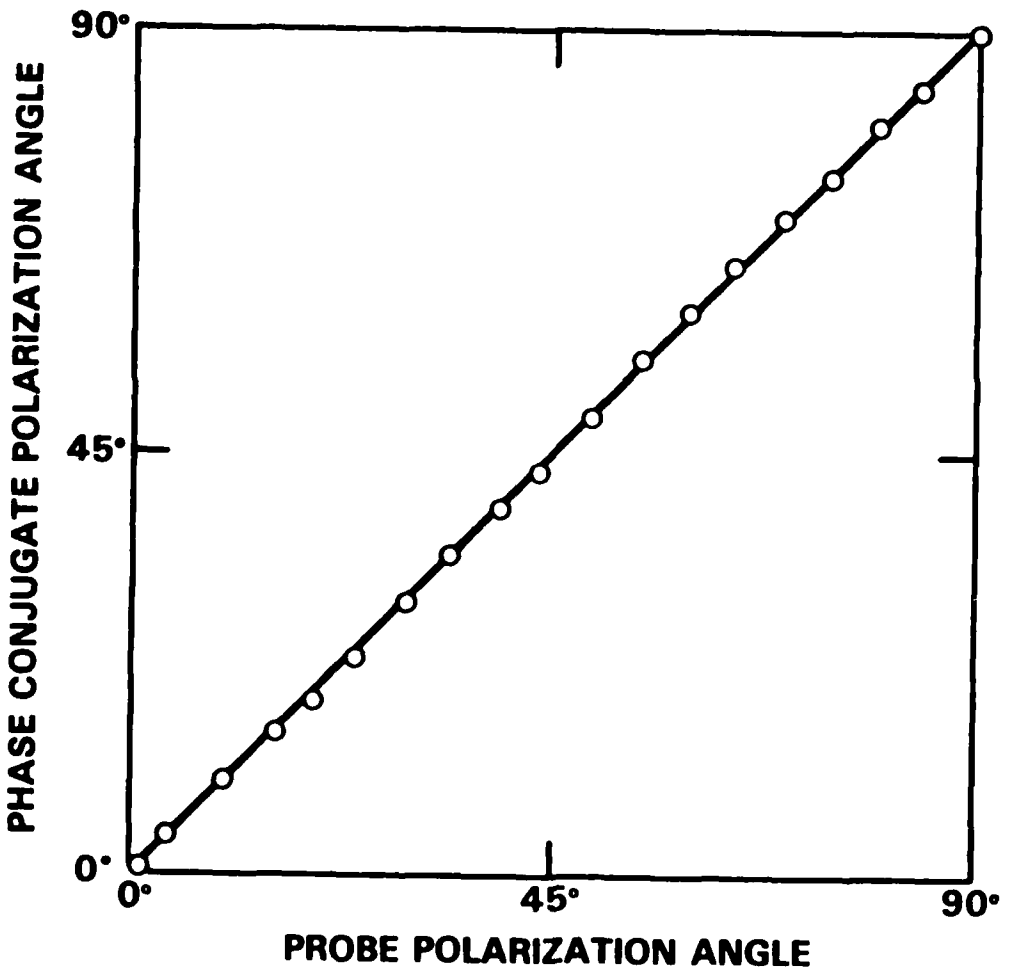
90°
45°
0°
0°
45°
90°
PHASE CONJUGATE POLARIZATION ANGLE
PROBE POLARIZATION ANGLE

SC85-31392

0°

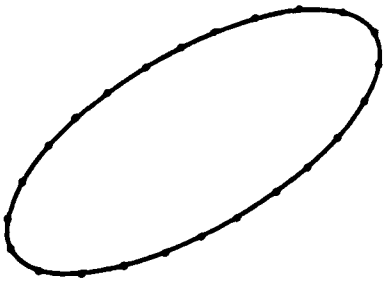

−34°

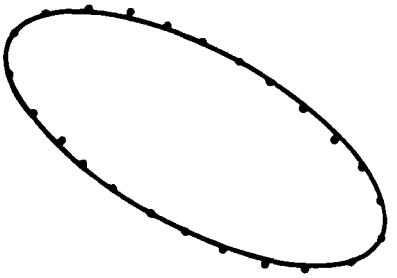

+34°

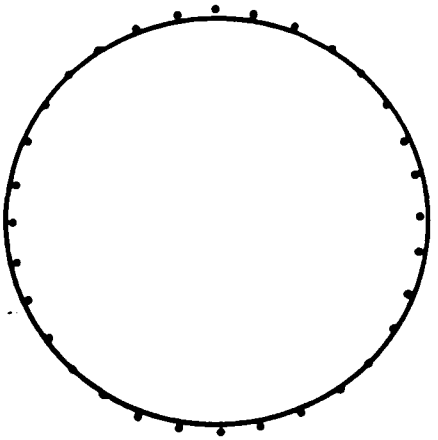

−45°

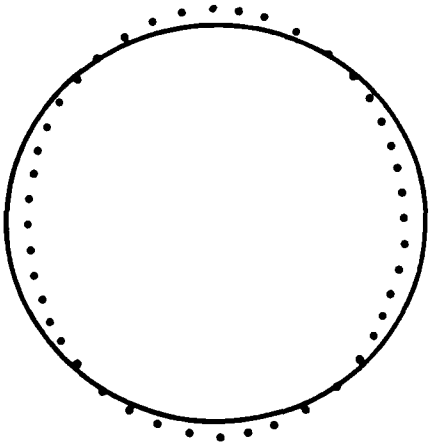

+45°

SC85-31388

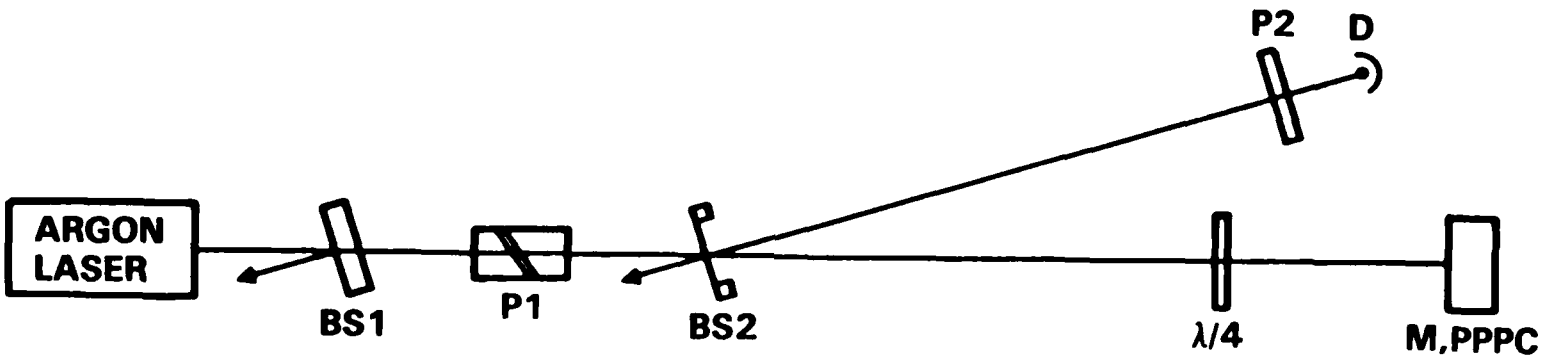

SC85-31391

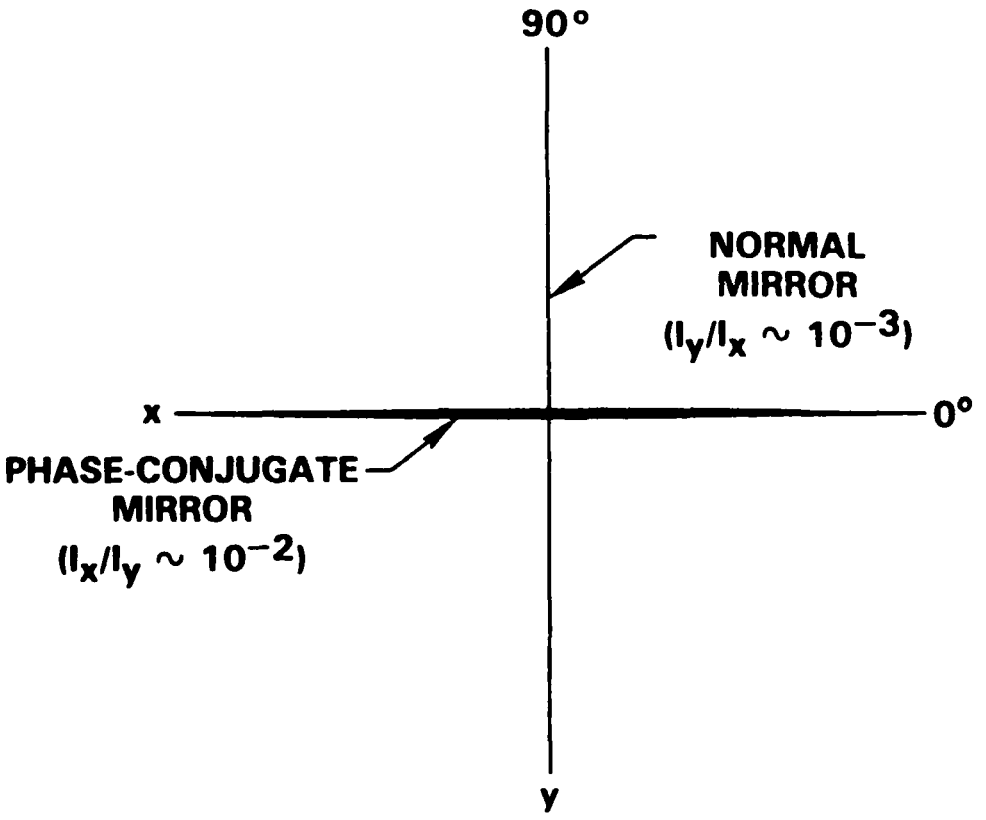

POLARIZATION AFTER
DOUBLE PASS THROUGH
QUARTER-WAVE RETARDER

APPENDIX 5.3

Absolute Phase Shift of Phase Conjugators

(Paper to appear in Proc. SPIE 613 (1986))

SC5424.AR

Absolute Phase Shift of Phase Conjugators

Ian McMichael, Pochi Yeh and Monte Khoshnevisan

Rockwell International Science Center
1049 Camino Dos Rios, Thousand Oaks, CA 91360

Abstract

We present theoretical expressions and experimental measurements of the absolute phase shifts of phase conjugators. Photorefractive media, transparent media, saturable absorbers and saturable amplifiers are considered in the analysis. Experimental measurements of the absolute phase shifts are presented for barium titanate, strontium barium niobate and ruby.

Introduction

Although the reflectivity of phase conjugators has been of significant interest recently, the phase of the phase-conjugate wave has received little attention. This phase determines the operating point of some phase-conjugate interferometers. If this phase can be controlled, the interferometers can be biased at the operating point of highest sensitivity and linear response (quadrature). With this motivation, we have studied the absolute phase of phase conjugators theoretically and experimentally.

Theory

We consider the usual case of degenerate four-wave mixing of two counterpropagating pump waves having amplitudes A_1 and A_2 with a probe wave having amplitude A_4 propagating in the +z direction and a phase-conjugate wave A_3 propagating in the -z direction. Let the phase of the phase-conjugate reflection ϕ_3, where $A_n = |A_n|e^{i\Phi_n}$, be written as,

$$\phi_3 = \phi_0 + \phi_1 + \phi_2 - \phi_4 \quad (1)$$

We then refer to ϕ_0 as the absolute phase shift of the phase conjugator. The phase shift ϕ_0 can be obtained from the solution of the coupled-wave equations describing the degenerate four-wave mixing. In general, ϕ_0 depends on the type of grating (index, absorption, or gain) involved in the degenerate four-wave mixing, the phase shift of this grating with respect to the light intensity pattern that produces the grating, and the intensities of the interacting waves.

For a photorefractive medium, the complex amplitude of the phase-conjugate wave at the input to the medium (z = 0) is given by,[1]

$$A_3(0) = A_4^*(0)(A_1/A_2^*)(e^{-\gamma L} - 1)/(r^{-1}e^{-\gamma L} + 1) \quad (2)$$

where L is the length of the medium, r is the pump-beam intensity ratio,

$$r = |A_2/A_1|^2 \quad (3)$$

and γ is the complex coupling constant that depends on the physical process involved in the generation of the hologram. If ones makes the usual assumption that the phase grating in photorefractive media is shifted by $\pi/2$ radians with respect to the intensity pattern, then γ is real and the phase shift of a photorefractive phase conjugator is

$$\phi_0 = 0 \text{ for } \gamma < 0$$

$$= \pi \text{ for } \gamma > 0 \quad (4)$$

For degenerate four-wave mixing in a transparent medium with a local response (no phase shift of the index grating with respect to the intensity pattern), the amplitude of the phase-conjugate wave at the input of the medium is given by,[2]

$$A_3(0) = -iA_4^*(0)(|\kappa^*|/\kappa) \tan |\kappa|L \tag{5}$$

where κ is the complex coupling constant,

$$\kappa^* = (2\pi\omega/cn)\chi A_1 A_2 \tag{6}$$

From Equations (5) and (6), we obtain the phase of the phase conjugator for a transparent medium with a local response,

$$\begin{aligned}\phi_0 &= -\pi/2 \text{ for } \chi > 0 \\ &= +\pi/2 \text{ for } \chi < 0\end{aligned} \tag{7}$$

Finally, for degenerate four-wave mixing in a saturable absorber or amplifier with a local response, the amplitude of the phase-conjugate wave at the input of the medium is given by,[3]

$$A_3(0) = -iK^*A_4^*(0)\ [\sin wL/(w \cos wL + \alpha_R \sin wL)] \tag{8}$$

$$K^* = i\alpha_0[(1-i\delta)/(1 + \delta^2)]\ (2A_1A_2/I_S)/(1 + 4I/I_S)^{3/2} \tag{9}$$

$$\alpha = \alpha_0[(1 - i\delta)/(1 + \delta^2)]\ (1 + 2I/I_S)/(1 + 4I/I_S)^{3/2} = \alpha_R - i\alpha_I \tag{10}$$

$$w = (|K|^2 - \alpha_R^2)^{1/2} \tag{11}$$

α_0 is the line-center small-signal field attenuation or gain coefficient, I_S is the saturation intensity for the detuning from line center δ, and I is the intensity of the pump waves ($I_1 = I_2 = I$). If the frequency of the interacting waves is on resonance with the atomic transition of the medium, then $\delta = 0$ and w is imaginary. From Equation (8), we obtain the phase of the phase conjugator for degenerate four-wave mixing on resonance with a saturable absorber or gain medium,

$$\phi_0 = 0 \text{ for } \alpha_0 > 0$$

$$= \pi \text{ for } \alpha_0 < 0 \qquad (12)$$

Experiment

To measure the phase of the phase-conjugate reflection ϕ_0, we use the experimental setup shown in Figure 1. Light from a laser is split by beamsplitter BS into two arms of an interferometer. In the reference arm of the interferometer, the light transmitted by BS passes through a photorefractive crystal XTL, and is retroreflected by mirror M1. This provides the counterpropagating pump waves for degenerate four-wave mixing in the crystal. In the signal arm of the interferometer, the light reflected by BS is then reflected by mirror M2 to provide the probe beam for degenerate four-wave mixing. The intensity measured by detector D is given by

$$I = I_1 + I_2 - 2\sqrt{I_1 I_2} \cos \phi_0 \qquad (13)$$

where I_1 and I_2 are the intensities of the combining waves. This equation indicates that the operating point of this interferometer is completely determined by the absolute phase of the phase conjugator ϕ_0, and is independent of phases of the pumping and probe waves.

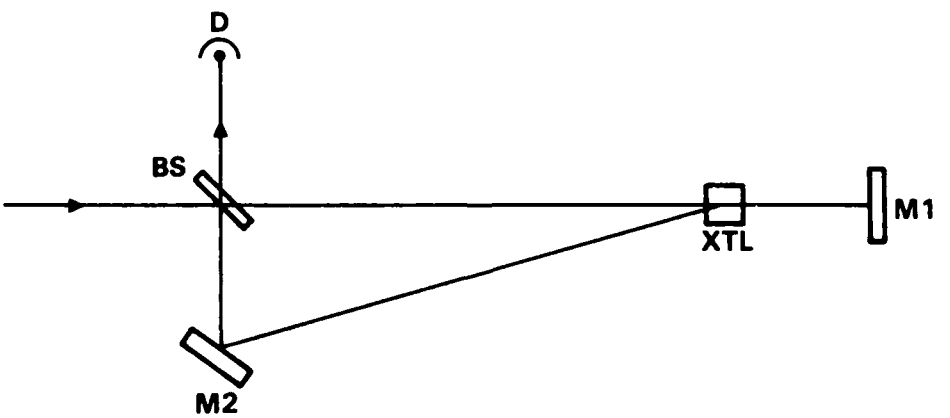

Fig. 1 Experimental setup used to measure the absolute phase of phase conjugators.

To derive Equation (13), we consider a light wave of unit amplitude that is incident on the beamsplitter BS. The amplitudes of the transmitted and externally reflected waves are then t and r, respectively. The amplitudes of the pumping waves at the crystal are $te^{i\Phi 1}$ and $te^{i\Phi 2}$, and the amplitude of the probe wave is $re^{i\Phi 4}$, where the phase factors Φ describe the accumulated phase for propagation from the beamsplitter to the nonlinear medium. These three waves interact in the nonlinear medium to produce a phase-conjugate wave with an amplitude A_3,

$$A_3 = \rho t^2 r^* e^{i(\phi_0 + \Phi_1 + \Phi_2 - \Phi_4)} \tag{14}$$

where ρ is a real constant describing the reflectivity of the phase conjugator. When this wave returns to the beamsplitter, it combines with the wave retroreflected by mirror M1 to produce an intensity I at the detector D given by

$$I = \left|\rho t^2 r^* e^{i(\phi_0 + \Phi_1 + \Phi_2)} + tr' e^{i(\Phi_1 + \Phi_2)}\right|^2 \tag{15}$$

where r' is the amplitude reflection coefficient for internal reflection from the beamsplitter. Using the Stoke's relation $tr^* = -t^*r'$, we can obtain Equation (13) from Equation (15).

In principle, ϕ_0 can be determined from a measurement of the intensities. However, in practice, the uncertainties in measuring the intensities do not allow for an accurate determination of ϕ_0. A more accurate determination can be made by modulating the phase of the cosine term at a frequency ω and measuring the ration R of the fundamental power to the second harmonic power at the detector. In the experiment, a piezoelectric transducer is attached to the mirror M_2 to produce a phase modulation $\phi_m \sin \omega t$. The phase modulation is faster than the response time of the nonlinear medium in which the degenerate four-wave mixing takes place so that it is not compensated by phase conjugation. The amplitude of the phase modulation is small ($\phi_m << \pi$) so that the gratings involved in the degenerate four-wave mixing are not washed out. The time varying intensity at the detector D is proportional to,

$$-\cos(\phi_0 + \phi_m \sin \omega t) \tag{16}$$

From this equation, we obtain the ratio R of the fundamental power to the second harmonic power

$$R = [J_1(\phi_m)/J_2(\phi_m)]\tan\phi_0 \tag{17}$$

where J_1 and J_2 are Bessel functions. For $\phi_m << \pi$, the absolute phase shift of the phase-conjugate reflection is given by

$$\phi_0 \approx \tan^{-1} (R\phi_m/4) \tag{18}$$

Results

Using the technique described above, we have measured the phase shift of the phase-conjugate reflections from barium titanate, strontium barium niobate and ruby. Our results are given in Table 1, where θ is the angle between the grating k vector and the crystal axis.

Table 1

Phase of Phase-Conjugate Reflections

Material	θ	ϕ_0
$BaTiO_3$	0°	(19 ± 3)°
	45°	(6 ± 4)°
	135°	(176 ± 3)°
	180°	(164 ± 3)°
SBN	0°	(3 ± 3)°
	180°	(175 ± 5)°
Ruby	-	(80 ± 5)°

For the photorefractive materials $BaTiO_3$ and SBN, the measured values of ϕ_0 compare well with the expected values from Equation (4). The differences between the expected values $\phi_0 = 0°$ and 180°, and the measured values $\phi_0 = (19 \pm 3)°$ and $(164 \pm 3)°$ for $BaTiO_3$ at $\theta = 0°$ and 180° indicate that the index grating is not shifted by exactly $\pi/2$ radians, as is often assumed. We have verified this fact by an independent measurement of the two-wave mixing gain Γ as a function of the frequency detuning between the two waves. The fact that for ruby, ϕ_0 is close to 90°, indicates that the grating involved is predominantly an index grating rather than an absorption grating.

Summary

We have presented theoretical expressions and experimental measurements of the absolute phase shifts of phase conjugators. Photorefractive media, transparent media, saturable absorbers and saturable amplifiers were considered in the analysis. Experimental measurements of the absolute phase shifts for barium titanate, strontium barium niobate and ruby are in good agreement with the theory.

Acknowledgements

This work is supported by the Office of Naval Research.

References

1. Fisher, B., Cronin-Golomb, M., White, J., and Yariv, A., "Amplified Reflection, Transmission, and Self-oscillation in Real-time Holography," Opt. Lett., Vol. 6, pp. 519-521, 1981.

2. Yariv, A. and Pepper, D, "Amplified Reflection, Phase Conjugation, and Oscillation in Degenerate Four-Wave Mixing," Opt. Lett., Vol. 1, pp. 16-18, 1977.

3. Abrams, R. and Lind, R., "Degenerate Four-Wave Mixing in an Absorbing Media," Opt. Lett., Vol. 2, pp. 94-96. 1978; "Errata," Opt. Lett., Vol. 3, p 205, 1978.

APPENDIX 5.4

Phase-Conjugate Fiber-Optic Gyro

(Paper appeared in Appl. Opt. 25, 1029 (1986))

Reprinted from Applied Optics, Vol. 25, Page 1029, April 1, 1986

Phase-conjugate fiber-optic gyro

Pochi Yeh, Ian McMichael, and Monte Khoshnevisan

Rockwell International Science Center, 1049 Camino Dos Rios, Thousand Oaks, California 91360.
Received 23 December 1985.
0003-6935/86/071029-02$02.00/0.

Several types of phase-conjugate gyro are proposed in the literature.[1-4] In this Letter, we describe a new type of fiber-optic gyro that uses the phase-reversal property of polarization-preserving phase conjugation. Although the insensitivity of phase-conjugate gyros to reciprocal phase shifts and their sensitivity to nonreciprocal phase shifts such as the Faraday effect have been reported,[3,4] to date no one has demonstrated rotation sensing. In this Letter, we report the first demonstration of rotation sensing with a phase-conjugate gyro.

Polarization scrambling is a well-known source of signal fading and noise in fiber-optic gyros. Polarization-preserving fibers and couplers must be used to decouple the two states of polarization and hence improve the sensitivity.[5] In the phase-conjugate fiber-optic gyro, a polarization-preserving phase conjugator is used to restore the severely scrambled waves to their original state of polarization.[6-8] This eliminates the signal fading and noise due to polarization scrambling without the need for polarization-preserving fiber.

Referring to Fig. 1, we consider a phase-conjugate Michelson interferometer[9] in which a fiber loop is inserted in the arm that contains the phase-conjugate reflector ϕ^*. We now examine the phase shift of light as it propagates along the fiber. From point A to point B, the light experiences a phase shift of

$$\phi_1 = kL - \frac{2\pi RL\Omega}{\lambda c}, \tag{1}$$

where $k = (2\pi n)/\lambda$ is the wave number and L is the length of fiber, R is the radius of the fiber coil, Ω is the rotation rate, λ is the wavelength, and c is the velocity of light. The second term in Eq. (1) is due to rotation. In the return trip, the phase shift is

$$\phi_2 = kL + \frac{2\pi RL\Omega}{\lambda c}, \tag{2}$$

where we notice that the term due to rotation is reversed because of the change in propagation direction relative to the rotation. If there were no phase conjugation, the total round-trip phase shift due to regular mirror reflection would be $2kL$. However, because of the phase reversal on phase-conjugate reflection, the round-trip phase shift becomes

$$\phi = \frac{4\pi RL\Omega}{\lambda c}. \tag{3}$$

This phase shift can be measured by using the interference with the reference beam from the other arm. Notice that as a result of the phase reversal on reflection, the reciprocal phase shift kL is canceled on completion of a round trip. The net phase shift left is due to anything nonreciprocal such as rotation.

This net phase shift is proportional to the rotation rate and can be used for rotation sensing. In addition, if the phase-conjugate reflector is polarization-preserving,[6-8] it will produce a true time-reversed version of the incident wave and will undo all the reciprocal changes (e.g., polarization scrambling, modal aberration, temperature fluctuation) when the light completes the round trip in the fiber. Since the polarization scrambling and modal aberration of multimode fibers can be corrected by polarization-preserving phase conjugation, multimode fibers can replace the polarization-preserving single-mode fiber in this new type of gyro.

Figure 2 shows a schematic diagram of the experimental setup used to demonstrate the phase-conjugate fiber-optic gyro. Since this experiment does not use a polarization-preserving phase-conjugate mirror, it does not demonstrate the correction of polarization scrambling. However, the experiment does measure the phase shift described by Eq. (3). A highly reflective beam splitter $BS1$ isolates the argon laser from retroreflections of its output. The light reflected by $BS2$ is focused by lens $L1$ (60-cm focal length) into a crystal of barium titanate to provide the pumping waves for degenerate four-wave mixing (DFWM). The light transmitted by $BS2$ is split into two arms of a Michelson interferometer by $BS5$. One arm of the interferometer contains a 10-cm radius coil of ~7 m of optical fiber. Since the phase-conjugate mirror in this experiment is not polarization-preserving, we use single-mode polarization-preserving optical fiber. Light exiting the fiber provides the probe wave for DFWM. The c-axis of the barium titanate crystal is parallel to the long faces of the crystal and points in the direction of beam splitter $BS3$. The pumping waves from mirrors $M2$ and $M3$ have powers of 18 and 3 mW, respectively, and their angle of incidence is ~45°. The probe wave, exiting from the end of the fiber loop, makes a small angle (<10°) with the pumping wave from mirror $M2$ and has a power of 0.7 mW. Under these conditions we obtain a phase-conjugate reflectivity of 50% and a response time of 0.1 s. The reference arm of the interferometer is terminated by a mirror $M4$ mounted on a piezoelectric transducer so that the operating point of the interferometer can be set at quadrature. Light from both arms combines to form complementary fringe patterns at detectors $D3$ and $D4$. Detectors $D1$ and $D2$ measure the powers in the recombining waves.

The fiber coil is rotated with the rest of the setup remaining fixed at various rotation rates [first clockwise (CW), then

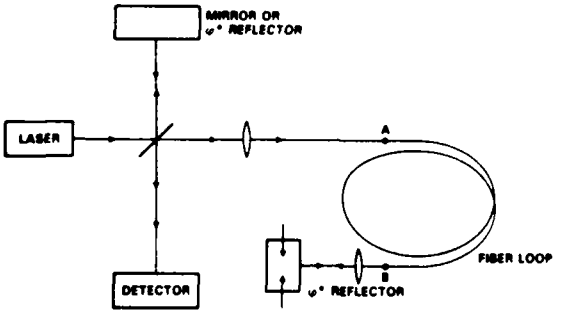

Fig. 1. Schematic drawing of the phase-conjugate fiber-optic gyro.

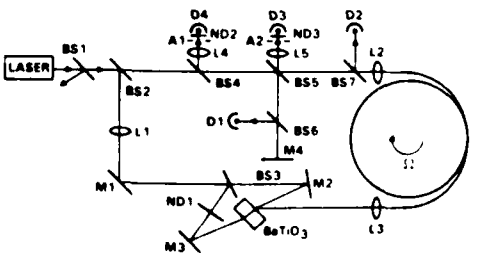

Fig. 2. Experimental setup of the phase-conjugate fiber-optic gyro.

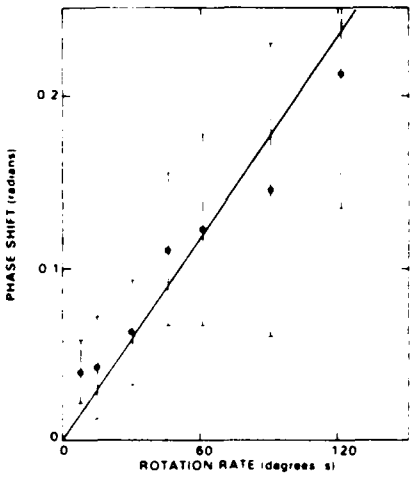

Fig. 3. Measured phase shift as a function of applied rotation rate.

counterclockwise (CCW), etc.] in a square wave fashion for 10 cycles with an amplitude of 120°. The measured powers from all detectors are used to calculate the average phase shift between rotation in the CW and CCW directions of rotation. Figure 3 shows a plot of the measured phase shift as a function of the rotation rate. The solid line indicates the expected rotation-induced Sagnac phase shift. The large uncertainty in the data is due to rapid (faster than the response time of the DFWM) phase changes that are produced by the twisting of the fiber when the fiber loop is rotated and that act as a source of noise.

In conclusion, we have proposed a new type of fiber-optic gyro that uses polarization-preserving optical phase conjugation, and we have presented the first demonstration of rotation sensing by a phase-conjugate gyro.

This research is partially supported by the Office of Naval Research.

References

1. J.-C. Diels and I. C. McMichael, "Influence of Wave-Front-Conjugated Coupling on the Operation of a Laser Gyro," Opt. Lett. **6**, 219 (1981).
2. P. Yeh, J. Tracy, and M. Khoshnevisan, "Phase-Conjugate Ring Gyroscopes," Proc. Soc. Photo-Opt. Instrum. Eng. **412**, 240 (1983).
3. C. J. Bode, "Phase Conjugate Optics and Applications to Interferometry and to Laser Gyroscope," in *Experimental Gravitation and Measurement Theory*, P. Meystre and M. O. Scully, Eds (Plenum, New York, 1983), pp. 269–291.
4. B. Fischer and Shmuel Sternklar, "New Optical Gyroscope Based on the Ring Passive Phase Conjugator," Appl. Phys. Lett. **47**, 1 (1985).
5. W. K. Burns, R. P. Moeller, C. A. Villarruel, and M. Abebe, "Fiber Optic Gyroscopes with Polarization Holding Fiber," Opt. Lett. **8**, 540 (1983).
6. P. Yeh, "Scalar Phase Conjugation for Polarization Correction," Opt. Commun. **51**, 195 (1984).
7. I. McMichael and M. Khoshnevisan, "Scalar Phase Conjugation Using a Barium Titanate Crystal," in *Technical Digest, Conference on Lasers and Electro-Optics* (Optical Society of America, Washington, D.C., 1985), paper THN1.
8. I. McMichael, M. Khoshnevisan, and P. Yeh, "Polarization-Preserving Phase Conjugator," submitted to Opt. Lett.
9. M. D. Ewbank, M. Khoshnevisan, and P. Yeh, "Phase-Conjugate Interferometry," Proc. Soc. Photo-Opt. Instrum. Eng. **464**, 2 (1984).

APPENDIX 5.5

Theory of Unidirectional Photorefractive Ring Oscillators

Reprinted from Journal of the Optical Society of America B, Vol. 2, page 1924, December 1985

Theory of unidirectional photorefractive ring oscillators

Pochi Yeh

Rockwell International Science Center, Thousand Oaks, California 91360

Received March 11, 1985; accepted July 11, 1985

Amplification owing to holographic two-wave mixing in photorefractive crystals can be utilized to achieve unidirectional ring oscillation. Unlike for the conventional gain medium (e.g., He–Ne), the gain bandwidth of photorefractive two-wave coupling is very narrow (a few hertz for $BaTiO_3$). Despite this fact, the ring resonator can still oscillate over a large range of cavity detuning. A theory is presented that describes how the oscillating mode attains the round-trip phase condition.

INTRODUCTION

The photorefractive effect in electro-optic crystals (e.g., $BaTiO_3$, $LiNbO_3$) has been widely studied for many applications. These include real-time holography, optical data storage, and phase-conjugate wave-front generation. Recently, increasing attention has been focused on using coherent signal beam amplification in two-wave mixing. These new applications include image amplification,[1] vibrational analysis,[2] nonreciprocal transmission,[3,4] and laser-gyro biasing.[5] The coherent signal beam amplification in two-wave mixing can also be used to provide parametric gain for unidirectional oscillation in ring resonators. Although such an oscillation has been observed by using a $BaTiO_3$ crystal in a ring resonator,[6] a general theory is not available. The present state of the theory does not address such problems as the round-trip phase condition or even oscillation frequency.

In this paper we describe a theory of parametric ring oscillation using holographic two-wave mixing in photorefractive crystals. The theory shows that oscillation can occur at almost any cavity length despite the narrow-band nature of the coherent two-wave coupling gain, provided that the coupling is strong enough. A similar situation also occurs in phase-conjugate parametric oscillators.[7] The theory also provides explicit expressions for the oscillation frequency, intensity, and threshold conditions.

FORMULATION OF THE PROBLEM

Referring to Fig. 1, we consider an optical ring resonator consisting of three partially reflecting mirrors. A photorefractive medium, which is pumped by an external laser beam, is inserted into the cavity. To investigate the properties of such oscillators, we must first treat the problem of two-wave coupling in photorefractive media. This problem has been formulated and solved by many workers.[8–10] However, most work has been focused on the degenerate two-wave mixing. For the purpose of developing our theory, we need to address nearly degenerate two-wave mixing.

Let us focus our attention on the region occupied by the photorefractive crystal, so that the electric field of the two waves can be written as

$$E_j = A_j(z)\exp[i(\mathbf{k}_j \cdot \mathbf{r} - \omega_j t)] + \text{c.c.}, \quad j = 1, 2, \tag{1}$$

where z is measured along the bisector of the two beams, $\mathbf{k}_1$ and $\mathbf{k}_2$ are the wave vectors of the beams, and c.c. denotes a term that is the complex conjugate to the first term. In Eq. (1), we assume for simplicity that both waves have the same state of polarization and the photorefractive medium does not exhibit optical rotation. A_1 and A_2 are the wave amplitudes and are taken as functions of z only for steady-state situations.

In the photorefractive medium (from zero to $z = l$), these two waves generate an interference pattern (traveling if $\omega_1 \neq \omega_2$). This pattern may generate and redistribute photocarriers. As a result, a spatial charge field (also traveling if $\omega_1 \neq \omega_2$) is created in the medium. This field induces a volume index grating by means of the Pockels effect. In general, the index grating will have a finite spatial phase shift relative to the interference pattern,[9] so that, following the notation of Ref. 11, we can write the fundamental component of the intensity-induced grating as

$$n = n_0 + \frac{n_1}{2}\left\{e^{i\phi}\frac{A_1 A_2^*}{I_0}\exp[i(\mathbf{K}\cdot\mathbf{r} - \Omega t)] + \text{c.c.}\right\}, \tag{2}$$

where

$$I_0 = I_1 + I_2 \equiv |A_1|^2 + |A_2|^2. \tag{3}$$

ϕ is real and n_1 is a real and positive number, $\mathbf{K} = \mathbf{k}_1 - \mathbf{k}_2$, and $\Omega = \omega_1 - \omega_2$. Here again, for the sake of simplicity, we assume a scalar grating. The phase ϕ indicates the degree to which the index grating is shifted spatially with respect to the light interference pattern. According to Ref. 1, ϕ and n_1 can be written, respectively, as

$$\phi = \phi_0 + \tan^{-1}(\Omega\tau) \tag{4}$$

and

$$n_1 = \frac{2}{(1 + \Omega^2\tau^2)^{1/2}}\Delta n_s, \tag{5}$$

where τ is the decay time constant of the holograph grating, Δn_s is the saturation value of the photoinduced index change, and ϕ_0 is a constant phase shift related to the nonlocal response of the crystal under fringe illumination. Both parameters Δn_s and ϕ_0 depend on the grating spacing ($2\pi/K$) and its direction as well as on the material properties of the crystal, e.g., the electro-optic coefficients. Expressions for

0740-3224/85/121924-05$02.00

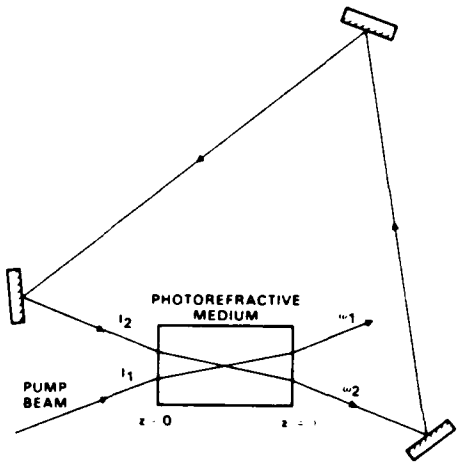

Fig. 1. Schematic drawing of a unidirectional photorefractive ring resonator.

Δn, and ϕ_0 can be found in Refs. 10 and 12. In photorefractive media, e.g., $BaTiO_3$, that operate by diffusion only (i.e., no external static field) the magnitude of ϕ_0 is $\pi/2$, with its sign depending on the direction of the c axis.

Now, by using expression (2) for n and the scalar-wave equation and by using the parabolic approximation (i.e., slowly varying amplitudes), we can derive the following coupled equations:

$$\frac{d}{dz} A_1 = i \frac{\pi n_1}{\lambda I_0 \cos\theta} e^{i\phi} |A_2|^2 A_1 - \frac{\alpha}{2} A_1,$$

$$\frac{d}{dz} A_2 = i \frac{\pi n_1}{\lambda I_0 \cos\theta} e^{-i\phi} |A_1|^2 A_2 - \frac{\alpha}{2} A_2, \tag{6}$$

where θ is the half-angle between the beams and α is the absorption coefficient.

We now write

$$A_1 = \sqrt{I_1} \exp(i\psi_1),$$

$$A_2 = \sqrt{I_2} \exp(i\psi_2), \tag{7}$$

where ψ_1 and ψ_2 are phases of the amplitudes A_1 and A_2, respectively. Using Eqs. (7) and (3), the coupled Eqs. (6) can be written as

$$\frac{d}{dz} I_1 = -\gamma \frac{I_1 I_2}{I_1 + I_2} - \alpha I_1,$$

$$\frac{d}{dz} I_2 = \gamma \frac{I_1 I_2}{I_1 + I_2} - \alpha I_2, \tag{8}$$

and

$$\frac{d}{dz} \psi_1 = \beta \frac{I_2}{I_1 + I_2},$$

$$\frac{d}{dz} \psi_2 = \beta \frac{I_2}{I_1 + I_2}, \tag{9}$$

where

$$\gamma = \frac{2\pi n_1}{\lambda \cos\phi} \sin\phi, \tag{10}$$

$$\beta = \frac{\pi n_1}{\lambda \cos\theta} \cos\phi. \tag{11}$$

The solutions for the intensities $I_1(z)$ and $I_2(z)$ are

$$I_1(z) = I_1(0) \frac{1 + m^{-1}}{1 + m^{-1} e^{\gamma z}} e^{-\alpha z}, \tag{12}$$

$$I_2(z) = I_2(0) \frac{1 + m}{1 + m e^{-\gamma z}} e^{-\alpha z}, \tag{13}$$

where m is the input intensity ratio

$$m = \frac{I_1(0)}{I_2(0)}. \tag{14}$$

Note that in the absence of absorption ($\alpha = 0$), $I_2(z)$ is an increasing function of z and $I_1(z)$ is a decreasing function of z, provided that γ is positive. The sign of γ depends on the direction of the c axis. As a result of the coupling for $\gamma > 0$ in Fig. 1, beam 2 gains energy from beam 1. If this two-wave mixing gain is large enough to overcome the absorption loss, then beam 2 is amplified. Such an amplification is responsible for the oscillation.

With $I_1(z)$ and $I_2(z)$ known, the phases ψ_1 and ψ_2 can be integrated directly from Eqs. (9). The phase shift in traversing through the photorefractive medium for beam 2 is

$$\frac{2\pi}{\lambda} n_0 l + \psi_2(l) - \psi_2(0), \tag{15}$$

where $2\pi n_0 l/\lambda$ is the phase shift in the absence of photorefractive coupling. The additional phase shift

$$\Delta\psi \equiv \psi_2(l) - \psi_2(0), \tag{16}$$

which is due to the photorefractive two-wave coupling, can be obtained by integrating Eqs. (9). Substituting Eqs. (12) and (13) into Eqs. (9) for I_1 and I_2, respectively, we obtain

$$\Delta\psi = \psi_2(l) - \psi_2(0) = \int_0^l \frac{\beta dz}{1 + m^{-1} e^{\gamma z}}. \tag{17}$$

Note that this photorefractive phase shift is independent of the absorption coefficient α. Carrying out the integration in Eq. (17), we obtain

$$\Delta\psi = \psi_2(l) - \psi_2(0) = -\frac{\beta}{\gamma} \log\left(\frac{1 + m}{1 + m e^{-\gamma l}}\right). \tag{18}$$

Equations (18) and (13) can now be used to investigate the properties of the unidirectional ring oscillation.

OSCILLATION FREQUENCY AND INTENSITY

In a conventional ring resonator, the oscillation occurs at those frequencies

$$f = N \frac{c}{L}, \qquad N = \text{integer} \tag{19}$$

that lie within the gain curve of the laser medium (e.g., He-Ne). Here, L is the effective length of a complete loop and N is a large integer. For $L \leq 30$ cm, these frequencies [Eq. (19)] are separated by the mode spacing $c/L \geq 1$ GHz. Since the width of the gain curve for the conventional gain medium is typically several gigahertz, principally because of Doppler broadening, oscillation can occur at almost any cavity length L. On the contrary, if the bandwidth of the gain curve is

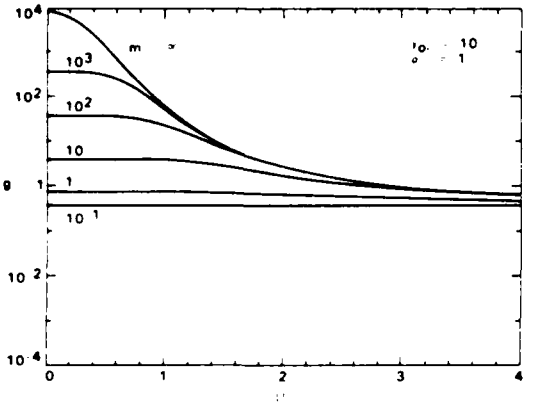

Fig. 2. Photorefractive gain g as a function of $\Omega\tau$ for various values of m.

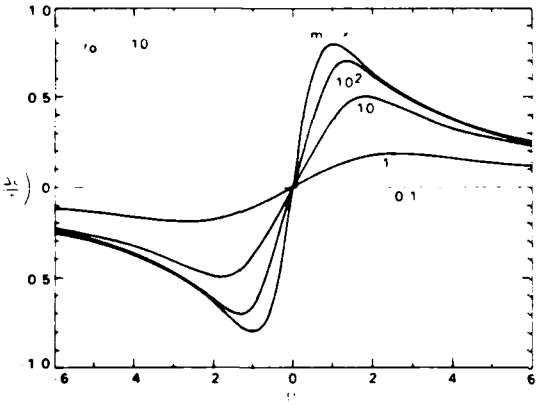

Fig. 3. Photorefractive phase shift $\Delta\psi$ as a function of $\Omega\tau$ for various values of m.

narrower than the mode spacing c/L, then oscillation can be sustained, provided that the cavity loop is kept at the appropriate length.

Unlike in the conventional gain medium, the bandwidth of the photorefractive two-wave mixing is very narrow. By using photorefractive crystals, e.g., $BaTiO_3$, that operate by diffusion only, the coupling constant can be written, according to Eqs. (4), (5), and (10), as

$$\gamma = \gamma_0/[1 + (\Omega\tau)^2], \tag{20}$$

where γ_0 is the coupling constant for the case of degenerate two-wave mixing (i.e., $\Omega = \omega_1 - \omega_2 = 0$) and is given by

$$\gamma_0 = \frac{4\pi\Delta n_s}{\lambda \cos\theta}. \tag{21}$$

In deriving Eq. (20), we have used $\pi/2$ for ϕ_0 in Eq. (4).

The parametric two-wave mixing gain can be defined as

$$g \equiv \frac{I_2(l)}{I_2(0)} = \frac{1 + m}{1 + me^{-\gamma l}} e^{-\alpha l}, \tag{22}$$

where we recall that m is the input beam ratio $m = I_1(0)/I_2(0)$ and l is the length of interaction. Note that amplification ($g > 1$) is possible only when $\gamma > \alpha$ and $m > (1 - e^{-\alpha l})/(e^{-\alpha l} - e^{-\gamma l})$. Also note that g is an increasing function of m (i.e., $\partial g/\partial m > 0$) and g is an increasing function of l, provided that $\gamma > \alpha$ and

$$l \leq \frac{1}{\gamma} \log\left[\frac{m(\gamma - \alpha)}{\alpha}\right]. \tag{23}$$

The gain as a function of frequency ω_2 (or equivalently as a function of $\Omega = \omega_1 - \omega_2$) is plotted in Fig. 2 for various values of m. Note that gain is significant only when $|\omega_1 - \omega_2|\tau < 1$. For materials such as $BaTiO_3$ and SBN, τ is between 1 and 0.1 sec. Thus the gain bandwidth is only a few hertz. In spite of such an extremely narrow bandwidth, unidirectional oscillation can still be observed easily at any cavity length in ring resonators by using $BaTiO_3$ crystals as the photorefractive medium.[13] Such a phenomenon can be explained in terms of the additional phase shift [Eq. (18)] introduced by the photorefractive coupling. This phase shift is a function of the oscillation frequency and is plotted in Fig. 3 as a function of $\Omega\tau$. For $BaTiO_3$ crystals with $\gamma_0 l > 4\pi$, this phase shift can vary from $-\pi$ to $+\pi$ for a frequency drift of $\Delta\Omega\tau = \pm 1$. Such a phase shift is responsible for the oscillation of the ring resonator, which requires a round-trip phase shift of an integer times 2π.

OSCILLATION CONDITIONS

It is interesting to note the initiation of the oscillation. Like laser oscillators, the oscillation of this ring resonator starts from noises that are due to physical processes such as scattering and quantum fluctuation. In photorefractive crystals the scattering dominates the noise contribution. At the beginning, there may be a slight amount of light scattered along the direction of the ring resonator. This slight amount of light will be amplified by the two-wave mixing process in the photorefractive crystal, provided that the frequencies are not appreciably different. As the intensity in the resonator builds up, the parameter m, defined by Eq. (14), decreases. The buildup of oscillation intensity leads to a saturation of the gain (see Fig. 2; the gain decreases as m decreases). At steady-state oscillation, the electric field must reproduce itself, both in phase and intensity, after each round trip. In other words, the oscillation conditions can be written as

$$\Delta\psi + \int k\,ds = 2N\pi \tag{24}$$

and

$$gR = 1, \tag{25}$$

where $\Delta\psi$ is the additional phase shift owing to photorefractive coupling, the integration is over a round-trip beam path, the parameter R is the product of the mirror reflectivities, and g is the parametric gain of Eq. (22).

If we define a cavity-detuning parameter $\Delta\Gamma$ as

$$\Delta\Gamma = 2N'\pi - \int k\,ds, \tag{26}$$

where N' is an integer chosen in such a way that $\Delta\Gamma$ lies between $-\pi$ and $+\pi$, then the oscillation condition [Eq. (24)] can be written as

$$\Delta\psi = \Delta\Gamma + 2M\pi, \tag{27}$$

where M is an integer. In other words, oscillation can be achieved only when the cavity detuning can be compensated for by the photorefractive phase shift.

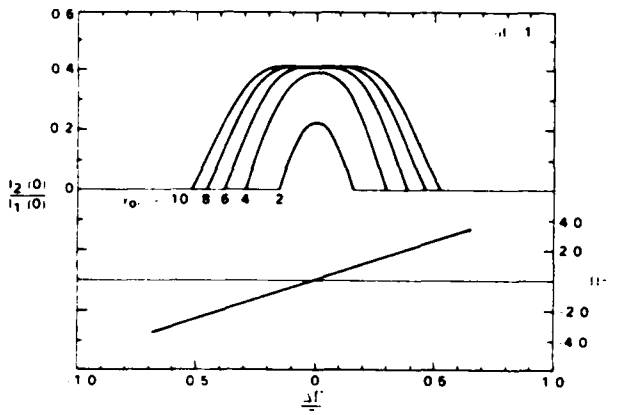

Fig. 4. Oscillation intensity and frequency as functions of cavity detuning $\Delta\Gamma$ for various values of $\gamma_0 l$.

Equations (24) and (25) may be used to solve for the two unknown quantities $m = I_1(0)/I_2(0)$ and $\Omega = \omega_1 - \omega_2$. If we fix the pump intensity $I_1(0)$ and the pump frequency ω_1, then Eqs. (24) and (25) can be solved for the oscillation frequency ω_2 and the oscillation intensity $I_2(0)$. Substituting Eq. (22) for g in Eq. (25) and using Eq. (18), we obtain

$$\Delta\psi = -\frac{\beta}{\gamma}\log(Re^{-\alpha l}). \tag{28}$$

This equation can now be used to solve for the oscillation frequency $\Omega\tau$. For the case of pure diffusion, using Eq. (4) for ϕ with $\phi_0 = \pi/2$ and Eqs. (10) and (11), we obtain from Eq. (28)

$$\Omega\tau = \frac{-2\Delta\psi}{\alpha l - \log R} = \frac{-2(\Delta\Gamma + 2M\pi)}{\alpha l - \log R}, \tag{29}$$

where $\Delta\Gamma$ is the cavity detuning and is given by Eq. (26). Substituting Eq. (22) for g in Eq. (25), we can solve for m and obtain

$$m = \frac{I_1(0)}{I_2(0)} = \frac{1 - Re^{-\alpha l}}{Re^{-\alpha l} - e^{-\gamma l}}. \tag{30}$$

Since m must be positive, we obtain from Eq. (30) the threshold condition for oscillation

$$\gamma l > \gamma_t l \equiv \alpha l - \log R, \tag{31}$$

where γ_t is the threshold parametric gain constant. Since γ is a function of frequency Ω, Eq. (31) dictates that the parametric gain is above threshold only in a finite spectral regime. When Eq. (20) is used for γ, Eq. (31) becomes

$$|\Omega\tau| < \left(\frac{\gamma_0 l}{\alpha l - \log R} - 1\right)^{1/2}, \tag{32}$$

where we recall that γ_0 is the parametric gain at $\Omega = \omega_1 - \omega_2 = 0$. Inequality (32) defines the spectral regime where the parametric gain γ is above threshold (i.e., $\gamma > \gamma_t$).

We have thus far obtained expressions for the oscillation frequency [Eq. (29)] and the spectral regime where the gain is above threshold. The ring resonator will oscillate only when the oscillation frequency falls within this spectral region. The oscillation frequency $\omega_2 = \omega_1 - \Omega$ is determined by Eq. (29), with $\Delta\Gamma$ being the cavity detuning [Eq. (26)].

The same oscillation frequency must also satisfy expression (32). Thus we obtain the following oscillation condition:

$$\frac{2|\Delta\psi|}{\alpha l - \log R} < \left[\frac{\gamma_0 l}{\alpha l - \log R} - 1\right]^{1/2}, \tag{33}$$

which can also be written as

$$\gamma_0 l > \gamma_t l + \frac{1}{\gamma_t l}(2\Delta\psi)^2 \equiv G_t l, \tag{34}$$

where γ_t is the threshold parametric gain of Eq. (31) for the case when $\Delta\psi = 0$ and G_t may be considered the threshold gain for the case when $\Delta\psi \neq 0$. According to Eq. (34), the threshold gain increases as a function of the cavity detuning $\Delta\Gamma$. The cavity detuning $\Delta\Gamma$ not only determines the oscillation frequency [Eq. (29)] but also determines the threshold gain G_t.

The $\Delta\Gamma$ in Eq. (26) is the cavity detuning and is defined between $-\pi$ and π. However, the photorefractive phase shift [Eq. (18)] can be greater than π. When this happens, the unidirectional ring resonator may oscillate at more than one frequency. These frequencies are given by Eq. (29), with $M = 0, \pm 1, \pm 2, \ldots$, etc., and with their corresponding threshold gain given by

$$G_t l = \gamma_t l + \frac{1}{\gamma_t l}[2(\Delta\psi + 2M\pi)]^2. \tag{35}$$

In other words, for each cavity detuning $\Delta\Gamma$, the ring resonator can support multimode oscillation, provided that the coupling constant γ_0 is large enough. Figure 4 shows the oscillation intensity as well as the oscillation frequency as functions of cavity detuning $\Delta\Gamma$. Note that for larger $\gamma_0 l$ the resonator can oscillate at almost any cavity detuning $\Delta\Gamma$, whereas for small $\gamma_0 l$ oscillation occurs only when the cavity detuning is limited to some small region around $\Delta\Gamma = 0$.

CONCLUSION AND DISCUSSION

In conclusion, we have derived a theory of unidirectional ring oscillators using parametric photorefractive two-wave mixing. By using the simple coupled-mode theory, we obtain an expression for the photorefractive phase shift. Such a photorefractive phase shift can compensate for cavity detuning and thus can allow the oscillation to occur. According to this theory, the oscillation frequency will be slightly detuned from the pump frequency. Such a frequency offset is necessary to produce the photorefractive phase shift to compensate for the cavity detuning. The photorefractive phase shift is proportional to the coupling constant. Thus, when materials with a large coupling constant (e.g., $BaTiO_3$) are used, oscillation can occur at almost any cavity detuning. Such a theory has been validated by the author and his coworker.[14] The same theory can also be applied to linear oscillators and thus can be employed to explain the frequency shift of self-pumped phase conjugators.[6,13]

ACKNOWLEDGMENTS

The author acknowledges helpful discussions with M. Khoshnevisan and M. Ewbank (Rockwell Science Center) and J. Feinberg (University of Southern California).

REFERENCES

1. J. P. Huignard and A. Marrackchi, "Coherent signal beam amplification in two-wave mixing experiments with photorefractive BSO crystals," Opt. Commun. **38**, 249 (1981).
2. J. P. Huignard and A. Marrackchi, "Two-wave mixing and energy transfer in $Bi_{12}SiO_{20}$ crystals: amplification and vibration analysis," Opt. Let. **6**, 622 (1981).
3. P. Yeh, "Contradirectional two-wave mixing in photorefractive media," Opt. Commun. **45**, 323 (1983).
4. P. Yeh, "Electromagnetic propagation in a photorefractive layered medium," J. Opt. Soc. Am. **73**, 1268 (1983).
5. P. Yeh, "Photorefractive coupling in ring resonators," Appl. Opt. **23**, 2974 (1984).
6. J. O. White, M. Cronin-Golomb, B. Fischer, and A. Yariv, "Coherent oscillation by self-induced gratings in photorefractive crystals," Appl. Phys. Lett. **40**, 450 (1982).
7. P. Yeh, "Theory of phase-conjugate oscillators," J. Opt. Soc. Am. A **2**, 727–730 (1985).
8. D. L. Staebler and J. J. Amodei, "Coupled wave analysis of holographic storage in LiNbO$_3$," J. Appl. Phys. **34**, 1042 (1972).
9. V. L. Vinetskii, N. V. Kukhtarev, S. G. Odulov, and M. S. Soskin, "Dynamic self-diffraction of coherent light beams," Sov. Phys. Usp. **22**, 742 (1979).
10. N. V. Kukhtarev, V. B. Markov, S. G. Odulov, M. S. Soskin, and V. L. Vinetskii, "Holographic storage in electro-optics crystals: beam coupling and light amplification," Ferroelectrics **22**, 961 (1979).
11. B. Fischer, M. Cronin-Golomb, J. O. White, and A. Yariv, "Amplified reflection, transmission, and self-oscillation in real-time holography," Opt. Lett. **6**, 519 (1981).
12. J. Feinberg, D. Heiman, A. R. Tanguay, and R. Hellwarth, J. Appl. Phys. **51**, 1297 (1980).
13. J. Feinberg and G. D. Bacher, "Self-scanning of a continuous-wave dye laser having a phase-conjugating resonator cavity," Opt. Lett. **9**, 420 (1984).
14. M. D. Ewbank and P. Yeh, "Frequency shift and cavity detuning in photorefractive resonators," Opt. Lett. **10**, 496–498 (1985).

APPENDIX 5.6

Frequency Shift and Cavity Length in Photorefractive Resonators

Reprinted from Optics Letters, Vol. 10, page 496, October, 1985

Frequency shift and cavity length in photorefractive resonators

M. D. Ewbank and P. Yeh

Rockwell International Science Center, Thousand Oaks, California 91360

Received April 22, 1985; accepted July 22, 1985

Photorefractive resonators exhibit an extremely small frequency difference ($\Delta\omega/\omega \sim 10^{-15}$) between the oscillating and pumping beams. The observed frequency difference is proportional to cavity-length detuning. This dependence is explained by a photorefractive phase shift that is due to slightly nondegenerate two-wave mixing that compensates for cavity detuning and satisfies the round-trip phase condition for steady-state oscillation. The measured onset or threshold of oscillation as a function of photorefractive gain and intensity agrees with theory.

Despite the attention that self-pumped phase conjugators and optical resonators utilizing photorefractive $BaTiO_3$ have received recently,[1-3] two dilemmas remain unresolved. First, self-pumped phase conjugation in $BaTiO_3$ exhibits a slight frequency shift (~1-Hz),[4-7] attributed to a Doppler shift from moving photorefractive phase gratings.[4] Second, resonators using photorefractive gain media apparently oscillate at any optical cavity length.[4,8] In this Letter we show that these two dilemmas are interrelated and reveal the origin of the moving gratings and frequency shifts.

For simplicity, consider a unidirectional ring oscillator with photorefractive two-wave mixing providing the gain. The optical arrangement (Fig. 1) is chosen because only two-wave mixing occurs. The frequency difference between the unidirectional oscillation beam and the pump can be controlled by small changes ($<\lambda$) in ring-cavity length. In fact, both the *sign and the magnitude of the frequency shift exhibit a one-to-one correspondence to the cavity-length detuning.*

The above observations are predicted by a theory for unidirectional photorefractive ring resonators.[9] Oscillation occurs when the two-wave mixing gain dominates cavity losses and the round-trip optical phase reproduces itself (to within an integer multiple of 2π). The condition on phase is unique because of a significant *optical phase shift owing to nondegenerate two-wave mixing.* This condition is satisfied at any cavity length if the oscillation frequency is detuned from the pump frequency, since the photorefractive phase shift depends on the detuning. The frequency difference Ω between the pumping and oscillating beams is[9]

$$\Omega = -[2(\Delta\Gamma + 2m\pi)/\tau A], \tag{1}$$

where $\Delta\Gamma$ is the cavity-length detuning with respect to an integer multiple of optical pump waves in the cavity, m is an integer, τ is the photorefractive time response, and A represents the total cavity loss. There are threshold conditions for oscillation involving cavity loss and gain (taking m to be zero):

$$|\Omega| \leq (1/\tau)(\gamma L/A - 1)^{1/2}, \tag{2a}$$

$$|\Delta\Gamma| \leq (A/2)(\gamma L/A - 1)^{1/2}, \tag{2b}$$

where γ is the degenerate two-wave mixing coupling coefficient, where L is the interaction length, and $A = -\ln(RT_sT_p)$ [with R the product of the reflectivities of the cavity mirrors and output coupler; T_s the transmission through the $BaTiO_3$ sample accounting for the absorption, Fresnel reflections, and scattering (or beam fanning); and T_p the effective transmission through the pinhole aperture].

This theory predicts that the unidirectional ring resonator will oscillate at a frequency different from the pump frequency by an amount directly proportional to the cavity-length detuning. Furthermore, in a photorefractive material with moderate slow τ, the theory postulates a threshold where oscillation will cease if the cavity detuning (frequency difference) becomes too large.

The experiments performed to examine the above theory will now be discussed in detail. Referring to Fig. 1, a single-mode argon-ion laser (514.5 nm) serves multiple purposes: It pumps the $BaTiO_3$ crystal with the beam reflected from BS_1 and focused by lens L_1 (F = 700 mm) to a beam diameter of 0.5 mm at the crystal, it is a reference beam to determine interferometrically the relative frequency of the ring-cavity oscillation at BS_5, and it provides an accurate method to align the ring-cavity components (unblocking the beam reflected from BS_2) by monitoring the Fabry–Perot peaks when

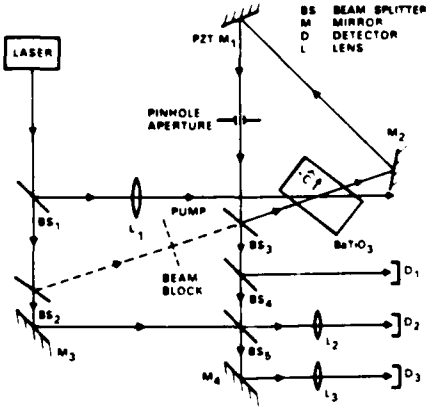

Fig. 1. Optical setup for the photorefractive unidirectional ring resonator with variable cavity length. The beat frequency between the self-oscillation and pump beams is derived from the motion of the interferograms at D_2 or D_3.

0146-9592/85/100496-03$2.00/0

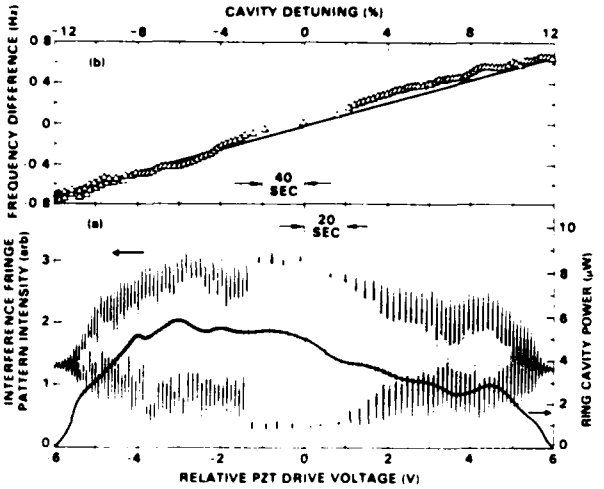

Fig. 2. Characteristics of the unidirectional self-oscillation as a function of ring-cavity length (i.e., PZT voltage or cavity detuning, where 100% implies a detuning of one full optical wave): (a) ring-cavity intensity (right) and beat-frequency signature (left); (b) frequency difference between the self-oscillation and the pumping beam.

rapidly scanning the piezo mirror PZT-M_1. Two-wave mixing in $BaTiO_3$ couples light into the unidirectional ring cavity, formed by two planar mirrors (M_1 and M_2) and a planar beam splitter (BS_3), even when the alignment beam is blocked. The ring-cavity beam is sampled through the output coupler BS_3, its intensity being detected at D_1 while the beat frequency between it and the pumping beam is determined using complementary fringe patterns formed at detectors D_2 and D_3. Without a ring-cavity pinhole aperture, unidirectional oscillation is observed at any cavity length. However, dynamically unstable multiple spatial modes are evident[4,10] in the fringe patterns at D_2 and D_3. To obtain a single mode (and clean fringe patterns), a 200-μm pinhole is placed in the ring cavity.

The basic premises of the theory[9] are verified by slowly ramping the PZT voltage and observing the beat frequency, along with the ring-cavity oscillation intensity. Typical results are shown in Fig. 2(a) for an 80-mW pump beam incident at 40° from the c axis of $BaTiO_3$ and at 20° from the oscillating beam (both angles are external in air). A triangle waveform (amplitude 250 V and period 10,000 sec) drives the PZT. The slow PZT scanning rate approximates steady-state two-wave mixing in $BaTiO_3$ while simultaneously permitting a controlled variation of the cavity length.

The unidirectional ring-cavity intensity versus cavity length [Fig. 2(a)] indicates threshold gain conditions [expressions (2a) and (2b)]. The beat frequency between oscillating and pumping beams, as observed in the time variation of the fringe-pattern intensity [Fig. 2(a)], clearly corresponds to the position of the PZT-M_1. This beat frequency is not simply due to the Doppler shift caused by the moving PZT-M_1 since this Doppler shift is 3 orders of magnitude smaller than the observed beat frequency. When M_1 is exactly at the correct position (chosen as the origin), the fringe pattern is stationary, i.e., there is no frequency shift. As M_1 moves away from this origin, the fringe motion becomes faster and the frequency difference increases. Figure 2(b) shows the linear dependence of the frequency difference on cavity detuning with the ramping period equal to 20,000 sec for improved resolution. This frequency difference is estimated from the beat-frequency signature [similar to Fig. 2(a)] by measuring the time interval between intensity maxima.

The frequency difference changes sign as M_1 slowly moves through the origin. The frequency of oscillation is upshifted with respect to the frequency of the pumping beam when the position of M_1 is negative, corresponding to a decrease in ring-cavity length from that where no frequency shift occurs. The observed sign is consistent with the sign of the phase shift between the light intensity pattern and index modulation that determines the direction of energy exchange in two-wave mixing.

The beat-frequency signature [Fig. 2(a)] is also a periodic function of PZT mirror position. The Fabry–Perot peak spacing detected at D_1 during alignment of the passive ring cavity calibrates the PZT motion (~50-V/free-spectral range for 514.5 nm). The observed beat-frequency signature reproduces itself with a M_1 displacement of every $\sim \lambda/2$, as expected (i.e., a cavity length detuning periodicity of λ).

Experimentally, the frequency threshold for oscillation is approximately a linear function of the pumping-beam intensity, as shown in Fig. 3(a). According to Eq. 2(a), this frequency threshold is inversely proportional to τ, but τ can be approximately proportional to the inverse of the pump intensity (assuming that the cavity intensity is negligible by comparison) when the photoconductivities dominate.[11] Therefore, the observed dependence [Fig. 3(a)] agrees with theory.

The oscillation conditions for the unidirectional ring resonator are dependent on the two-wave mixing gain (γL) in the photorefractive medium. γL is varied by

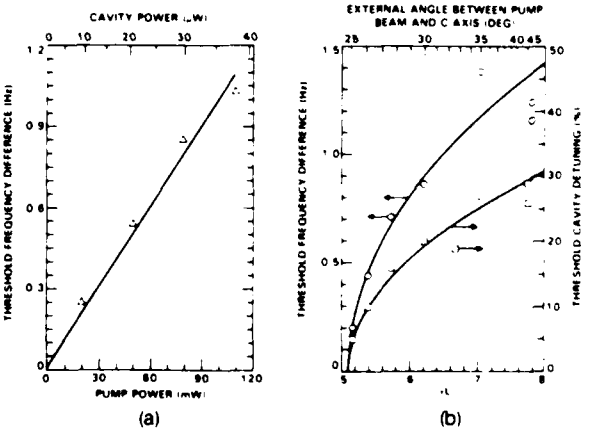

Fig. 3. Oscillation threshold behavior for the unidirectional ring resonator: (a) maximum beat frequency as a function of pumping-beam or ring-cavity power along with a linear fit (solid line); (b) maximum beat frequency (left) and cavity detuning (right) as a function of two-wave mixing gain, γL, where γL is related to the external angle that the pumping beam makes the crystal's c axis as shown (top scale). Note: the two solid curves in (b) correspond to the evaluation of expressions (2a) and (2b) as described in text.

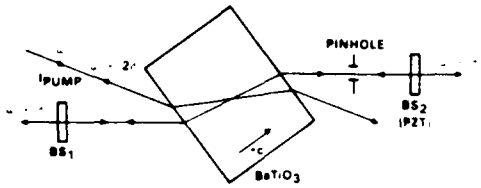

Fig. 4. Self-pumped phase conjugator using external reflectors to generate the self-oscillation with a frequency shift δ and the phase-conjugate reflection with a frequency shift 2δ, where δ is proportional to the linear cavity length.

rotating the $BaTiO_3$ crystal with respect to the pumping and oscillating beams.[12] When the gain is too small, no unidirectional oscillation is observed, regardless of ring-cavity length. For γL just above threshold, two pronounced differences are evident, contrasting with γL large. First, the amount of cavity detuning that is accommodated before oscillation ceases is greatly reduced. Second, the maximum frequency difference between the pumping and oscillating beams is much less. The quantitative trends of these two effects are given in Fig. 3(b) for a pump power of 80 mW.

The threshold oscillation conditions given in expressions (2a) and (2b) agree with the data [Fig. 3(b)]. The solid curve associated with the left-hand scale of Fig. 3(b) is generated from expression (2a) for $A = 5.1$ and $\tau = 0.53$ sec. This cavity-loss factor, A, is estimated independently from $R = 0.99 \times 0.91 \times 0.81$ (for M_1, M_2 and BS_3, respectively), $T_s = 0.52$ and $T_p = 0.016$ (for a cavity length of 50 cm). Accumulating these contributions gives $A = 5.2$, in excellent agreement with the observed 5.1. The right-hand scale of Fig. 3(b) shows the dependence of threshold cavity detuning (i.e., the maximum detuning that will still support self-oscillation) on γL, along with the prediction from Eq. 2(b), where $\Delta\Gamma$ is normalized by 2π. Remarkable agreement is obtained using $A = 5.1$ from Fig. 3(a) and no adjustable parameters.

The interdependence of the optical cavity length and the beat frequency between the oscillating and pumping beams is a general property of photorefractive resonators. These results are not unique to the optical setup shown in Fig. 1. Similar behavior is observed with other configurations. First, the orientation of the $BaTiO_3$ crystal in Fig. 1 can be altered so that the pumping and oscillating beams enter the *a* face but in such a way that no self-pumping occurs.[4] Second, the $BaTiO_3$ can be replaced by crystals of strontium barium niobate[13,14] (nominally undoped and cerium doped). Third, a linear resonator (Fig. 4) acts as a *self-pumped phase conjugator*.[1] The observed frequency shift of the phase-conjugate beam is exactly twice that of the self-oscillation, which is necessary to satisfy energy conservation for slightly nondegenerate four-wave mixing.[15] In all three variations, the measured frequency differences correlate with cavity length detuning; results equivalent to those shown in Fig. 2 are obtained.

Finally, consider another self-pumped phase conjugator, in which the four-wave mixing pumping beams arise from internal reflections at the crystal faces instead of external mirrors.[3-7] A resonance cavity containing the self-pumping beams is formed from the internal reflections off the crystal surfaces (but the cavity length cannot be systematically varied and the spatial modes cannot be restricted with an aperture). The frequencies of the beams can again be compared interferometrically. One self-pumping beam is monitored using the uncollimated light escaping the crystal's corner during reflection. Preliminary experiments indicate that the phase-conjugate beam sometimes exhibits a frequency shift exactly double that of a self-pumping beam, just as in Fig. 4. Even though four-wave mixing is occurring in all cases of self-pumped phase conjugators, two-wave mixing might be the dominating process in determining the oscillation conditions necessary for generating the self-pumping beams.

In conclusion, the frequency difference between the self-oscillating and pumping beams in the unidirectional ring resonator experimentally depends on the optical cavity length. This dependence supports a theory[9] that uses a photorefractive phase shift associated with slightly nondegenerate two-wave mixing to satisfy the round-trip phase-oscillation condition for the resonating beam. Similarly, the observed frequency shifts in other photorefractive resonators, including self-pumped phase conjugators, may also be explained by the same mechanism.

The authors acknowledge discussions with M. Khoshnevisan and A. Chiou of Rockwell International Science Center and J. Feinberg of the University of Southern California.

References

1. J. O. White, M. Cronin-Golomb, B. Fischer, and A. Yariv, Appl. Phys. Lett. **40**, 450 (1982).
2. R. McFarlane and D. Steel, Opt. Lett. **8**, 208 (1983).
3. J. Feinberg, Opt. Lett. **8**, 480 (1983).
4. J. Feinberg and G. D. Bacher, Opt. Lett. **9**, 420 (1984).
5. K. R. MacDonald and J. Feinberg, J. Opt. Soc. Am. A **1**, 1213 (A) 1984.
6. J. F. Lam, J. Opt. Soc. Am. A **1**, 1223 (A) 1984.
7. W. Whitten and J. Ramsey, Opt. Lett. **9**, 44 (1984).
8. H. Rajbenbach and J. P. Huignard, Opt. Lett. **10**, 137 (1985).
9. P. Yeh, J. Opt. Soc. Am. B **2** (to be published, November 1985).
10. G. Valley and G. Dunning, Opt. Lett. **9**, 513 (1984).
11. P. Gunter, Phys. Rep. **93**, 199 (1982).
12. As the orientation of the two-wave mixing fringe pattern with respect to the crystal axes changes, the effective electro-optic coefficient (and coupling efficiency of the index grating) is modified. γL is independently measured by removing ring-cavity mirror M_2 and using an attenuated probe beam from BS_2 with an external angle of 20° between probe and pump beams.
13. Provided by R. Neurganokar, Rockwell International, Thousand Oaks, Calif.
14. B. Fischer, M. Cronin-Goulomb, J. O. White, A. Yariv, and R. Neurgaonkar, Appl. Phys. Lett. **40**, 863 (1982).
15. P. Yeh, M. D. Ewbank, M. Khoshnevisan, and J. M. Tracy, Opt. Lett. **9**, 41 (1984).

APPENDIX 5.7

Frequency Shift of Self-Pumped Phase Conjugator

Frequency shifts of self-pumped phase conjugators

M.D. Ewbank and P. Yeh

Rockwell International Science Center
1049 Camino Dos Rios, Thousand Oaks, California 91360

Abstract

The reflection from most photorefractive, self-pumped phase conjugators differs in frequency from the incident beam by a small amount ($\Delta\omega/\omega \sim 10^{-15}$). A theory and the supporting experiments which explain such frequency shifts are presented. In our theory, four-wave mixing is responsible for the generation of the conjugated wave where a self-oscillation arising from photorefractive coupling provides the customary pumping beams. The frequency of these pumping beams is determined by a resonance cavity geometry and may be slightly different from that of the incident beam. Nondegenerate four-wave mixing using these self-oscillating pumping beams give rise to the frequency shift of the phase-conjugate reflection. Experimental results are in good agreement with theory.

Introduction

Self-pumped phase-conjugate reflectors[1-3] using photorefractive $BaTiO_3$ have recently received considerable attention because 30-50% reflectivities are relatively easy to achieve even with low-power lasers. In self-pumped (or passive) phase conjugators, the counter-propagating pumping beams needed in the four-wave mixing process are automatically generated by light photorefractively diffracted out of the incident beam. However, the phase-conjugate reflection is generally shifted slightly in frequency when compared to the incident beam (on the order of 1 Hz depending on intensity). This frequency shift has been attributed to moving photorefractive gratings which Doppler shift the diffracted light.[4] The physical mechanism, which is responsible for the moving gratings, is, however, not well understood.

The frequency shift first manifested itself as a frequency scanning when self-pumped $BaTiO_3$ was coupled to a dye laser.[4-6] Since those initial observations, numerous experiments and theories involving self-pumped phase conjugators and/or photorefractive resonators have addressed, either directly or indirectly, the frequency shift issue.[7-16] However, a general theory and the conclusive experiments are not available.

In this paper we present a theory and the supporting experiments which explain such frequency shifts of most self-pumped phase conjugators. In our theory, self-pumped phase conjugation results from an internal self-oscillation. The optical resonance cavity which supports such oscillation is formed by either external mirrors or crystal surfaces. The oscillating beams provide the counterpropagating pump beams which are required in the four-wave mixing process. The theory shows that despite the narrow gain bandwidth of the photorefractive two-wave coupling, internal oscillation can still occur over a large range of cavity length detuning. The frequency shift is proportional to the cavity length detuning. Such a dependence is explained by a photorefractive phase shift that is due to slightly nondegenerate two-wave mixing. The additional photorefractive phase shift compensates for cavity length detuning and satisfies the round-trip phase condition for steady-state oscillation.

When the self-pumping beams are spontaneously generated via photorefractive coupling in a linear resonance cavity with two external mirrors on opposite sides of a photorefractive crystal such as $BaTiO_3$, we observe that the frequency shift of the phase-conjugate reflection is directly proportional to cavity-length detuning. In the case where the self-pumping beams arise from internal reflections off the photorefractive crystal's surfaces, we experimentally prove that a previous description[2] of the self-pumping process is inadequate and we show that a closed-looped resonance cavity forming inside the crystal is a better description.

Theory

The theory is an extension of our earlier theory on unidirectional photorefractive ring oscillators.[16] In this theory, amplification owing to holographic two-wave mixing in the photorefractive crystal is responsible for the self-oscillation. When the configuration of the resonance cavity relative to the crystal supports bi-directional oscillation, a phase-conjugate beam is generated via the four-wave mixing process. The parametric two-wave mixing gain, defined as the output to input intensity ratio, is given by[16]

$$g = \frac{1 + m}{1 + me^{-\gamma \ell}} \, e^{-\alpha \ell} = g_o e^{-\alpha \ell} \quad , \tag{1}$$

where m is the ratio of the pump beam intensity to oscillating beam intensity, α is the bulk absorption coefficient, ℓ is the length of interaction γ is the intensity coupling constant, and g_o is the gain where there is no loss. For crystals such as $BaTiO_3$, this gain can be several thousand per pass. Thus oscillation can be sustained even in cavities with high scattering, diffraction, and/or mirror losses.

The phase shift in traversing through the photorefractive medium for the oscillating beam is

$$\frac{2\pi}{\lambda} n_o \ell + \Delta\phi \quad , \tag{2}$$

where $2\pi n_o \ell/\lambda$ is the phase shift in the absence of photorefractive coupling. The additional phase shift, $\Delta\phi$, is due to the photorefractive two-wave coupling and is given by[16]

$$\Delta\phi = -\frac{\beta}{\gamma} \log \left(\frac{1 + m}{1 + me^{-\gamma \ell}}\right) = \frac{-\beta}{\gamma} \log (g_o) \tag{3}$$

where β is the phase-coupling constant.[16] Note that this phase shift, $\Delta\phi$, is independent of absorption losses.

According to a nonlinear model of the photorefractive two-wave mixing, these coupling constants (i.e., β and γ) are given by

$$\gamma = \frac{2\pi n_1}{\lambda \cos\theta} \sin\phi \tag{4}$$

$$\beta = \frac{\pi n_1}{\lambda \cos\theta} \cos\phi \quad , \tag{5}$$

where θ is the half-angle between the pump beam and the oscillating beam. The parameters ϕ and n_1 can be written, respectively,

$$\phi = \phi_o + \tan^{-1} (\Omega\tau) \tag{6}$$

and

$$n_1 = \frac{2}{\sqrt{1 + \Omega^2 \tau^2}} \Delta n_s \tag{7}$$

where τ is the decay time constant of the holograph grating, Δn_s is the saturation value of the photoinduced index change for degenerate two-wave mixing, ϕ_o is a constant phase shift related to the nonlocal response of the crystal under fringe illumination, and Ω is the frequency shift between the oscillating and pumping beams. According to Equation (1), amplification is possible (i.e., $g > 1$) only when $\gamma > \alpha$. Note that gain is significant only when $\Omega\tau < 1$. For materials such as $BaTiO_3$ and SBN, τ is typically between 0.1 s and 1.0 s for nominal laser intensities (1-10 W/cm^2). Thus, the gain bandwidth is only a few Hertz. In spite of such an extremely narrow bandwidth, self-oscillation can still be observed easily at "any" cavity length using $BaTiO_3$ crystals as the photorefractive medium. Such a phenomenon can be explained in terms of the additional phase shift (Equation (3)) introduced by the photorefractive coupling. This phase shift is a function of the oscillation frequency. For $BaTiO_3$ crystals with $\gamma\ell > 4\pi$, this phase shift can vary from $-\pi$ to $+\pi$ for a frequency drift of $\Delta\Omega\tau = \pm 1$. Such a phase shift contributes to the round-trip phase shift so that the latter can be an integer times 2π, a condition required for oscillation.

Concerning the initiation of the oscillation in the photorefractive resonator, like laser oscillators, the oscillation starts from noises that are due to physical processes such as scattering and quantum fluctuation. In photorefractive crystals, the scattering dominates the noise contribution. At the beginning, a slight amount of light may be scattered along the direction of the resonator. This slight amount of light will be amplified by the two-wave mixing process in the photorefractive crystal, provided that the frequencies are not appreciably different. As the intensity in the resonator builds up, the beam ratio parameter, m, decreases. The buildup of oscillation intensity leads to a saturation of the gain (see Equation (1) where the gain decreases as m decreases). At steady-state oscillation,

the electric field must reproduce itself, both in phase and intensity, after each round trip. In other words, the oscillation conditions can be written as

$$\Delta\phi + \int kds = 2N\pi \tag{8}$$

and

$$gR = 1 \quad , \tag{9}$$

where $\Delta\phi$ is the additional phase shift owing to photorefractive coupling, the integration is over a round-trip beam path, N is an integer, the parameter R represents the cavity losses (e.g., the product of the mirror reflectivities), and g is the parametric gain of Equation (1).

If we define a cavity-detuning parameter $\Delta\Gamma$ as

$$\Delta\Gamma = 2N'\pi - \int kds \quad , \tag{10}$$

where N' is an integer chosen in such a way that $\Delta\Gamma$ lies between $-\pi$ and $+\pi$, then the oscillation condition (Equation (8)) can be written as

$$\Delta\phi = \Delta\Gamma + 2M\pi \quad , \tag{11}$$

where M is an integer. In other words, oscillation can be achieved only when the cavity detuning can be compensated by the photorefractive phase shift.

Equations (8) and (9) may be used to solve for the two unknown quantities m and Ω. If we fix the pump intensity and the pump frequency, then Equations (8) and (9) can be solved for the oscillation frequency and the oscillation intensity. Substituting Equation (1) for g in Equation (9) and using Equation (3), we obtain

$$\Delta\phi = \frac{\beta}{\gamma} \log\left(Re^{-\alpha\ell}\right) \quad . \tag{12}$$

This equation can now be used to solve for the frequency shift Ω. For the case of pure diffusion, using Equation (6) for ϕ with $\phi_o = \pi/2$ and Equations (4) and (5), we obtain from Equation (12)

$$\Omega\tau = \frac{-2\,\Delta\phi}{\alpha\ell - \log R} = \frac{-2(\Delta\Gamma + 2M\pi)}{\alpha\ell - \log R} \tag{13}$$

where $\Delta\Gamma$ is the cavity detuning and is given by Equation (10). Substituting Equation (1) for g in Equation (9), we can solve for m and obtain

$$m = \frac{1-Re^{-\alpha\ell}}{Re^{-\alpha\ell}-e^{-\gamma\ell}} \quad . \tag{14}$$

Since m must be positive, we obtain from Equation (14) the threshold condition for oscillation

$$\gamma\ell > \gamma_t\ell \equiv \alpha\ell - \log R \tag{15}$$

where γ_t is the threshold parametric gain constant. Since γ is a function of frequency Ω, Equation (15) dictates that the parametric gain is above threshold only in a finite spectral regime. Using Equation (1) for γ, Equation (15) becomes

$$|\Omega\tau| < \left[\frac{\gamma_o\ell}{\alpha\ell - \log R} - 1\right]^{1/2} \tag{16}$$

where γ_o is the parametric gain at $\Omega = 0$. Equation (16) defines the spectral regime where the parametric gain γ is above threshold (i.e., $\gamma > \gamma_t$).

We have obtained expressions for the oscillation frequency (Equation (13)) and the spectral regime where the gain is above threshold. The self-oscillation will be sustained only when the parametric gain is greater than the round-trip cavity loss and the oscillation frequency falls within this spectral region. The frequency shift is determined by Equation (13), with $\Delta\Gamma$ being the cavity detuning given by Equation (10). According to Equations

(15) and (16), the resonator can be made to fall below threshold by decreasing the reflectivity, R. When this happens, oscillations ceases.

The $\Delta\Gamma$ in Equation (10) is the cavity detuning and is defined between $-\pi$ and π. However, the photorefractive phase shift (3) can be greater than π. When this happens, the internal oscillation may occur at more than one frequency. These frequencies are given by Equation (13), with $M = 0, \pm1, \pm2, \ldots$ etc. In other words, for each cavity detuning $\Delta\Gamma$, the resonator can support multimode oscillation, provided the coupling constant γ_o is large enough. Note that when $\gamma_o\ell$ is large compared to the natural logarithm of the cavity losses, the resonator can oscillate at almost any cavity detuning $\Delta\Gamma$; whereas when $\gamma_o\ell$ is small, oscillation occurs only when the cavity detuning is limited to some small region around $\Delta\Gamma = 0$.

The interdependence of the cavity length detuning and the frequency shift between the oscillating and pumping beams is a general property of photorefractive resonators. Such frequency shifts have been measured in unidirectional ring resonators and self-pumped phase conjugators using external mirrors.[15] In these two types of resonators, the cavity length, cavity losses and two-wave mixing gain (via crystal orientation) can be varied in a controlled fashion. The results, described below, show that the frequency shift of the self-oscillation is directly proportional to cavity length detuning for both of these resonators in excellent agreement with the above theory.

In self-pumped phase conjugator using internal reflections, bi-directional internal oscillations must simultaneously be present. These two counterpropagating beams act as the customary pumping beams of the four-wave mixing process. If each of these pumping beams is frequency shifted by Ω, then the generated phase conjugate beam has a frequency shift of 2Ω as required by conservation of energy.

Experiments

Unidirectional Ring Oscillator

Before describing the frequency shift experiments with self-pumped phase conjugators, let's first review similar experiments performed on a unidirectional ring oscillator[15] with only two-wave mixing photorefractive gain. The optical arrangement is shown in Figure 1 where two-wave mixing in $BaTiO_3$ couples light from an argon ion laser into the unidirectional ring cavity, formed by two planar mirrors (M_1 and M_2 with the former being piezoelectrically (PZT) driven) and a planar beamsplitter (BS_3). The unidirectional oscillation in the ring cavity (confined to a single mode by the pinhole aperture[17]) is sampled via the output coupler BS_3, its intensity being measured at detector D_1 and the frequency shift between the self-oscillating and pumping beams being determined interferometrically using complementary fringe patterns at detectors D_2 and D_3.

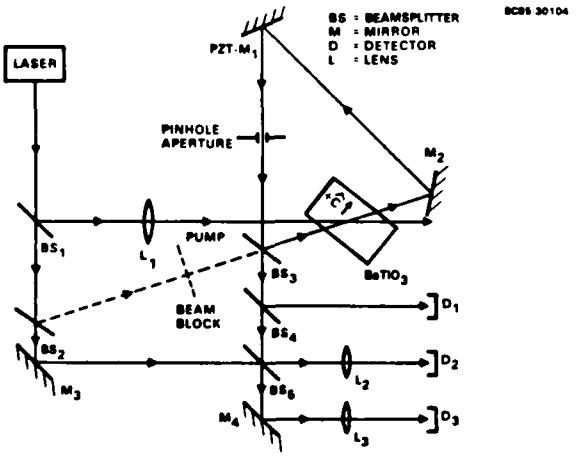

Figure 1 Optical setup for a photorefractive unidirectional ring resonator with variable cavity length. Two-wave mixing coupling in $BaTiO_3$ provides the gain for self-oscillation. The beat frequency between the pumping and self-oscillating beams is derived from the motion of the interferograms at D_2 and D_3.

Figure 2a shows the beat frequency, along with the ring cavity oscillation intensity, as a function of PZT mirror position or cavity detuning. A slow ramping rate of the PZT mirror is used to mimic steady-state for the two-wave mixing process in the slow photorefractive $BaTiO_3$ while, at the same time, permitting a controlled variation of the ring cavity

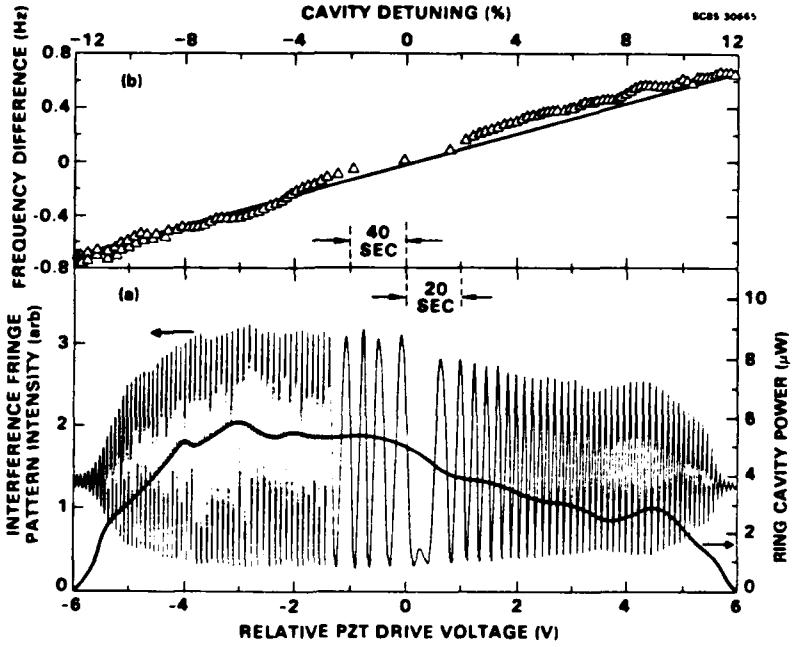

Figure 2 Characteristics of the unidirectional self-oscillation as a function of ring cavity length (i.e., PZT voltage or cavity detuning where 100% implies a detuning of one full optical wave): (a) ring cavity intensity (right) and beat-frequency signature (left); (b) frequency difference between the self-oscillation and pumping beam (solid line is a linear least squares fit to data).

length. The frequency difference between the pump beam and the unidirectional oscillation, as observed in the time-variation of the fringe pattern intensity shown in Figure 2a, is clearly related to position of the PZT mirror. When the mirror is exactly at the correct position (here, arbitrarily assigned to be the "origin"), the fringe pattern is stationary, i.e., no frequency shift. The farther the PZT moves away from this "origin," the faster the fringe motion and, hence, the larger the frequency difference, until the self-oscillation ceases (recall Equation 16 above). Figure 2b shows the linear dependence of the frequency difference on cavity detuning, determined from the time intervals between the maxima in the beat-frequency signature. This dependence agrees with Equation (13). Minor deviations from the linear behavior could be due to air currents or the nonlinear response in the PZT. Note that the observed beat-frequency signature vs cavity length also reproduces itself periodically as the PZT mirror moves every half optical wavelength (see Equation (11)).

In the above experiment, unidirectional oscillation is observed only when the ring cavity length is "tuned" to an appropriate length by the PZT mirror and the beat frequency between the unidirectional oscillation and pumping beam is directly proportional to the cavity length detuning. These observations are explained by the theory presented above. Specifically , self-oscillation occurs only when the two-wave mixing gain, which is a function of the frequency shift, is sufficient to overcome the cavity losses and when the ring cavity roundtrip optical phase reproduces itself (to within an integer multiple of 2π).

Self-Pumped Phase Conjugator with External Linear Cavity

The frequency shifts in the self-pumped phase conjugator with two external mirrors forming a linear cavity are observed to be very similar to those described above for the unidirectional ring resonator. Specifically, both the sign and magnitude of the frequency shift can be controlled by the linear cavity length detuning. The optical setup is shown in Figure 3 where light from a single incident beam is photorefractively coupled by the $BaTiO_3$ crystal into the linear cavity formed between two highly reflecting beam splitters (BS_8 and BS_9). This self-oscillation serves as the counterpropagating pumping beams in a traditional four-wave mixing geometry to phase conjugate the incident beam.[1]

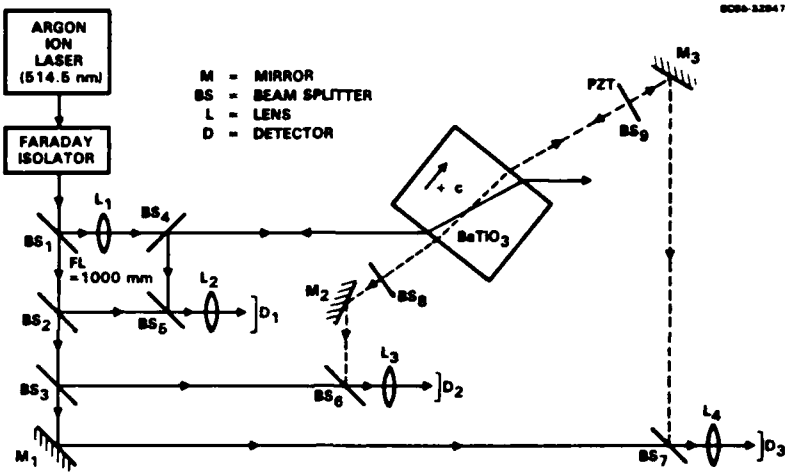

Figure 3 Optical setup for a self-pumped phase conjugator with external linear cavity. Photorefractive coupling in $BaTiO_3$ generates the self-oscillations in the resonant cavity (with variable length) formed by beam splitters BS_8 and BS_9. The beat frequencies for the phase-conjugate reflection and both of the two counter-propagating self-oscillations (relative to the incident beam) are derived from the motion of the interferograms at D_1, D_2 and D_3, respectively.

While only two-wave mixing occurs in the unidirectional ring oscillator previously described, both two- and four-wave mixing are occurring simultaneously in this self-pumped phase conjugator with external mirrors forming a linear cavity. The photorefractive coupling process is considerably more complicated in this latter situation.

As illustrated in Figure 3, the frequency shifts (relative to the incident beam) appearing on the phase-conjugate reflection and the two counterpropagating self-oscillations are simultaneously measured at detectors, D_1, D_2 and D_3, using the same interferometric techniques described in the unidirectional ring oscillator experiment. The resulting beat-frequency signatures, as a function of linear cavity length detuning, are shown in Figure 4 for the phase-conjugate reflection and one self-oscillating beam. Note that the other counter-propagating self-oscillation beat-frequency signature appears identical to the one shown.

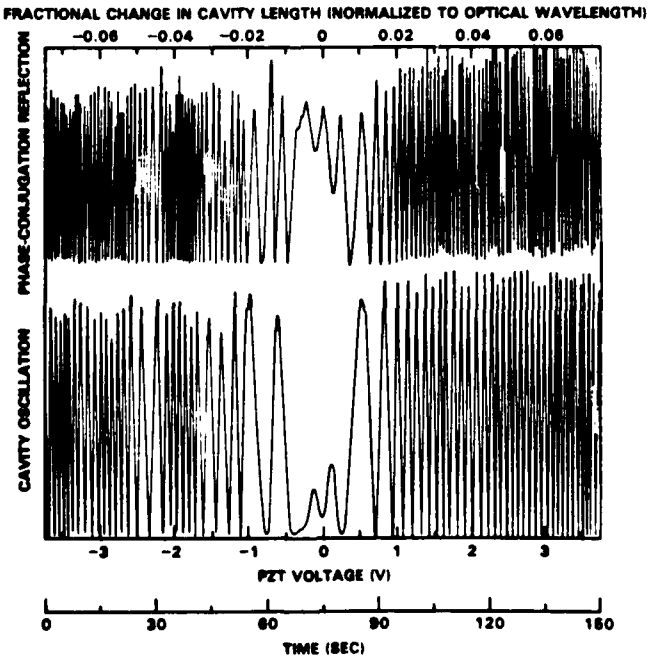

Figure 4 Self-pumped phase conjugator with external linear cavity: Dependence of the beat frequencies (relative to the incident beam) for the phase-conjugate reflection (top) and one self-oscillation (bottom) on cavity length detuning.

Regarding the beat-frequency signatures shown in Figure 4, two important features are evident. First, the frequency shift of the phase-conjugate reflection is exactly a factor of two larger than that of either self-oscillation. In fact, this is simply the conservation of energy constraint for slightly nondegenerate four-wave mixing when the two counterpropagating pump beams are the same frequency.[18] Second, the signs and magnitudes of the beat frequencies of the phase-conjugate reflection and the counterpropagating self-oscillations depend on the external linear cavity length detuning, similar to the unidirectional ring oscillator. That is, the beat frequencies are directly proportional to the detuning (see Equation (13)), becoming faster and faster as the cavity length detuning increases or decreases away from the length that gives no frequency shift.

Two additional observations concerning the beat-frequency signatures are not shown in Figure 4. First, if the cavity length detuning is increased or decreased far enough, the self-oscillation ceases because the frequency shift required by the phase oscillation condition could not be supported by the slow response time of the photorefractive $BaTiO_3$ (i.e., the threshold condition for oscillation as described by Equation (16)). Second, the beat-frequency signatures are periodic in cavity length detuning with the entire patterns repeating for every half wavelength change in PZT beam splitter position (see Equation (11)). Note that both of these effects are also present in the unidirectional ring resonator.

Self-Pumped Phase Conjugator with Internal Reflections

The self-pumped phase conjugator, where the "pumping beams" for the four-wave mixing process arise entirely from internal reflections at the crystal faces instead of external mirrors, is the simplest self-pumped phase conjugator configuration[2] since it does not require any additional optical components. This self-pumped phase conjugator also exhibits a frequency shift in its phase-conjugate reflection.[4]

We have speculated that the frequency shift observed in this self-pumped phase conjugator using internal reflections is due to the "oscillation conditions" (see Equations (8) and (9)) involving an optical resonance cavity,[15,16] just as in the unidirectional ring oscillator and in the self-pumped phase conjugator with an external linear cavity described above. A number of experiments investigating the self-pumped phase conjugator with internal reflections provide conclusive evidence that the aforementioned speculation is indeed the case.

In the first experiment where the optical setup is shown in Figure 5, the frequency shift of the phase-conjugate reflection is compared to frequency shifts on the internal self-pumping beams. The beat frequency of the phase-conjugate reflection is determined in the usual way (i.e., interferometrically) at detector, D_1. The frequency shifts on the internal self-pumping beams are inferred by observing the beat frequency for the scattered light that emanates from the primary self-pumping corner of the crystal. Upon interfering with a portion of the incident beam as shown in Figure 5, this scattered light forms a discernable fringe pattern at detector, D_2, only after it is spatially filtered to some degree by an aperture.

The results of this frequency shift comparison are shown in Figure 6. During the period where the frequency shift of the phase-conjugate reflection is constant, the beat-frequency signature of the scattered light is also reasonably consistent considering the poor quality of the fringe pattern used to make the determination. After taking the average of the time intervals between maxima in the beat-frequency signatures, we note that the frequency shift of the phase-conjugate reflection is approximately twice that of the scattered light. Just as with the self-pumped phase conjugator with an external linear cavity, this factor of two results from conservation of energy for slightly nondegenerate four-wave mixing (assuming, of course, that the frequency shift of the scattered light is the same as the frequency shift of the internal pumping beams). The deviation from two may be due to a multimode oscillation inside the crystal.

Unlike the unidirectional ring resonator and the self-pumped phase conjugator with an external linear cavity, any resonant cavity length in the self-pumped phase conjugator using internal reflections cannot be varied by simply moving a PZT mirror as was done previously. Any resonant cavity in the self-pumped phase conjugator with internal reflections is completely contained inside the photorefractive crystal. In a second experiment, attempts have been made to systematically vary the internal cavity length via thermal expansion by controlling the temperature.[19] The results of this investigation are currently inconclusive because small changes in temperature ($< 1°C$) induce instabilities in the frequency shift and intensity of the phase-conjugate reflection. We speculate that these instabilities are due to competition between the multiple spatial resonant cavity modes supported by a variety of internal reflections from the crystal surfaces. In the unidirectional ring oscillator and the self-pumped phase conjugator with an external linear cavity, the spatial modes of the resonance cavities were well-defined by the pinhole aperture. In this experiment with the self-pumped phase conjugator using internal reflections, it is impossible to place an aperture inside the crystal for mode selection.

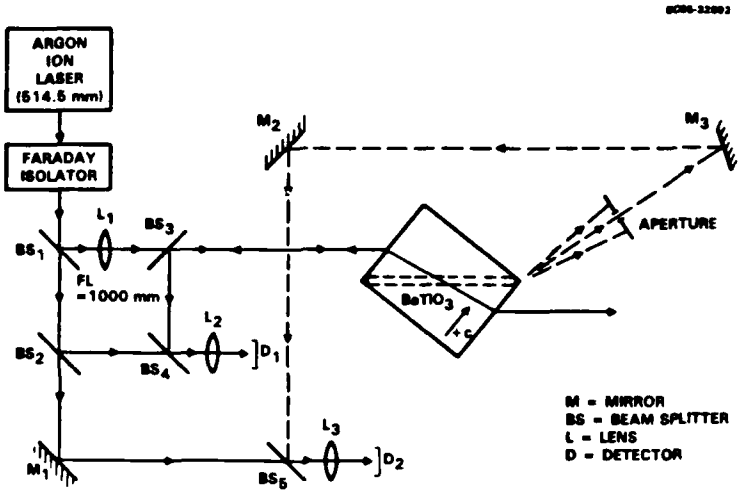

Figure 5 Optical setup for a self-pumped phase conjugator using internal reflections. Photorefractive coupling and internal reflections from the $BaTiO_3$ crystal surface automatically generate the self-pumping beams inside the crystal. The beat frequencies for the phase-conjugate reflection and the light scattered from the primary self-pumping corner (relative to the incident beam) are derived from the motion of the interferograms at D_1 and D_2, respectively.

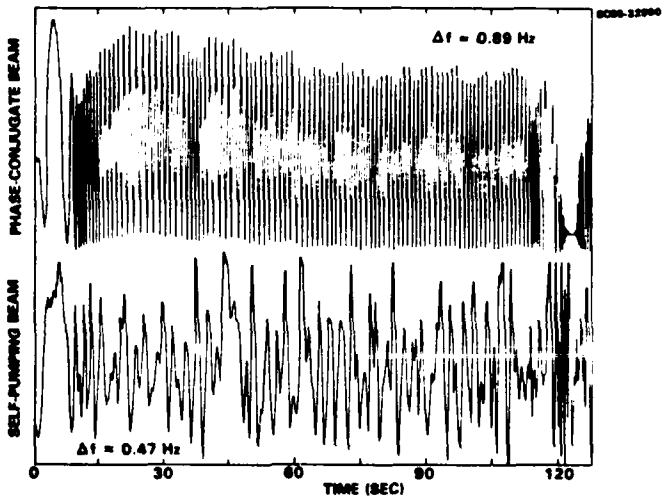

Figure 6 Self-pumped phase conjugator using internal reflections off crystal faces: correlation of the beat frequencies (relative to the incident beam) for the phase-conjugate reflection (top) and the light scattered from the primary self-pumping corner (bottom).

In a third experiment, we conclusively show that the old model[2,12,20] for the self-pumped phase conjugator using internal reflections in $BaTiO_3$ is incorrect and that the phase oscillation condition associated with a closed-loop resonance cavity is applicable to the self-pumped phase conjugator using internal reflections, as well as the previously described photorefractive resonators.[15] The picture of the old model[2,12,20] for the self-pumped phase conjugator using internal reflections in $BaTiO_3$ is schematically illustrated in Figure 7. Simply stated, this model assumed a pair of four-wave mixing interaction regions where two counterpropagating (and mutually phase-conjugated) self-pumping beams

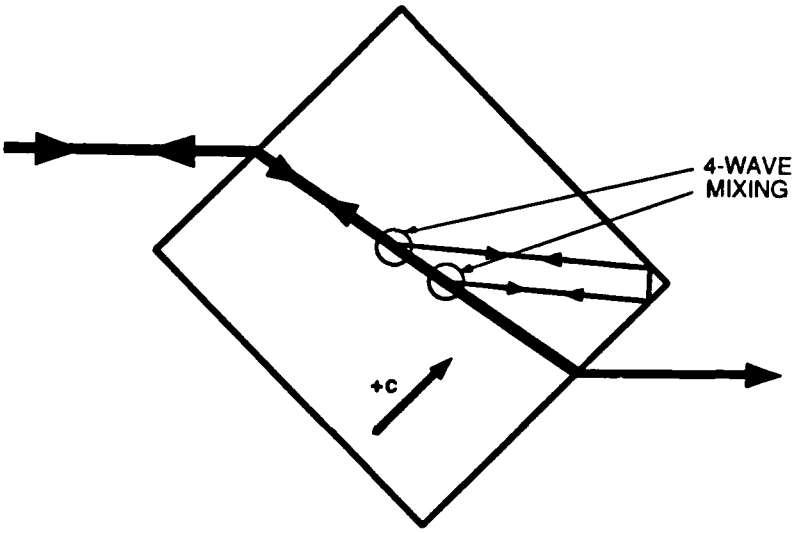

Figure 7 Schematic diagram for the self-pumped phase conjugator using internal reflections off crystal faces, showing the pair of four-wave mixing regions where the incident beams interact with the self-pumping beams to generate the phase-conjugate reflection.

underwent total internal reflection in one corner (the primary self-pumping corner) of the $BaTiO_3$ crystal. Using this model, the incident beam and its phase-conjugate reflection can also serve as the four-wave mixing "pumping beams" to produce the double-phase-conjugate oscillation[8,9] between the two interaction regions which make up the self-pumping beams.

The accuracy of this old model[2,12,20] can be ascertained by examining the pictures shown in Figure 8. An actual micrograph of the interacting beams in self-pumped $BaTiO_3$ is shown in Figure 8a and tends to support the old model. However, by increasing the exposure time by a factor of ten in the same micrograph, it becomes evident that more than the two self-pumping beams are present, as shown in Figure 8b.

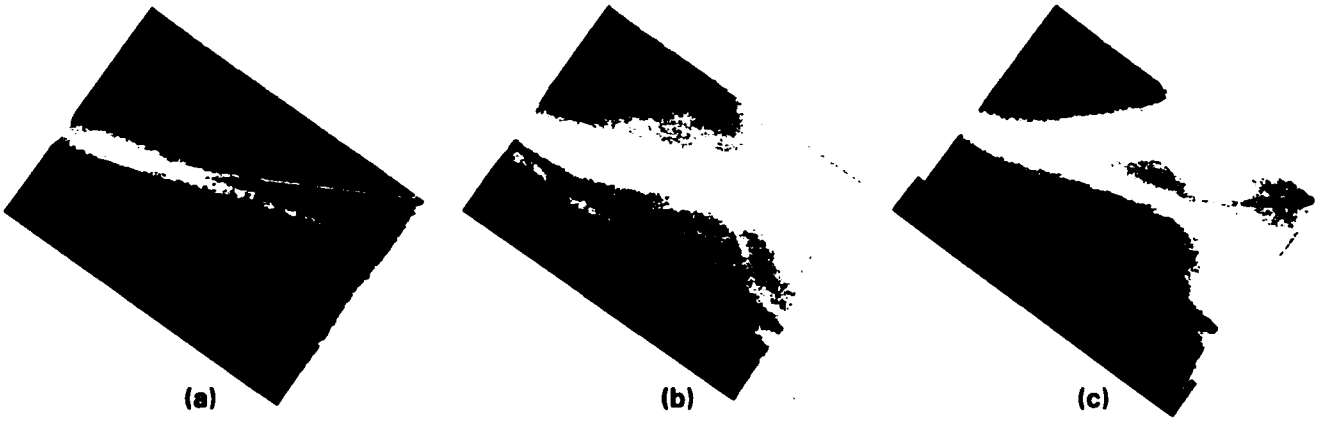

Figure 8 Microscope photographs of self-pumping process using internal reflections in a crystal of $BaTiO_3$, (a) 12 s exposure showing only the primary self-pumping beams along with the incident beam, (b) 120 s exposure showing primary and secondary self-pumping beams along with the incident beam and (c) 120 s exposure after painting lower-left crystal face black showing the incident beam and the broad fan of photorefractively scattered light. Note that the phase-conjugate reflection and all self-pumping beams vanished after painting even though primary self-pumping corner (right corner) was not painted or changed in any way.

Finally, we have proven that these secondary beams which are apparent in Figure 8b are absolutely crucial to the operation of the self-pumped phase conjugator using internal reflections. It has been suggested that the surface reflectivity in photorefractive $BaTiO_3$ can be modified by painting the crystal faces.[11,21] We attempted to reduce the reflectivity of the lower-left surface of the crystal, as indicated in Figure 8c, by covering its entire width (all the way to the corners) with Krylon ultra-flat black paint, thereby attempting to eliminate the secondary beams shown in Figure 8b. When this painting was carried out "in-situ" (i.e., without disturbing the optical alignments used to obtain the self-pumping beam pictures shown in Figures 8a and 8b), not only did the secondary beams disappear, but the phase-conjugate reflections and primary self-pumping beams also vanish (as can be seen in Figure 8c) even though primary self-pumping corner of the $BaTiO_3$ crystal remained undisturbed. Only a broad fan of photorefractively scattered light, along with the incident beam, remains visible in Figure 8c. This observation agrees with our theory. According to Equation (16), the threshold oscillation condition depends on the roundtrip mirror reflectivity R. By decreasing the refectivity R, the internal cavity falls below threshold and thus oscillation dies. Furthermore, after painting, the crystal would not self-pump in any orientation (i.e., at any angle or position of the incident beam). This conclusively shows that self-pumping in $BaTiO_3$ involves more than the internal reflections from just one corner and that the old model[2,12,20] for the process is not correct. Also, the resonator model for the self-pumped phase conjugator using internal reflections which we proposed is consistent with the series of pictures shown in Figure 8.

Summary

In conclusion, we have presented a general theory and the supporting experiments which explain the frequency shifts of self-pumped phase conjugators. The cause of the slight frequency shifts (~ 1 Hz) observed in both the photorefractive unidirectional ring resonator and the self-pumped phase conjugator with an external linear cavity is unequivocally established[15] and is well understood. In addition, the previous description of the self-pumped phase conjugator using internal reflections[2,12,20] is proven inadequate. We view all photorefractive, self-pumped phase conjugators which exhibit a frequency shift in the phase-conjugate reflection as being almost equivalent. Note that only two known photorefractive, self-pumped phase conjugators do not show the ~ 1 Hz frequency shifts: the ring conjugator[22,23] and the stimulated-backscattering (2k-grating) conjugator.[24] The self-pumped phase conjugators which do exhibit a frequency shift all employ some sort of resonant cavity (using only internal reflections from crystal surfaces or using only external reflections from ordinary mirrors or using a combination of both) to automatically generate the self-pumping beams. Because a closed-loop resonance cavity forms, the frequency shift on the phase-conjugate reflection is dictated by the phase oscillation condition for this resonance cavity.

Acknowledgments

The authors acknowledge helpful discussions with M. Khoshnevisan (Rockwell Science Center), J. Feinberg (University of Southern California), S.K. Kwong (Caltech) and M. Cronin-Golomb (Ortel). This research is supported, in part, by the Office of Naval Research.

References

1. J.O. White, M. Cronin-Golomb, B. Fischer and A. Yariv, Appl. Phys. Lett. 40, 450 (1982).
2. J. Feinberg, Opt. Lett. 7, 486 (1982); J. Feinberg, Opt. Lett. 8, 480 (1983).
3. R.A. McFarlane and D.G. Steel, Opt. Lett. 8, 208 (1983).
4. J. Feinberg and G.D. Bacher, Opt. Lett. 9, 420 (1984).
5. W.B. Whitten abd J.M. Ramsey, Opt. Lett. 9, 44 (1984).
6. F.C. Jahoda, P.G. Weber and J. Feinberg, Opt. Lett. 9, 362 (1984).
7. H. Rajbenbach and J.P. Huignard, Opt. Lett. 10, 137 (1985).
8. M.D. Ewbank, P. Yeh, M. Khoshnevisan and J. Feinberg, Opt. Lett. 10, 282 (1985).
9. M. Cronin-Golomb, B. Fischer, S-K. Kwong, J.O. White and A. Yariv, Opt. Lett. 10, 353 (1985).
10. J.M. Ramsey and W.B. Whitten, Opt. Lett. 10, 362 (1985).
11. P. Gunter, E. Voit, M.Z. Zha and J. Albers, Opt. Comm. 55, 210 (1985).
12. K.R. MacDonald and J. Feinberg, Phys. Rev. Lett. 55, 821 (1985).
13. A. Yariv and S-K. Kwong, Opt. Lett. 10, 454 (1985).
14. S-K. Kwong, A. Yariv, M. Cronin-Golomb and I. Ury, Appl. Phys. Lett. 47, 460 (1985).
15. M.D. Ewbank and P. Yeh, Opt. Lett. 10, 496 (1985).
16. P. Yeh, J. Opt. Soc. Am. B2, 1924 (1985).
17. G.C. Valley and G.D. Dunning, Opt. Lett. 9, 513 (1984).
18. P. Yeh, M.D. Ewbank, M. Khoshnevisan and J.M. Tracy, Opt. Lett. 9, 41 (1984).
19. M. Khoshnevisan, Rockwell International Science Center, Thousand Oaks, CA, private communication.

20. K.R. MacDonald and J. Feinberg, J. Opt. Soc. Am. 73, 548 (1983).
21. S-K. Kwong, California Institute of Technology, Pasadena, CA, private communication.
22. M. Cronin-Golomb, B. Fischer, J.O. White and A. Yariv, Appl. Phys. Lett. 42, 919 (1983).
23. M. Cronin-Golomb, J. Paslaski and A. Yariv, Appl. Phys. Lett. 47, 1131 (1985).
24. T.Y. Chang and R.W. Hellwarth, Opt. Lett. 10, 408 (1985).

APPENDIX 5.8

Photorefractive Conical Diffraction in $BaTiO_3$

PHOTOREFRACTIVE CONICAL DIFFRACTION IN $BaTiO_3$

M.D. Ewbank and Pochi Yeh
Rockwell International Science Center
Thousand Oaks, California 91360

and

Jack Feinberg
Department of Physics
University of Southern California
Los Angeles, California 90089-0484

ABSTRACT

A laser beam incident on $BaTiO_3$ can cause a cone of light to exit the crystal. If the incident beam is polarized as an extraordinary ray, the cone of light is formed by ordinary rays. The cone angle is fixed by a phase-matching condition for the incident and cone beams. Measurement of this cone angle as a function of the incident angle is a simple and sensitive method for determining the birefringence of a $BaTiO_3$ crystal over the entire range of wavelengths where the sample is photorefractive.

A single beam of coherent light incident on a $BaTiO_3$ crystal can cause a cone of light to emerge from the far face of the crystal. This cone has a polarization orthogonal to that of the incident ray and appears when the incident beam is an extraordinary ray in the crystal. There have been previous accounts of rings, fans, and other forms of photoinduced light scattering in photorefractive crystals, which have been attributed to a variety of physical mechanisms.[1-9] Recently, similar light cones in $BaTiO_3$ have been reported and shown to be due to stimulated two-wave mixing via the photorefractive effect.[10] Here, we account for the phase-matching condition in $BaTiO_3$ for anisotropic Bragg scattering[11] by using a simple geometrical construction to predict the angular position of the light in the exit plane. We also show that precise measurements of the cone angle can be used to determine the dispersion of the birefringence, $\Delta n = n_e - n_o$, of a $BaTiO_3$ sample.

Figure 1 shows the experimental setup, with a laser beam incident on one of the a-faces of a $BaTiO_3$ crystal. The incident beam makes an angle θ in air with the face normal and is polarized to be an extraordinary ray, with its electric-field vector in the plane of incidence defined by the beam direction and the c-axis of the crystal. A broad fan[12] of extraordinary light is observed on the +c-axis side of the transmitted beam, as shown in Fig. 2a. Simultaneously, a single ring of light with ordinary polarization appears on the negative c-axis side of the transmitted beam (see the multiple exposure photograph in Fig. 2b). For an incident beam intensity of $\sim 1 W/cm^2$, the fan and the ring appear within a few seconds. As shown in Fig. 2b, the shape of the ring varies with the angle of incidence. The ring is visible for both positive and negative angles of incidence θ (with positive θ defined in Fig. 1), although for negative angles the ring intensity is diminished because self-pumped phase conjugation[13] depletes the incident beam intensity.

The rings observed in Fig. 2b for $BaTiO_3$ result from anisotropic Bragg scattering[11] of the incident beam off photorefractive gratings formed during beam fanning.[10] The incident beam, with wavevector $\vec{K}_i$, scatters from defects or impurities into a broad fan having a range of wavevectors $\vec{K}_f$. These scattered

beams interfere with the incident beam and create photorefractive index gratings with wavevectors $\vec{K}$ given by

$$\vec{K} = \vec{K}_f - \vec{K}_i \quad . \tag{1}$$

The incident beam then Bragg-scatters off these gratings and either reinforces or depletes the fanning beams by two-wave mixing[14] depending on the sign of the projection of $\vec{K}$ onto the positive c-axis direction. The collection of all amplified scattered beams is a broad fan of light directed towards the positive c-axis side of the crystal.

The photorefractive grating wavevectors $\vec{K}$ formed during beam fanning can also deflect the incident beam into a cone of light. As illustrated in Fig. 3a, some of these photorefractive gratings will have wavevectors of exactly the right length and direction $-\vec{K}$ to deflect the extraordinary incident wavevector $\vec{K}_i$ into an ordinary ring beam $\vec{K}_r$:

$$\vec{K}_r = \vec{K}_i - \vec{K} \quad . \tag{2}$$

Eliminating $\vec{K}$ from Eqs. (1) and (2) gives the phase-matching condition:

$$\vec{K}_r = 2\vec{K}_i - \vec{K}_f \quad . \tag{3}$$

Equation (3) selects a cone of wavevectors $\vec{K}_r$ as can be seen in the following simple geometric interpretation. The locus of all possible $\vec{K}_r$ (ordinary ring beams) is a sphere of radius $2\pi n_o/\lambda$. The locus of all possible $\vec{K}_f$ (extraordinary fanned beams) is an ellipsoid of revolution with semi-minor and semi-major axes of lengths $2\pi n_e/\lambda$ and $2\pi n_o/\lambda$, respectively. Displace the center of the ellipsoid from the center of the sphere by an amount $2\vec{K}_i$. Then the intersection of the ellipsoid and the sphere selects a cone of phase-matched wavevectors $\vec{K}_r$. Figure 3b shows this geometric construction in the x-z plane, while Fig. 3c extends it to three dimensions. As can be seen in Fig. 3c, the intersection of the two normal surfaces is a ring centered around the direction

AD-A170 203 STUDIES OF PHASE-CONJUGATE OPTICAL DEVICE CONCEPTS(U) 2/2
ROCKWELL INTERNATIONAL THOUSAND OAKS CA SCIENCE CENTER
P YEH ET AL. JUN 86 SC5424.AR N00014-85-C-0219
UNCLASSIFIED F/G 20/6 NL

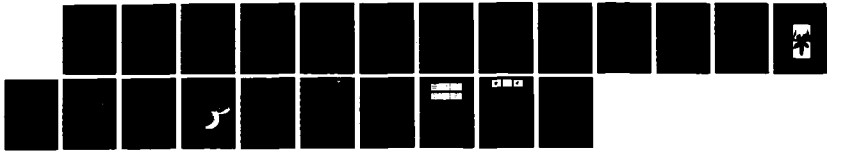

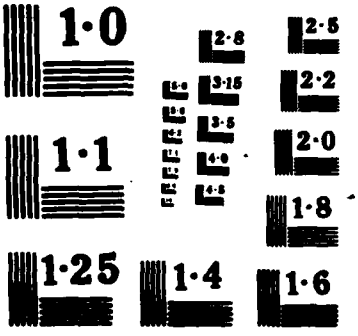
1·0
1·1
1·25
1·4
1·6
1·8
2·0
2·2
2·5

of the incident beam. For materials with small birefringence, this ring is approximately a circle inside the crystal.

The intensity and the polarization of the cone of light is determined by the electro-optic tensor of the crystal. $BaTiO_3$ has point group symmetry 4mm, and its largest electro-optic coefficient is $r_{42} = r_{51} = 1640$ pm/V.[15] A photorefractive space-charge electric field $E_{sc} = (E_x, E_y, E_z)$ formed during beam fanning will, through the r_{42} coefficient, cause a change in the susceptibility tensor $\Delta\chi$ given by[16]

$$\Delta\chi = \begin{pmatrix} 0 & 0 & ar_{42}E_x \\ 0 & 0 & ar_{42}E_y \\ ar_{42}E_x & ar_{42}E_y & 0 \end{pmatrix} \tag{4}$$

where $a \equiv -\varepsilon_a\varepsilon_c/4\pi$ with ε_a and ε_c being the static dielectric constants along the a- and c-axes, respectively. The $\Delta\chi_{13} = \Delta\chi_{31}$ components in Eq. (4) produce beam fanning by coupling the incident extraordinary beam, whose polarization vector is in the x-z plane, into the extraordinary fanned beams, which also have x-z polarization. The $\Delta\chi_{23} = \Delta\chi_{32}$ components produce anisotropic scattering of the incident extraordinary beam into the ring beam, which has ordinary (y) polarization. Anisotropic scattering of a beam into the x-z plane itself cannot occur because if the grating K lies entirely in the x-z plane then $E_y = 0$, and the intensity of the anisotropically scattering beam is zero.[10] This is evident in Fig. 2b, where the observed intensity of the conical diffraction vanishes along the plane of incidence.

The angular position and shape of the diffraction cone depend on the angle of incidence, as observed in Fig. 2b. Referring to Fig. 3b, for a given incident beam angle θ_i inside the crystal, the diffraction angle α_i inside the crystal in the plane of incidence can be obtained from

$$n_o^2v^2 + n_e^2w^2 = n_o^2n_e^2 \tag{5}$$

where

$$v \equiv 2n_1 \cos \theta_1 - n_o \cos (\theta_i + \alpha_i) \tag{6}$$

and

$$w \equiv 2n_1 \sin \theta_i - n_o \sin (\theta_i + \alpha_i) \tag{7}$$

with $n_1(\theta) = n_o n_e / \sqrt{n_e^2 \sin^2 \theta_i + n_o^2 \cos^2 \theta_i}$ the effective extraordinary refractive index at an incident angle θ_i.

For normal incidence ($\theta = \theta_i = 0$), the internal diffraction angle α_i in the plane containing the incident beam and the c-axis is given by

$$\cos \alpha_i = 2n_e/(n_o + n_e) \quad , \tag{8a}$$

and for scattering in the plane containing the incident beam but normal to the c-axis is given by

$$\cos \alpha_i = (3n_e^2 + n_o^2)/(4n_e n_o) \quad . \tag{8b}$$

For small birefringence, Eq. 8(a) is valid for any incident angle θ_i if n_e is replaced by the effective index $n_1(\theta_i)$, defined after Eq. (7) above.

Closed-form expressions for the diffraction angle α of the ring beam outside the crystal can be obtained using Snell's law. For normal incidence, assuming a fractional birefringence much less than unity ($[n_o - n_e]/n_o \approx 0.025$ in $BaTiO_3$) and using small angle approximations, the external scattering angle α becomes

$$\alpha \sim \sqrt{n_o(n_o - n_e)} \tag{9}$$

in both planes assoicated with Eqs. (8a) and (8b); that is, the external diffraction ring is nearly circular at $\theta = 0$. As a function of the incident angle θ outside of the crystal, the external diffraction angle α in the plane of incidence can be obtained from a quadratic solution to Eqs. (5) - (7) for small internal angles and Snell's law. Out of the plane of incidence, the external angle of diffraction can be determined numerically.

Figure 2c shows the calculated shape of the diffraction rings external to the crystal using the values[17] $n_o = 2.521$ and $n_e - n_o = -0.072$. Excellent agreement between theory and experiment is seen by comparing Figs. 2b and c. As the angle of incidence θ increases, portions of the diffraction ring eventually undergo total internal reflection at the crystal's exit face, and the rings become open-ended teardrop shapes, as shown in Figs. 2b and c.

At large scattering angles, where the diffracted ring approaches total internal reflection ($\theta + \alpha \sim 90°$ in the plane of incidence), the precise direction of the scattered light is a sensitive function of the birefringence $n_e - n_o$ in the crystal. Consequently, a measurement of α vs θ provides a simple method to determine the birefringence in a photorefractive $BaTiO_3$ sample. This method is independent of crystal length, unlike traditional methods of determining birefringence where a phase retardation between orthogonal polarizations is directly measured. Figure 4 shows the dependence of α on θ for one $BaTiO_3$ sample at a number of visible wavelengths (from HeNe, Ar^+ and R6G-dye laser sources). Since the intensity of the ring approaches zero in the x-z plane (see Eq. 4), the data were taken by projecting the path of the ring into this plane. Uncertainty in the precise orientation of the crystal's c-axis with respect to the fabricated faces is a possible source of error. However, we found that rotating the crystal by 180° about the y-axis gave the same measured values for the scattering angle (although now in the opposite direction), as long as care was taken to locate the angle $\theta = 0°$ by retroreflecting the incident beam off the back a-face of the crystal. By performing a nonlinear least squares fit to the data in Fig. 4 using the closed-form solution to Eq. (5) and by assuming a value for n_o,[17] the birefringence $n_e - n_o$ at each wavelength has been obtained with an

estimated accuracy of ~ 1.5%. The results of this fitting procedure are given in Table 1 and closely agree with the values previously reported in the literature.[17] (Note: the Sellmeier coefficients for $BaTiO_3$ reported in Reference 17 are better than those in Reference 18 for calculating the birefringence.) A measurement of the room-temperature birefringence in six different $BaTiO_3$ samples[19] at λ = 4880Å gave the same value with a standard deviation of 1.4×10^{-3}, even though these crystals exhibit different photorefractive behavior.

Multiple conical diffraction rings are observed in photorefractive $BaTiO_3$ in two different situations. First, if more than one beam is incident on a crystal, extra diffraction rings appear. For example, in two-wave mixing with two incident beams, each beam produces its own ring via the phase-matching process described in Fig. 3. In addition, two other diffraction rings are also present. Both of these extra rings are due to anisotropic Bragg diffraction of either incident beam off the photorefractive gratings generated via beam fanning of the other incident beam. Secondly, a transient diffraction ring is visible when the incident angle of a single beam is abruptly changed. The photorefractive gratings stored in the crystal from beam fanning for the previous angle of incidence can anisotropically Bragg-scatter the new incident beam into a transient ring. However, as the new fanned light and corresponding diffraction ring at the new angle of incidence become more intense, the previous photorefractive gratings are erased and the transient ring disappears.

In conclusion, we have observed and explained the appearance of conical diffraction rings, both transient and steady state, caused by anisotropic Bragg scattering off self-induced photorefractive gratings in $BaTiO_3$. Since these gratings are birefringent, the polarization of the rings is orthogonal to the extraordinary polarization of the incident beam. A precise measurement of the diffraction angle of the rings provides an accurate value for the birefringence of the $BaTiO_3$ crystal.

ACKNOWLEDGEMENTS

The authors acknowledge the contributions of G. Bates, A. Chiou, and M. Khoshnevisan from Rockwell and W-H Chen of Chung Cheng Institute of Technology (Taiwan). This research was supported, in part, by contract N00014-85-C-0219 of the United States Office of Naval Research.

REFERENCES

1. W. Phillips, J.J. Amodei and D.L. Staebler, RCA Rev. 33, 94 (1972).

2. J.M. Morgan and I.P. Kaminow, Appl. Opt. 12, 1964 (1973).

3. M.R.B. Forhsaw, Appl. Opt. 13, 2 (1974).

4. R. Magnusson and T.K. Gaylord, Appl. Opt. 13, 1545 (1974).

5. S.I. Ragnarsson, Appl. Opt. 17, 116 (1978).

6. I.R. Dorosh, Yu.S. Kuzminov, N.M. Polozkov, A.M. Prokhorov, V.V. Osiko, N.V. Tkachenko, V.V. Voronov and D.Kh. Nurligareev, Phys. Stat. Sol. (a) 65, 513 (1981).

7. E.M. Avakyan, K.G. Belabaev and S.G. Odoulov, Sov. Phys. Sol. St. 25, 1887 (1983).

8. R. Grousson, S. Mallick and S. Odoulov, Opt. Comm. 51, 342 (1984).

9. S. Odoulov, K. Belabaev and I. Kiseleva, Opt. Lett. 10, 31 (1985).

10. D.A. Temple and C. Warde, J. Opt. Soc. Am. B3, 337 (1986).

11. N.V. Kukhtarev, E. Kratzig, H.C. Kulich and R.A. Rupp, Appl. Phys. B35, 17 (1984).

12. J. Feinberg, J. Opt. Soc. Am. 72, 46 (1982).

13. J. Feinberg, Opt. Lett. 7, 486 (1982).

14. See, for example, D. Rak, I. Ledoux and J.P. Huignard, Opt. Comm. 49, 302 (1984) and references cited therein.

15. A.R. Johnston and J.M. Weingart, J. Opt. Soc. Am. 55, 828 (1965).

16. See, for example, A. Yariv and P. Yeh, Optical Waves in Crystals, (John Wiley & Sons, New York, 1984) p. 228.

17. R.J. Pressley, ed., Handbook of Lasers, (Chemical Rubber Company, Cleveland, 1971) p. 509.

18. S.H. Wemple, M. DiDomenico, Jr., and I. Camlibel, J. Phys. Chem. Sol. 29, 1797 (1968).

19. All samples purchased from Sanders Associates, Nashua, NH 03061.

Table 1

Birefringence $\Delta n = n_e - n_o$ of $BaTiO_3$ at Various Visible Laser Wavelengths

λ(Å)	Calculated[a] n_o	Calculated[a] Δn	This Work[b] Δn
4579	2.560	-0.0791	-0.0777
4880	2.521	-0.0718	-0.0693
5145	2.494	-0.0668	-0.0634
5674	2.452	-0.0594	-0.0597
6003	2.432	-0.0564	-0.0554
6328	2.416	-0.0534	-0.0529

a. from the Sellmeier equations given in Reference 17.
b. from a nonlinear least squares fit to the θ vs α data shown in Fig. 4 assuming the reported value for n_o listed above.

FIGURE CAPTIONS

Fig. 1 A laser beam with extraordinary polarization incident on a photorefractive $BaTiO_3$ crystal causes fanned beams and a ring beam to appear. The fanned beams are polarized extraordinary and the ring beam is ordinary, as indicated.

Fig. 2 Patterns of scattered light observed on a viewing screen oriented normal to the transmitted beam: (a) Photograph (1/50 sec exposure) of beam fanning with extraordinary polarization for λ = 4880Å and incident angle θ = 30° (b) Multiple exposure photograph (1-20 sec exposures) of the anisotropically Bragg-scattered rings of light with ordinary polarization for λ = 4880Å and incident angles θ = 0°, 20°, 30°, 35° and 38°; (c) Calculation of light patterns for incident angles θ = 0°, 20°, 30°, 35° and 38° using the phase-matching condition for anisotropic Bragg scattering (Eq. 3).

Fig. 3. Phase matching for anisotropic Bragg scattering in photorefractive $BaTiO_3$. (a) Ordinary and extraordinary normal wave surfaces in the plane of incidence. Photorefractive gratings deflect the incident wavevector $\vec{K}_i$ into a range of fanned wavevectors $\vec{K}_f$. One particular grating, with wavevector $-\vec{K}$, also deflects the incident wavevector $\vec{K}_i$ and generates the ring beam with wavevector $\vec{K}_r$. Because the polarization of the incident and fanned beams is extraordinary and the ring beam is ordinary, only the one wavevector $-\vec{K}$ in the plane of incidence will permit the ring beam to be phase-matched. (b) A graphical solution in the plane of incidence to the phase-matching condition, $\vec{K}_r = 2\vec{K}_i - \vec{K}_f$. The ring wavevector $\vec{K}_r$ is determined by the intersection of a circle (representing all possible ordinary ring beams) and an ellipse (representing the extraordinary fanned beams) whose centers are separated by $2\vec{K}_i$. (c) Extending the geometric construction of Fig. 3b to three dimensions; the intersection of the two normal surfaces defines a cone of wavevectors (note that now $\vec{K}_r$ is shown coming out of the x-z plane), which produces the diffraction ring observed in Fig. 2b.

Fig. 4 Measured external ring diffraction angle α vs incident angle θ as a function of wavelength for one photorefractive $BaTiO_3$ crystal. The solid curves are nonlinear least squares fits to Eq. (5) (as described in the text) and provide the values for the birefringence listed in Table 1.

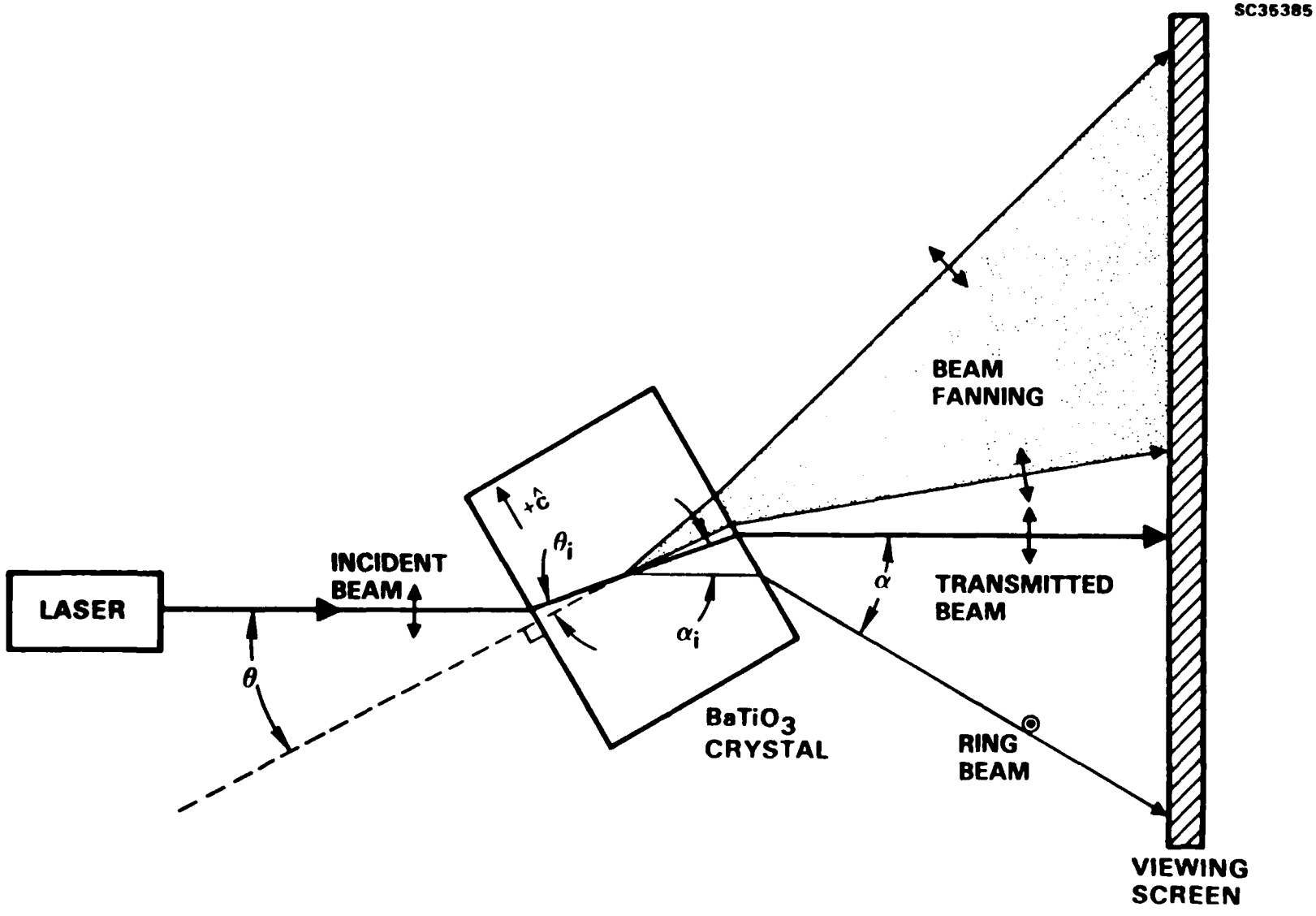
SC36385
BEAM
FANNING
+c
θ_i
INCIDENT
BEAM
LASER
θ
α_i
α
TRANSMITTED
BEAM
$BaTiO_3$
CRYSTAL
RING
BEAM
VIEWING
SCREEN

Figure 1

SC35383
SC35384

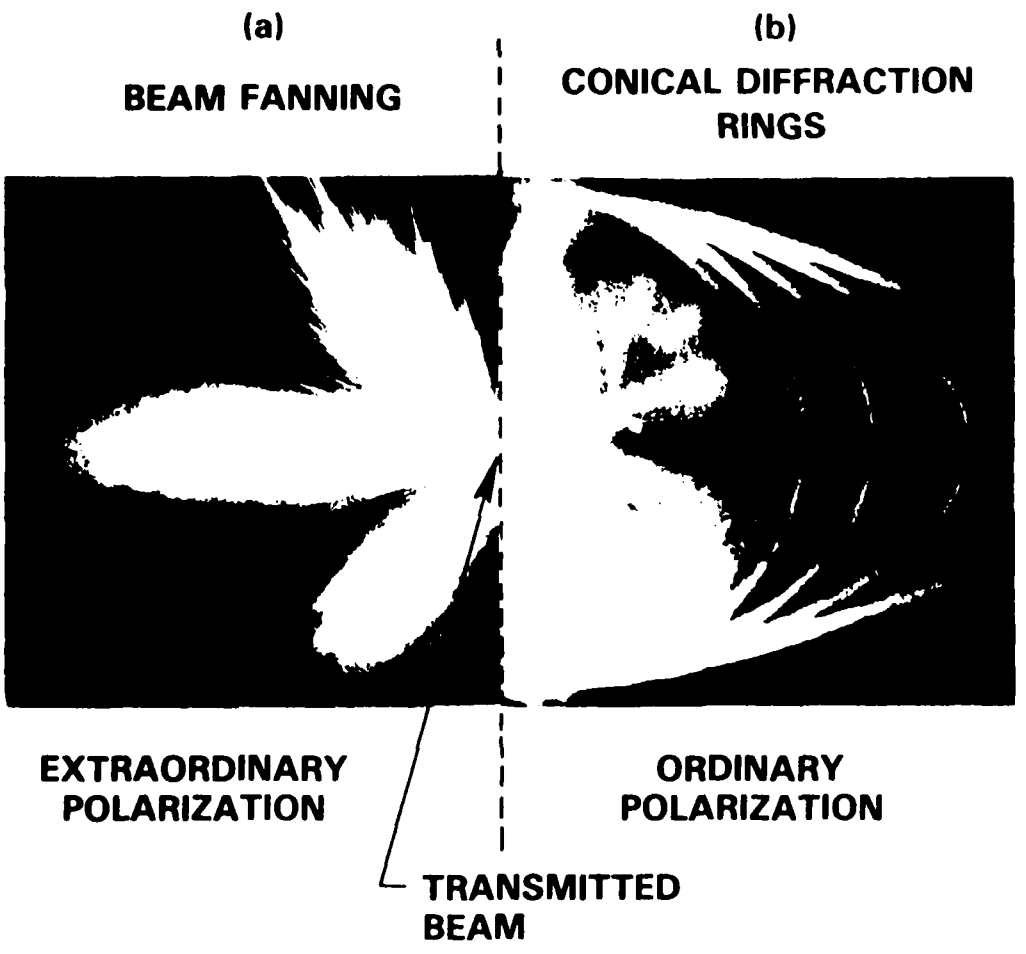

Figure 2a & b

SC35387

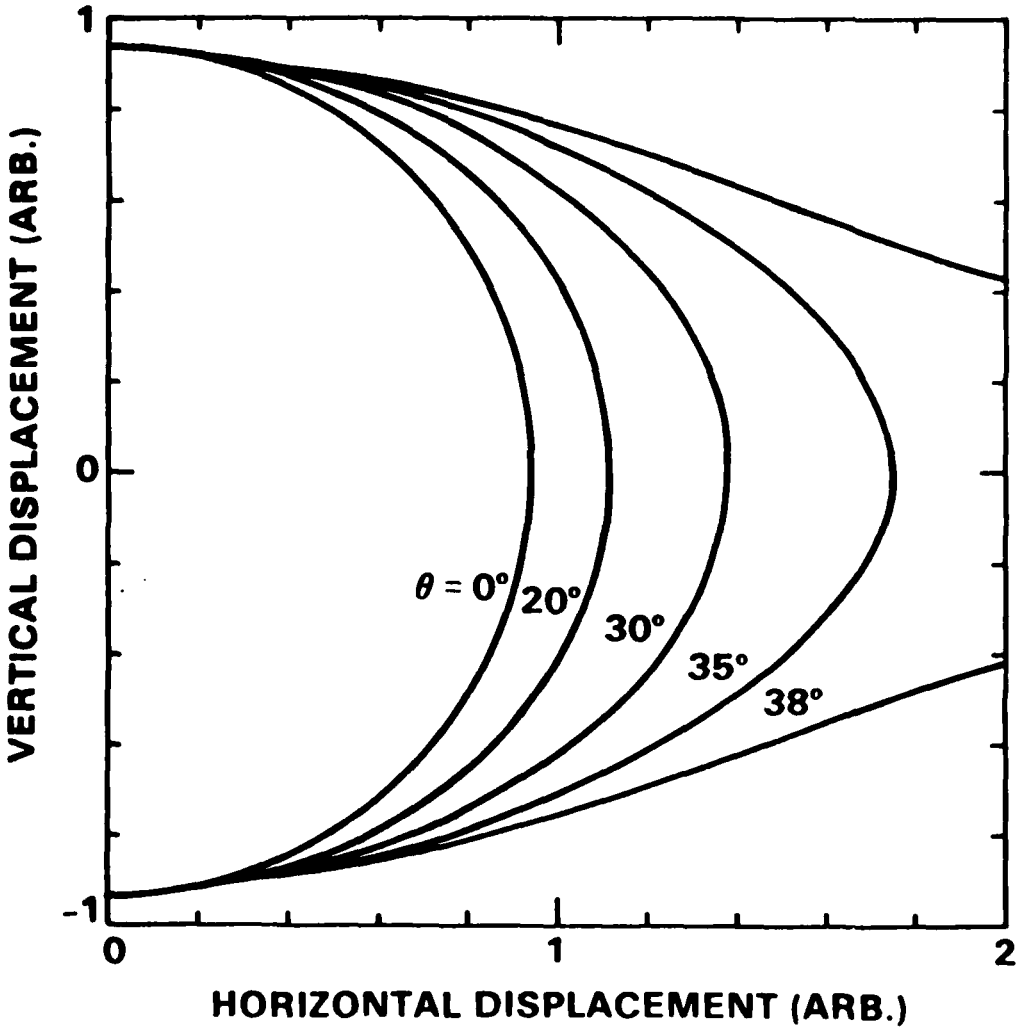

Figure 2c

SC35432

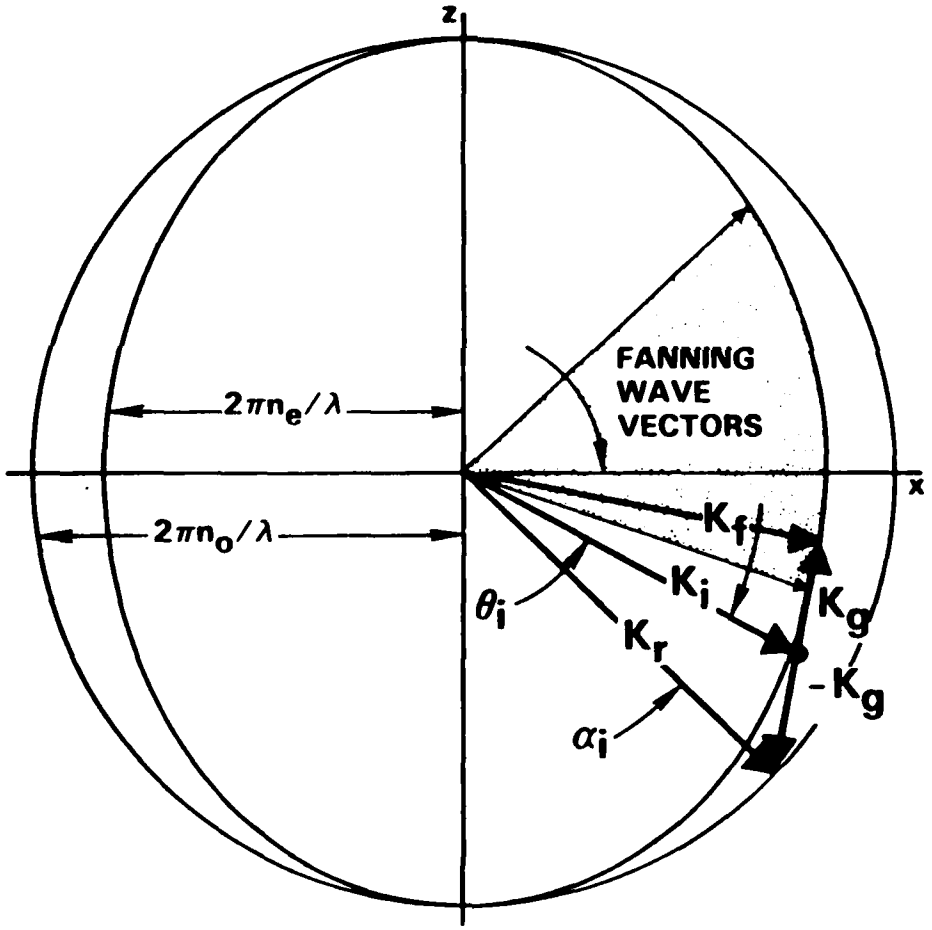

Figure 3a

SC35537

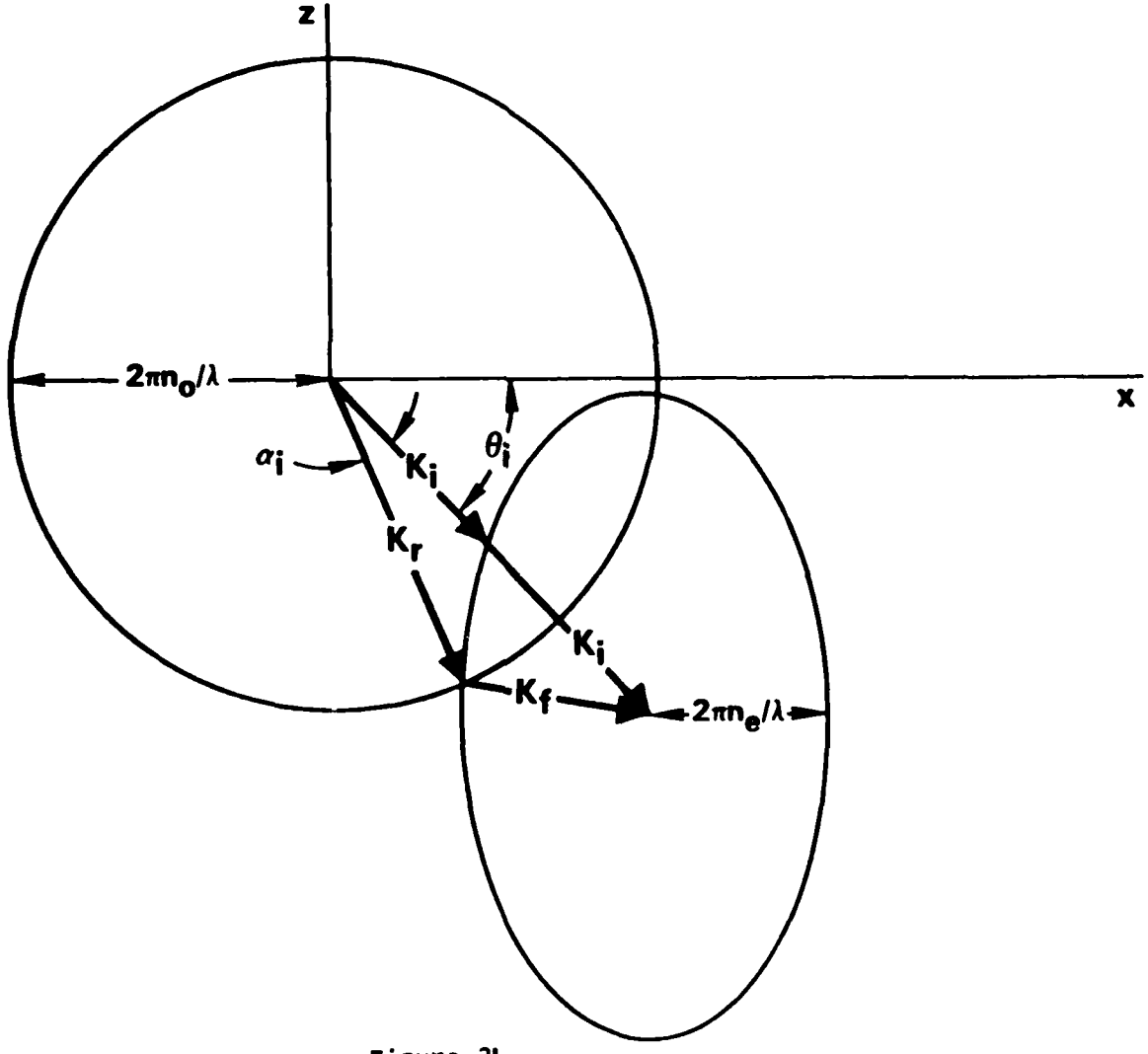

Figure 3b

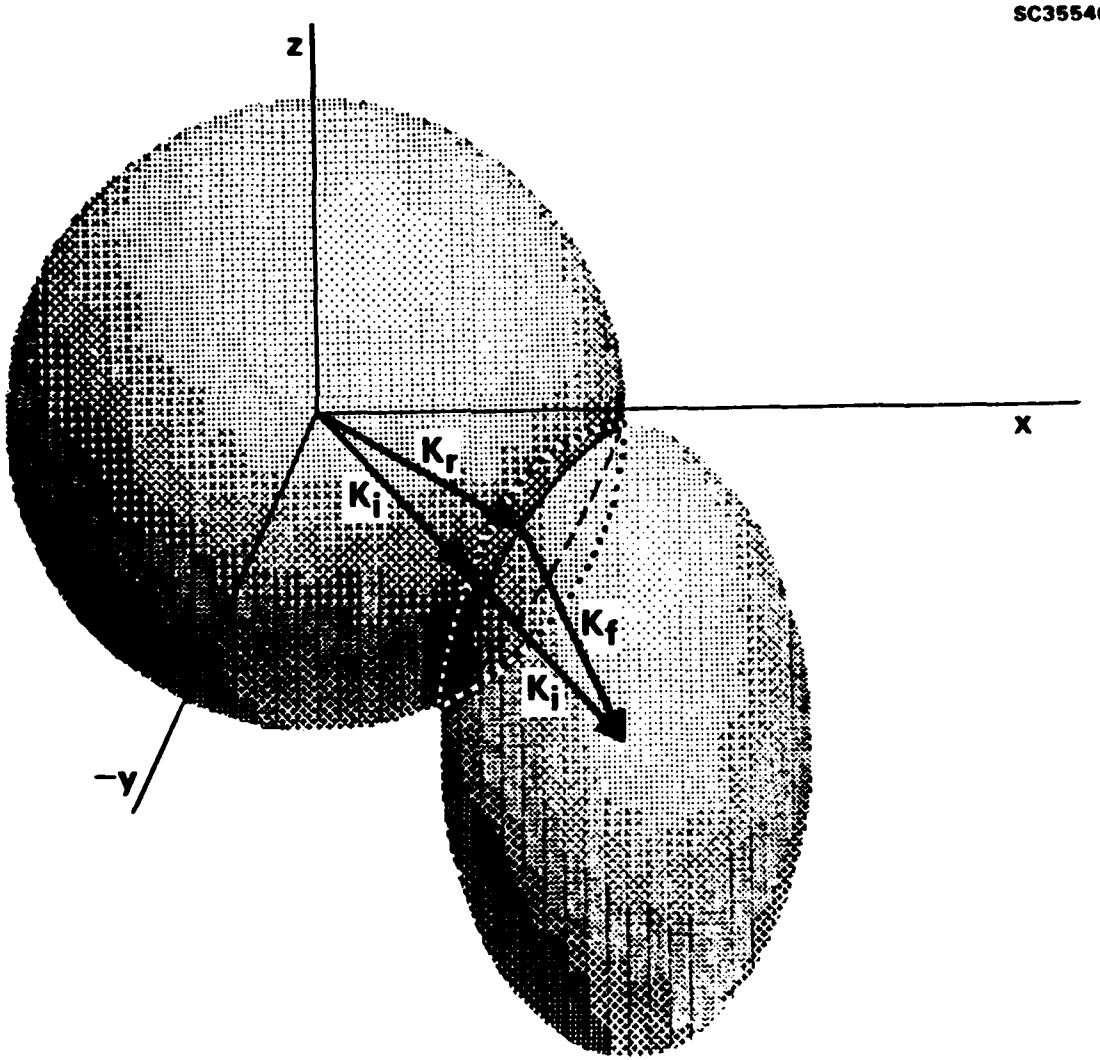

Figure 3c

SC35386

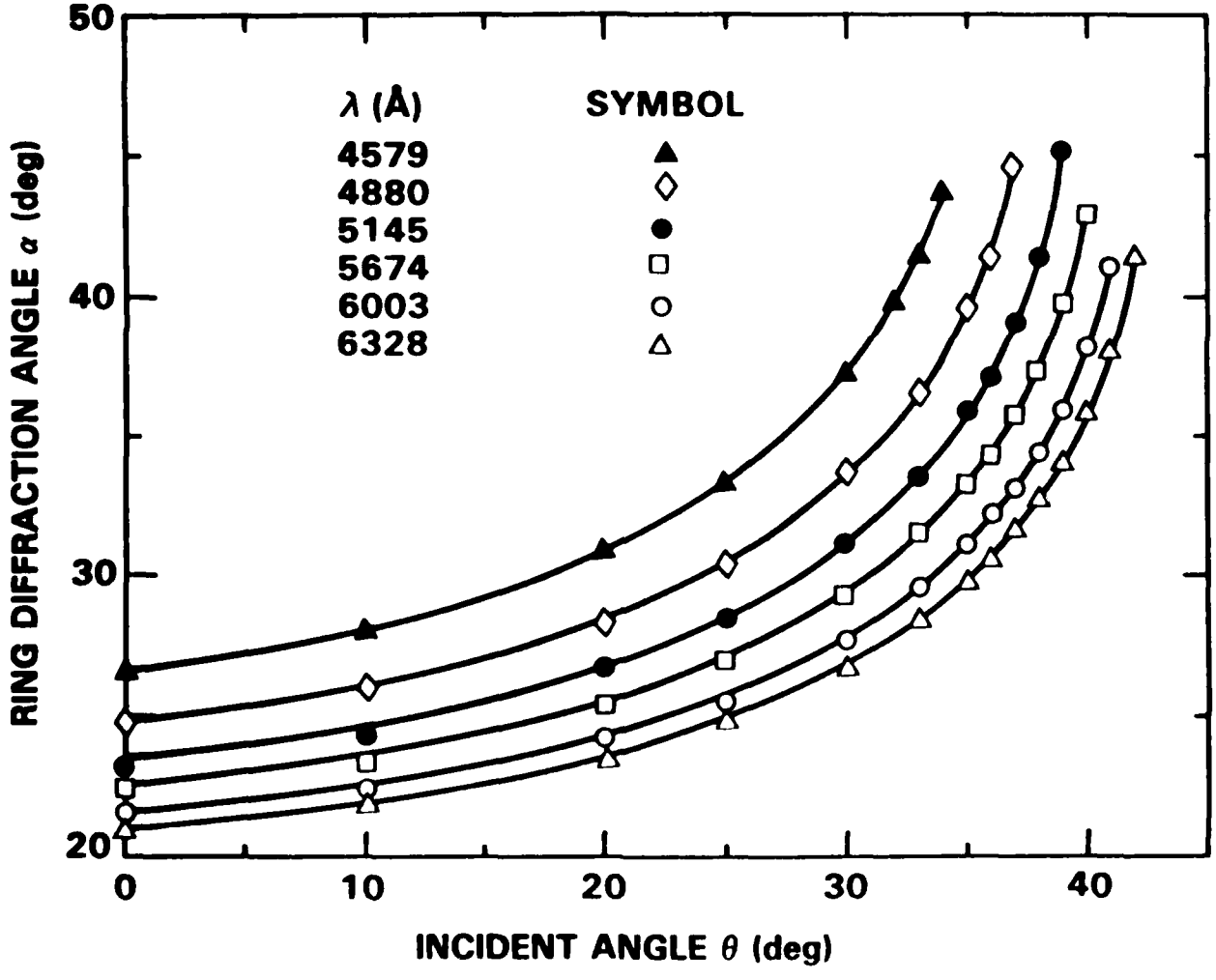

Figure 4

APPENDIX 5.9

Parallel Image Subtraction Using a Phase-Conjugate Michelson Interferometer

Reprinted from Optics Letters, Vol. 11, page 306, May, 1986.

Parallel image subtraction using a phase-conjugate Michelson interferometer

Arthur E. Chiou and Pochi Yeh

Rockwell International Science Center, Thousand Oaks, California 91360

Received December 2, 1985; accepted February 20, 1986

A phase-conjugate Michelson interferometer using an internally self-pumped barium titanate crystal as reflectors has been constructed to perform parallel image subtraction, intensity inversion, and exclusive OR logic operation. These operations are independent of the optical path differences and phase aberration.

We report parallel image subtraction, exclusive OR (XOR) logic operation, and intensity inversion using a phase-conjugate Michelson interferometer that consists of a beam splitter and a phase-conjugate reflector in place of the usual interferometer mirrors (see Fig. 1). Such an interferometer is equivalent to the double phase-conjugate interferometer and also exhibits time reversal.[1]

Image subtraction has been a subject of considerable interest in signal processing. Electronic digital processing of images is slow because of its serial nature. Optical techniques offer the capability of parallel processing over the entire images. The parallel processing is versatile and inherently faster. The technique of optical image synthesis by the addition and subtraction of the complex amplitude of light was first described by Gabor *et al.*[2] The basic principle consists of spatially modulating the two images by periodic waves that are mutually shifted by a phase of 180 deg.[3,4]

Although there are other techniques of image subtraction,[5-8] interferometers such as the Mach–Zehnder or Michelson offer convenient ways for the addition and subtraction of the complex amplitude of images.[9-11] In the interferometric methods the subtraction is obtained by introducing the two images symmetrically in the two arms of the interferometer where a path difference corresponding to π phase shift exists between them. It is known that the interferometers are extremely difficult to adjust and that they cannot easily maintain the fixed path difference. In addition, only the center fringe is useful for image subtraction or addition. In many cases the center fringe is not large enough to cover all the images. The new method of parallel image subtraction by phase-conjugate interferometry described in this Letter eliminates these two problems.

In our phase-conjugate Michelson interferometer, a plane wave with amplitude E is divided into two by the beam splitter BS_2. Each of these two beams passes through a transparency and is then reflected by a self-pumped $BaTiO_3$ phase conjugator.[12-15] When these two phase-conjugated beams recombine at the beam splitter, image subtraction is obtained at the usual interferometer output port A (see Fig. 1). Let the reflection coefficient of the phase conjugator be ρ.[16] The image intensity at the output port A is given by

$$I_A(x,y) = |E|^2|\rho|^2|t^*r'T_1(x,y) + r^*tT_2(x,y)|^2, \quad (1)$$

where r and r' are the amplitude reflection coefficients of the beam splitter BS_2 for beam incidence from the left and right sides, respectively; t is the amplitude-transmission coefficient; * denotes complex conjugation; and $T_1(x,y)$ and $T_2(x,y)$ are the intensity-transmittance functions of transparencies 1 and 2, respectively. Using Stokes's relation[17]

$$r't^* + r^*t = 0, \quad (2)$$

Eq. (1) for the intensity at the output port becomes

$$I_A(x,y) = |E|^2|\rho|^2RT|T_1(x,y) - T_2(x,y)|^2, \quad (3)$$

where R and T are intensity reflectance and transmittance, respectively, of the beam splitter BS_2. Note that the output intensity is proportional to the square of the difference of the intensity-transmittance functions.

The 180-deg phase shift between the two images as dictated by the Stokes's relation plays a crucial role in this image-subtraction technique. The Stokes relation holds for any lossless dielectric mirror and results directly from the time reversal. Such a relation was first predicted by Stokes[18] in the nineteenth century and was not proved experimentally until recently by using phase-conjugate reflectors.[1] The phase-conju-

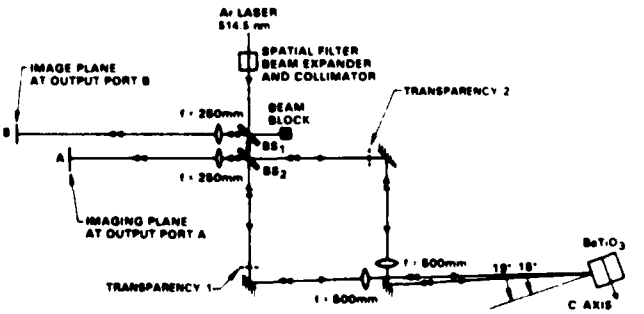

Fig. 1. Schematic diagram illustrating the basic idea of coherent image subtraction and addition by a phase-conjugate Michelson interferometer.

0146-9592/86/050306-03$2.00/00

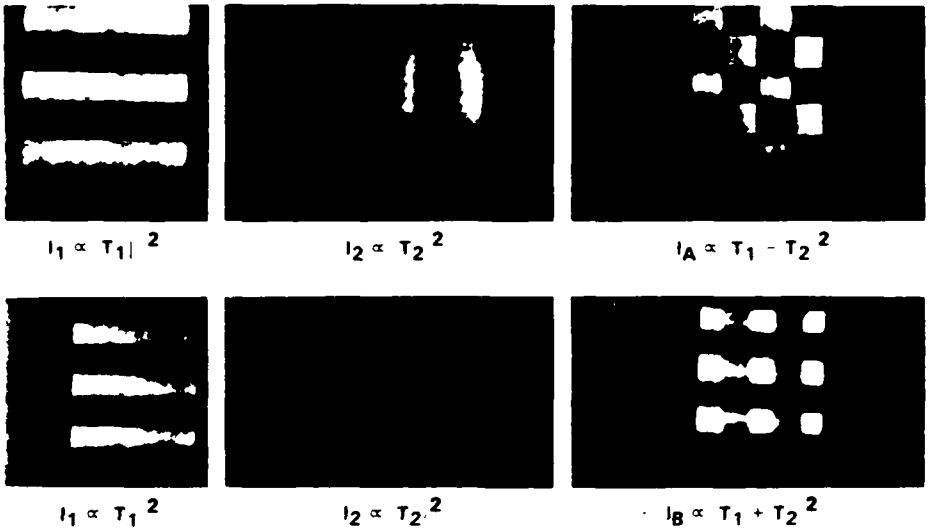

Fig. 2. Experimental results for the image subtraction and addition by the phase-conjugate Michelson interferometer. The horizontal and the vertical bars are the images of transparencies 1 and 2, respectively, when the illuminating beam for the other arm is blocked. The checkerboard patterns at upper and lower right are the intensity distribution of the coherent subtraction and addition, respectively, of the two images.

gation process also eliminates the problems of phase distortion and the critical alignment requirement associated with conventional interferometry.

At the image plane B (see Fig. 1) the intensity distribution is given by

$$I_B(x, y) = |E|^2|\rho|^2|TT_1(x, y) + RT_2(x, y)|^2. \quad (4)$$

In our experiment, an argon-ion laser (514.5 nm) with output power of a few hundred milliwatts is used as the coherent light source. The laser output, after spatial filtering through a 5× microscope objective and a 25-μm-diameter aperture, is expanded and collimated to a 1-cm-diameter beam size. The collimated beam is split into two by beam splitters BS_2 (intensity transmittance, 64%) to illuminate the two transparencies (the horizontal and the vertical triplet bars from the U.S. Air Force Resolution Chart). They are then redirected and focused (f-number, $f/50$) onto the a face of a $BaTiO_3$ crystal with angles of incidence of approximately 15 and 19 deg. These beams are polarized in the xz plane (i.e., the plane of incidence) and excite only extraordinary wave in the crystal. Both beams self-pump the crystal and are phase conjugated with a reflectance of about 32%. Each of the phase-conjugated beams retraces its incoming path backward through the transparencies, and the two recombine at the beam splitter BS_2. Note that the beam splitter BS_1 simply serves physically to separate the output port B from the input. It is not part of the interferometer. At each of the interferometer output ports, a lens (f-number, $f/25$) is used to image both objects onto the image plane.

We have experimentally demonstrated that the two images are subtracted from each other in the image plane A and are added together in the image plane B. These operations are independent of the optical path lengths of the two arms of the interferometer. According to Eq. (4), the addition of the two images is performed with weighing factors T and R, respectively. The subtraction, however, is independent of the ratio of R and T. Typical experimental results are shown in Fig. 2. The horizontal and the vertical bars in the upper photos are the images at output port A (see Fig. 1) of transparencies 1 and 2, respectively, when the illuminating beam for the other arm is blocked. The upper right checkerboard pattern represents the coherent subtraction of the two images due to destructive interference when both illuminating beams are present. Note that the intensity distribution where subtraction takes place is fairly uniform and is very close to that of the true dark background (four dark squares where the dark regions of the bars overlap). The lower photos are the corresponding results at output port B where image addition takes place.

The image subtracter can also perform logic operation. Consider the case when both transparencies are either 1 or 0. According to Eq. (3), a complete cancellation would require that these two transparencies be identical. An output intensity of 1 will appear at port A when only one of these two transparencies transmits. Thus such an image subtracter can act as an XOR gate. The truth table of such a logic operation is given in Table 1. In the case when the transparencies are encoded with a matrix of binary data, such an

Table 1. The Logic Operations Represented by the Intensity I_A

T_1	T_2	$I_A \propto \lvert T_1 - T_2 \rvert^2$
1	1	0
1	0	1
0	1	1
0	0	0

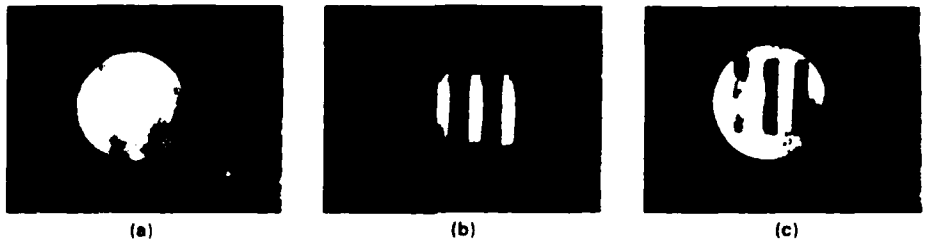

Fig. 3. Experimental results for the intensity inversion: (a) intensity distribution of the phase-conjugate beam in the first arm with the transparency removed, (b) image of the transparency in the second arm, and (c) the intensity inversion of (b). (a) $I_1 = T_1(x, y)|^2 = 1$, (b) $I_2 = T_2(x, y)|^2$, (c) $I_3 = T_1(x, y) - T_2(x, y)|^2 = |1 - T_2(x, y)|^2$.

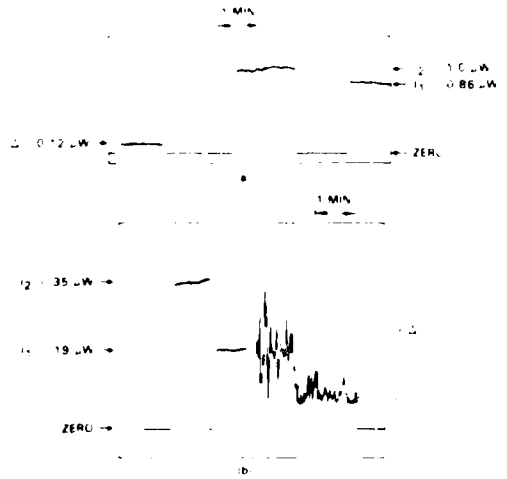

Fig. 4. Temporal fluctuation of the intensity of each image and their coherent subtraction for (a) a phase-conjugate Michelson interferometer, (b) a Mach–Zehnder interferometer with regular mirrors. Δ is the signal output at the subtraction port.

image subtracter acts as a two-dimensional array of XOR gates.

A special case of image subtraction is intensity inversion, which is obtained by removing one of the transparencies so that the transmittance $T_i(x, y)$ becomes unity in one arm. The experimental result is shown in Fig. 3.

The temporal stability of the subtracted image intensities is compared in Fig. 4 for the case of an interferometer with a phase conjugator and that of one with regular mirrors. For both cases, the centermost square of the checkerboard pattern (the upper right in Fig. 2) is imaged on the detector through a circular aperture with diameter slightly smaller than the side of the square. The temporal evolution of intensity I_1 and I_2 is recorded in turn when the illuminating beam in the other arm is blocked. The intensity difference Δ is then recorded when both beams are present. The improvement in temporal stability of the subtracted image intensity is dramatic.

In conclusion, we have demonstrated coherent image subtraction, intensity inversion, and exclusive OR logic operation using a phase-conjugate Michelson interferometer. The experimental results can be explained theoretically by the principle of time reversal.

Similar work has been carried out independently by Kwong *et al.*[19] and was reported recently.

The authors acknowledge technical discussions with M. Khoshnevisan, M. D. Ewbank, and I. McMichael. This research was supported partially by the U.S. Office of Naval Research under contract no. N00014-85-C-0219.

References

1. M. D. Ewbank, P. Yeh, M. Khoshnevisan, and J. Feinberg, Opt. Lett. **10**, 282 (1985).
2. D. Gabor, G. W. Stroke, R. Restrick, A. Funkhouser, and D. Brumm, Phys. Lett. **18**, 116 (1965).
3. See, for example, J. F. Ebersole, Opt. Eng. **14**, 436 (1975).
4. See, for example, G. Idebetouw, L. Bernardo, and M. Miller, Appl. Opt. **19**, 1218 (1980).
5. Y. H. Ja, Opt. Commun. **42**, 377 (1982).
6. C. P. Grover and R. Tremblay, Appl. Opt. **21**, 2666 (1982).
7. C. Warde and J. I. Thackara, Opt. Lett. **7**, 344 (1982).
8. G. G. Mu, C. K. Chiang, and H. K. Liu, Opt. Lett. **6**, 389 (1981).
9. K. Matsuda, N. Takeya, T. Tsujiuchi, and M. Shimoda, Opt. Commun. **2**, 425 (1971).
10. K. Patroski, S. Yokozeki, and T. Suzuki, Nouv. Rev. Opt. **6**, 25 (1975).
11. W. T. Cathey, Jr., and J. G. Doidge, J. Opt. Soc. Am. **56**, 1139 (1966).
12. J. O. White, M. Cronin-Golomb, B. Fischer, and A. Yariv, Appl. Phys. Lett. **40**, 450 (1982).
13. M. Gronin-Golomb, B. Fischer, J. O. White, and A. Yariv, Appl. Phys. Lett. **41**, 689 (1982).
14. J. Feinberg, Opt. Lett. **7**, 486 (1982).
15. K. R. McDonald and J. Feinberg, J. Opt. Soc. Am. **73**, 458 (1983).
16. These two beams enter the $BaTiO_3$ phase conjugator at the same spot with approximately the same angle of incidence and are considered parts of a composite beam. Thus the assumption of a unique phase-conjugate reflectivity is legitimate. This has also been proved experimentally.
17. Z. Knittl, *Optics of Thin Films* (Wiley, New York, 1976), p. 242.
18. G. G. Stokes, Camb. Dubl. Math. J. **4**, 1 (1849).
19. S. K. Kwong G. A. Rakuljuc, and A. Yariv, Appl. Phys. Lett. **48**, 201 (1985).

END

DTIC

9-86